

**RELIABILITY EVALUATION OF ELECTRIC POWER  
SYSTEMS INCLUDING WIND POWER AND ENERGY  
STORAGE**

A Thesis

Submitted to the College of Graduate Studies and Research  
In Partial Fulfillment of the Requirements for the Degree of

Doctor of Philosophy

in the

Department of Electrical and Computer Engineering

University of Saskatchewan

Saskatoon

By

Po Hu

© Copyright Po Hu, October 2009. All rights reserved.

## **PERMISSION TO USE**

In presenting this thesis in partial fulfillment of the requirements for the Doctor of Philosophy degree from the University of Saskatchewan, the author agree that the Libraries of this University may make it freely available for inspection. The author further agree that permission for copying of this thesis in any manner, in whole or in part, for scholarly purposes may be granted by the professor or professors who supervised this thesis work or, in their absence, by the Head of Department or the Dean of the College in which the thesis work was done. It is understood that any copying or publication or use of this thesis for financial gain shall not be allowed without the author's written permission. It is also understood that due recognition shall be given to the author of this thesis and to the University of Saskatchewan in any scholarly use which may be made of any material in my thesis.

Requests for permission to copy or to make other use of material in this thesis in whole or in part should be addressed to:

Head of the Department of Electrical and Computer Engineering  
57 Campus Drive  
University of Saskatchewan  
Saskatoon, Saskatchewan  
Canada S7N 5A9

## **ACKNOWLEDGEMENTS**

First of all, the author would like to express his sincere appreciation and gratitude to his supervisor, Dr. Rajesh Karki, for his invaluable guidance, patience, encouragement and support throughout the course of this research work and in the preparation of this thesis. He has greatly benefited from Dr. Karki's in-depth knowledge of power system reliability.

The author would like to express his sincere gratitude to Dr. Roy Billinton for his guidance during Dr. Karki's sabbatical leave. The author would like to thank the advisory committee members, Professors R. Billinton, V. Meda, and H. Nguyen for their suggestions and guidance in this work. The author would also like to thank his graduate study teachers, Dr. S. O. Faried, Dr. M. S. Sachdev, and Dr. N. A. Chowdhury for strengthening his knowledge on electrical power engineering.

The author would like to take this opportunity to acknowledge the constant encouragement, patience and support from his parents, Xinlian Hu and Yong Huang and wife, Yaling Yin. The author presents this thesis as a gift to them.

Financial assistances from the College of Graduate Studies and Research in the form of the Dean's Scholarship, from the Department of Electrical and Computer Engineering at the University of Saskatchewan in the form of a Graduate Scholarship, and from the Natural Science and Engineering Research Council of Canada in the form of a Graduate Scholarship are gratefully acknowledged.

## **ABSTRACT**

Global environmental concerns associated with conventional energy generation have led to the rapid growth of wind energy applications in electric power systems. Growing demand for electrical energy and concerns associated with limited reserves of fossil fuels are also responsible for the development and increase in wind energy utilization. Many jurisdictions around the world have set high wind penetration targets in their energy generation mix.

The contribution of wind farms to the overall system reliability is limited by the uncertainty in power output from the highly variable energy source. High wind penetration can lead to high risk levels in power system reliability and stability. In order to maintain the system stability, wind energy dispatch is usually restricted and energy storage is considered to smooth out the fluctuations and improve supply continuity. The research work presented in this thesis is focused on developing reliability models for evaluating the benefits associated with wind power and energy storage in electric power generating systems. An interactive method using a sequential Monte Carlo simulation technique that incorporates wind farm and energy storage operating strategies is developed and employed in this research. Different operating strategies are compared and the resulting benefits are evaluated. Important system impacts on the reliability benefits from wind power and energy storage are illustrated. Hydro facilities with energy storage capability can alleviate the impact of wind power fluctuations and also contribute to system adequacy. A simulation technique for an energy limited hydro plant and wind farm coordination is developed considering the chronological variation in the wind, water and the energy demand. The IEEE four-state model is incorporated in the developed technique to recognize the intermittent operation of hydro units. Quantitative assessment of reliability benefits from effective utilization of wind and water resources are conducted through a range of sensitivity studies. The information provided and the examples illustrated in this thesis should prove useful to power system planners and wind developers to assess the reliability benefit from utilizing wind energy and energy storage and the coordination between wind and hydro power in electric power systems.

## TABLE OF CONTENTS

<b>PERMISSION TO USE.....</b>	<b>i</b>
<b>ACKNOWLEDGEMENTS.....</b>	<b>ii</b>
<b>ABSTRACT.....</b>	<b>iii</b>
<b>TABLE OF CONTENTS.....</b>	<b>iv</b>
<b>LIST OF FIGURES.....</b>	<b>vii</b>
<b>LIST OF TABLES.....</b>	<b>xii</b>
<b>LIST OF ABBREVIATIONS.....</b>	<b>xiii</b>
<b>1 INTRODUCTION.....</b>	<b>1</b>
1.1 Power System Reliability Evaluation.....	1
1.2 Wind Energy and Power System Reliability.....	3
1.3 Reliability Considerations in Generating Systems Containing Wind Power and Energy Storage.....	8
1.4 Power Systems including Wind and Hydro Power Generation.....	9
1.5 Research Objectives.....	10
1.6 Outline of the Thesis.....	13
<b>2 BASIC CONCEPTS AND TECHNIQUES FOR GENERATING SYSTEM ADEQUACY ASSESSMENT.....</b>	<b>16</b>
2.1 Introduction.....	16
2.2 System Modeling in Probabilistic Methods.....	18
2.2.1 Generation Model.....	19
2.2.2 Load Model.....	22
2.2.3 System Risk Model.....	24
2.3 Probabilistic Adequacy Evaluation Methods.....	25
2.3.1 Analytical Techniques.....	25
2.3.2 Monte Carlo Simulation Method.....	30
2.3.2.1 State Sampling Method.....	31
2.3.2.2 Sequential Monte Carlo Simulation Method.....	32
2.3.2.3 Simulation Convergence.....	38

2.4	Summary.....	40
<b>3</b>	<b>MODELS FOR ADEQUACY ASSESSMENT OF GENERATING SYSTEMS INCLUDING WIND POWER AND ENERGY STORAGE.....</b>	<b>42</b>
3.1	Introduction.....	42
3.2	Models for Wind Energy Conversion System.....	43
3.2.1	Wind Speed Model.....	44
3.2.2	Wind Turbine Generator Model.....	50
3.3	Reliability Evaluation Model for Generating Systems Including Wind Power and Energy Storage.....	54
3.4	Models for Energy Limited Hydro Plants.....	59
3.4.1	Peaking Unit Model.....	60
3.4.2	Energy Limited Hydro Unit Model.....	62
3.5	Coordination between Wind Power and Hydro Units.....	66
3.6	Performance Indices Associated with Reliability Evaluation of Generating Systems Including Wind Power and Energy Storage.....	72
3.7	Summary.....	73
<b>4</b>	<b>ADEQUACY ASSESSMENT OF GENERATING SYSTEMS CONTAINING WIND POWER AND ENERGY STORAGE.....</b>	<b>75</b>
4.1	Introduction.....	75
4.2	Reliability Test System.....	76
4.3	Impact of Wind Penetration on Wind Energy Utilization and System Reliability.....	77
4.4	Wind Farm and Energy Storage Operating Strategies.....	84
4.5	Simulation Results and Analyses.....	87
4.5.1	Effect of Wind Site Location.....	90
4.5.2	Effect of Charging/discharging of Energy Storage.....	92
4.5.3	Effect of Energy Storage Capacity.....	94
4.5.4	Effect of Wind Power Dispatch Restrictions.....	96
4.6	Summary.....	99
<b>5</b>	<b>ADEQUACY EVALUATION CONSIDERING WIND AND HYDRO POWER COORDINATION.....</b>	<b>101</b>
5.1	Introduction.....	101
5.2	Base Case Studies.....	102
5.2.1	Impact of Energy Limited Hydro Units on System Reliability.....	102

5.2.2	Impact of Wind Power Dispatch Restriction on System Reliability.....	105
5.3	Effect of the Number of Hydro Units Coordinated with Wind Power.....	108
5.4	Effect of Water In-flow and Reservoir Volume.....	114
5.5	Effect of Wind Farm Location.....	120
5.6	Effect of Wind Power Penetration Level.....	126
5.7	Effect of System Load Level.....	132
5.8	Effect of Wind-hydro Coordination Criterion.....	135
5.9	Effect of Hydro Unit Starting Failures.....	140
5.10	Effect of Initial Water Volume in the Reservoir.....	147
5.11	Summary.....	153
<b>6</b>	<b>SUMMARY AND CONCLUSIONS.....</b>	<b>157</b>
<b>7</b>	<b>REFERENCES.....</b>	<b>165</b>
 <b>APPENDIX A: LOAD DATA AND GENERATING SYSTEM DATA</b>		
	<b>FOR THE IEEE-RTS.....</b>	<b>173</b>
 <b>APPENDIX B: GENERATING UNIT RATINGS AND RELIABILITY</b>		
	<b>DATA FOR THE RBTS.....</b>	<b>176</b>

## LIST OF FIGURES

Figure 1.1: Subdivision of system reliability.....	2
Figure 1.2: Hierarchical levels.....	3
Figure 1.3: World wind electricity-generating capacity, 1980-2008.....	5
Figure 2.1: System model for HL- I adequacy evaluation.....	16
Figure 2.2: Conceptual tasks in generating capacity reliability evaluation.....	19
Figure 2.3: Two-state model for a generating unit.....	20
Figure 2.4: Three-state model for a generating unit.....	21
Figure 2.5: IEEE 4-state model for a peaking unit.....	22
Figure 2.6: A sample load duration curve.....	23
Figure 2.7: Chronological hourly load model for the IEEE-RTS.....	24
Figure 2.8: Loss of load method.....	28
Figure 2.9: Loss of energy method.....	29
Figure 2.10: Operating history of a conventional generating unit.....	35
Figure 2.11: Operating history of individual generating units and the capacity states of an entire system.....	35
Figure 2.12: Superimposition of capacity states and the chronological load model.	36
Figure 2.13: Convergence of the LOEE.....	39
Figure 2.14: Convergence with different initial seeds.....	40
Figure 3.1: Hourly average wind speed for the Swift Current wind site .....	46
Figure 3.2: Hourly standard deviation of wind speed for the Swift Current wind site.....	47
Figure 3.3: Hourly average wind speed for the North Battleford wind site.....	47
Figure 3.4: Hourly standard deviation of wind speed for the North Battleford wind site.....	48
Figure 3.5: Simulated wind speed for the Swift Current site for a sample day.....	49
Figure 3.6: Simulated wind speed for the Swift Current site for a sample month....	49
Figure 3.7: Simulated wind speed for the Swift Current site for a sample year.....	50
Figure 3.8: Power curve of a typical WTG unit.....	52
Figure 3.9: Power output from a wind farm in a sample month.....	53
Figure 3.10: Power output from a wind farm in a sample year.....	53
Figure 3.11: Probability distribution of the simulated wind power generation.....	54
Figure 3.12: Basic model for a wind-conventional generating system including energy storage.....	56
Figure 3.13: Realistic model for a wind-conventional generating system including	



energy storage.....	57
Figure 3.14: Simulation process for a generating system including base-loaded units and peaking units.....	62
Figure 3.15: Simulation process for a generating system considering the coordination between energy limited hydro units and wind power.....	71
Figure 4.1: Single line diagram of the RBTS.....	77
Figure 4.2: LOLE versus wind energy penetration.....	78
Figure 4.3: LOEE versus wind energy penetration.....	79
Figure 4.4: ESWE versus wind energy penetration.....	80
Figure 4.5: ESWE versus wind capacity when wind power dispatch is restricted to a fixed percentage of the system load.....	81
Figure 4.6: Effect of energy storage on system LOLE.....	82
Figure 4.7: Effect of energy storage on LOLE with a wind power dispatch restriction equal to 40%.....	84
Figure 4.8: Effect of energy storage on LOLE with a wind power dispatch restriction equal to 20%.....	84
Figure 4.9: LOLE comparison of cases with and without energy storage in different scenarios.....	88
Figure 4.10: EESW comparison of cases with and without energy storage in different scenarios.....	89
Figure 4.11: Effect of wind farm location on the LOLE. (SC: Swift Current; NB: North Battleford).....	90
Figure 4.12: Effect of energy storage charging/discharging constraints on the LOLE.....	93
Figure 4.13: Effect of energy storage capacity on the LOLE.....	95
Figure 4.14: Effect of wind energy dispatch restriction on the LOLE.....	97
Figure 4.15: Effect of wind energy dispatch restriction on the LOEE.....	98
Figure 5.1: Comparison of LOLE for Cases 1, 2 and 3.....	104
Figure 5.2: Comparison of LOEE for Cases 1, 2 and 3.....	104
Figure 5.3: Comparison of LOLF for Cases 1, 2 and 3.....	105
Figure 5.4: Effect of wind power dispatch restriction on the LOLE.....	107
Figure 5.5: Effect of wind power dispatch restriction on the LOEE.....	107
Figure 5.6: Effect of wind power dispatch restriction on the LOLF.....	108
Figure 5.7: Effect of wind power dispatch restriction on the EWEU.....	108
Figure 5.8: Effect of the number of hydro units coordinated with wind power output on the system LOLE when the hydro units are not energy limited.....	109
Figure 5.9: Effect of the number of hydro units coordinated with wind power output on the system LOEE when the hydro units are not energy limited.....	109
Figure 5.10: Effect of the number of hydro units coordinated with wind power output on the system LOLF when the hydro units are not energy limited.....	110
Figure 5.11: Effect of the number of hydro units coordinated with wind power	

output on the system LOLE when the hydro units are energy limited.....	111
Figure 5.12: Effect of the number of hydro units coordinated with wind power output on the system LOEE when the hydro units are energy limited.....	111
Figure 5.13: Effect of the number of hydro units coordinated with wind power output on the system LOLF when the hydro units are energy limited.....	112
Figure 5.14: Effect of the number of hydro units coordinated with wind power output on the AWE when the hydro units are energy limited.....	113
Figure 5.15: Effect of the number of hydro units coordinated with wind power output on the AWS when the hydro units are energy limited.....	113
Figure 5.16: Effect of the number of hydro units coordinated with wind power output on the AVolume when the hydro units are energy limited.....	113
Figure 5.17: Effect of water inflow and reservoir volume on the system LOLE.....	116
Figure 5.18: Effect of water inflow and reservoir volume on the system LOEE.....	117
Figure 5.19: Effect of water inflow and reservoir volume on the system LOLF.....	117
Figure 5.20: Effect of water inflow and reservoir volume on the AWE.....	118
Figure 5.21: Effect of water inflow and reservoir volume on the AWS.....	119
Figure 5.22: Effect of water inflow and reservoir volume on the AVolume.....	120
Figure 5.23: Effect of wind farm location on the system LOLE with Reservoir A...	121
Figure 5.24: Effect of wind farm location on the system LOEE with Reservoir A...	121
Figure 5.25: Effect of wind farm location on the system LOLF with Reservoir A...	121
Figure 5.26: Effect of wind farm location on the AWE with Reservoir A.....	122
Figure 5.27: Effect of wind farm location on the AWS with Reservoir A .....	122
Figure 5.28: Effect of wind farm location on the AVolume with Reservoir A .....	123
Figure 5.29: Effect of wind farm location on the system LOLE with Reservoir B...	123
Figure 5.30: Effect of wind farm location on the system LOEE with Reservoir B...	124
Figure 5.31: Effect of wind farm location on the system LOLF with Reservoir B...	124
Figure 5.32: Effect of wind farm location on the AWE with Reservoir B.....	125
Figure 5.33: Effect of wind farm location on the AWS with Reservoir B.....	125
Figure 5.34: Effect of wind farm location on the AVolume with Reservoir B.....	126
Figure 5.35: Effect of wind power penetration level on the system LOLE with Reservoir A .....	126
Figure 5.36: Effect of wind power penetration level on the system LOEE with Reservoir A .....	127
Figure 5.37: Effect of wind power penetration level on the system LOLF with Reservoir A .....	127
Figure 5.38: Effect of wind power penetration level on the AWE with Reservoir A .....	128
Figure 5.39: Effect of wind power penetration level on AWS with Reservoir A .....	128
Figure 5.40: Effect of wind power penetration level on the AVolume with Reservoir A .....	129

Figure 5.41: Effect of wind power penetration level on the system LOLE with Reservoir B.....	130
Figure 5.42: Effect of wind power penetration level on the system LOEE with Reservoir B.....	130
Figure 5.43: Effect of wind power penetration level on the system LOLF with Reservoir B.....	130
Figure 5.44: Effect of wind power penetration level on the AWE with Reservoir B	131
Figure 5.45: Effect of wind power penetration level on the AWS with Reservoir B.	131
Figure 5.46: Effect of wind power penetration level on the AVolume with Reservoir B.....	132
Figure 5.47: Effect of system load on the system LOLE with Reservoir A.....	132
Figure 5.48: Effect of system load on the system LOEE with Reservoir A .....	133
Figure 5.49: Effect of system load on the system LOLF with Reservoir A .....	133
Figure 5.50: Effect of system load level on the AWE with Reservoir A .....	134
Figure 5.51: Effect of system load level on the AWS with Reservoir A .....	134
Figure 5.52: Effect of system load level on the AVolume with Reservoir A .....	134
Figure 5.53: Effect of coordination criterion on the system LOLE with Reservoir A .....	135
Figure 5.54: Effect of coordination criterion on the system LOEE with Reservoir A .....	136
Figure 5.55: Effect of coordination criterion on the system LOLF with Reservoir A.....	136
Figure 5.56: Effect of coordination criterion on the AWE with Reservoir A .....	137
Figure 5.57: Effect of coordination criterion on the AVolume with Reservoir A.....	137
Figure 5.58: Effect of coordination criterion on the system LOLE with Reservoir B.....	138
Figure 5.59: Effect of coordination criterion on the system LOEE with Reservoir B.....	138
Figure 5.60: Effect of coordination criterion on the system LOLF with Reservoir B.....	138
Figure 5.61: Effect of coordination criterion on the AWE with Reservoir B.....	139
Figure 5.62: Effect of coordination criterion on the AWS with Reservoir B.....	139
Figure 5.63: Effect of coordination criterion on the AVolume with Reservoir B.....	140
Figure 5.64: Effect of hydro unit starting failure probability on the system LOLE with Reservoir A .....	141
Figure 5.65: Effect of hydro unit starting failure probability on the system LOEE with Reservoir A .....	141
Figure 5.66: Effect of hydro unit starting failure probability on the system LOLF with Reservoir A .....	142
Figure 5.67: Effect of hydro unit starting failure probability on the AWE with Reservoir A .....	143

Figure 5.68: Effect of hydro unit starting failure probability on the AWS with Reservoir A .....	143
Figure 5.69: Effect of hydro unit starting failure probability on the AVolume with Reservoir A .....	144
Figure 5.70: Effect of hydro unit starting failure probability on the system LOLE with Reservoir B.....	145
Figure 5.71: Effect of hydro unit starting failure probability on the system LOEE with Reservoir B.....	145
Figure 5.72: Effect of hydro unit starting failure probability on the system LOLF with Reservoir B.....	145
Figure 5.73: Effect of hydro unit starting failure probability on the AWE with Reservoir B.....	146
Figure 5.74: Effect of hydro unit starting failure probability on the AWS with Reservoir B.....	146
Figure 5.75: Effect of hydro unit starting failure probability on the AVolume with Reservoir B.....	146
Figure 5.76: Effect of initial water volume in the reservoir on the system LOLE with Reservoir A.....	148
Figure 5.77: Effect of initial water volume in the reservoir on the system LOEE with Reservoir A .....	148
Figure 5.78: Effect of initial water volume in the reservoir on the system LOLF with Reservoir A .....	148
Figure 5.79: Effect of initial water volume in the reservoir on the AWE with Reservoir A .....	149
Figure 5.80: Effect of initial water volume in the reservoir on the AWS with Reservoir A .....	149
Figure 5.81: Effect of initial water volume in the reservoir on the AVolume with Reservoir A .....	150
Figure 5.82: Effect of initial water volume in the reservoir on the system LOLE with Reservoir B.....	151
Figure 5.83: Effect of initial water volume in the reservoir on the system LOEE with Reservoir B.....	151
Figure 5.84: Effect of initial water volume in the reservoir on the system LOLF with Reservoir B.....	151
Figure 5.85: Effect of initial water volume in the reservoir on the AWE with Reservoir B.....	152
Figure 5.86: Effect of initial water volume in the reservoir on the AWS with Reservoir B.....	153
Figure 5.87: Effect of initial water volume in the reservoir on the AVolume with Reservoir B.....	153

## LIST OF TABLES

Table 3.1: Mean value of water in-flow.....	63
Table 3.2: Hydro plant data.....	66
Table 4.1: Effect of wind farm location on the EWEB.....	92
Table 4.2: Effect of energy storage charging/discharging constraints on the EWEB.....	94
Table 4.3: Effect of energy storage capacity on the EWEB.....	95
Table 5.1: System configurations for the cases in Section 5.2.1.....	103
Table 5.2: Relationship between water head and reservoir volume for Reservoir A.	114
Table 5.3: Relationship between water head and reservoir volume for Reservoir B.	115
Table 5.4: Example data for wind farm and hydro plant.....	116

## **LIST OF ABBREVIATIONS**

A	Availability
AR	Auto-Regressive
ARMA	Auto-Regressive and Moving Average
AVolume	Average Volume of reservoir
AWE	Average Water used to produce Electricity
AWS	Average Water Spilled
CGU	Conventional Generation Units
COPT	Capacity Outage Probability Table
CRM	Capacity Reserve Margin
DPLVC	Daily Peak Load Variation Curve
EESW	Expected Energy Supplied by Wind
ESWE	Expected Surplus Wind Energy
EWEB	Expected Wind Energy stored in Battery
EWEU	Expected Wind Energy Utilized
FOR	Forced Outage Rate
HL	Hierarchical Levels
HL-I	Hierarchical Level-I
HL-II	Hierarchical Level-II
HL-III	Hierarchical Level-III
HT-RTS	Hydro-Thermal Reliability Test System
IEEE-RTS	IEEE Reliability Test System

km	Kilometer
LDC	Load Duration Curve
LLU	Loss of the Largest Unit
LOEE	Loss of Energy Expectation
LOLE	Loss of Load Expectation
LOLF	Loss of Load Frequency
LOLP	Loss of Load Probability
m	Meter
MCS	Monte Carlo Simulation
Mm <sup>3</sup>	Mega cubic meter
MTTF	Mean Time to Failure
MTTR	Mean Time to Repair
MW	Megawatt
NB	North Battleford
NID	Normally Independent Distribution
RBTS	Roy Billinton Test System
RPS	Renewable Portfolio Standard
SC	Swift Current
sec	Second
U	Unavailability
VRB	Vanadium Redox Battery
WECS	Wind Energy Conversion System
WTG	Wind Turbine Generator

# **1. INTRODUCTION**

## **1.1 Power System Reliability Evaluation**

The primary function of an electric power system is to supply its customers with electrical energy as economically as possible and with a reasonable degree of continuity and quality [1]. Many modern electric power systems around the world have undergone de-regulation with major changes in structure, operation and regulation. Individual parties such as, power plant owners, transmission system owners and operators, regulators, and the end customers are all involved in the complex system. The development of modern society is significantly dependent on electric supply availability. People in modern societies have difficulty appreciating how life would be without electricity. It is expected that demands for high quality, and reliable power supply will continue to increase.

The reliability associated with a power system is a measure of the overall ability of the system to satisfy the customer demand for electrical energy. Power system reliability can be further subdivided into the two different categories of system adequacy and system security [1] as shown in Figure 1.1 in order to provide a more specific meaning in power system applications.

System adequacy relates to the existence of sufficient facilities within the system to satisfy the customer demand. These facilities include those necessary to generate sufficient energy and the associated transmission and distribution networks required to transport the energy to the actual consumer load points. Adequacy is considered to be



associated with static conditions rather than system disturbances. System security, on the other hand, is considered to relate to the ability of the system to respond to disturbances arising within that system [1].

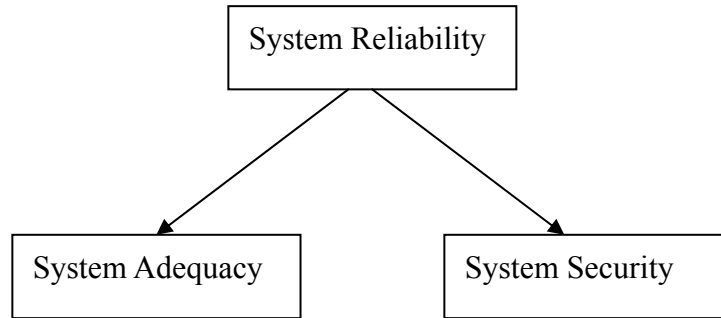


Figure 1.1: Subdivision of system reliability.

Modern electric power systems are very complex, highly integrated. It is very difficult and impractical to attempt to analyze the whole power system as a single entity in a completely realistic and exhaustive manner. The overall power system can be divided into the three main functional zones of generation, transmission, and distribution. These functional zones can be combined to create the three hierarchical levels shown in Figure 1.2.

Reliability assessment at Hierarchical Level I (HL-I) is only concerned with the generation facilities. At this level, the total system generation including interconnected assistance is examined to determine its ability to meet the total system load demand. Reliability assessment at HL-I is normally defined as generating capacity adequacy evaluation. The transmission network and the distribution facilities are not included in an assessment at the HL-I level.

Adequacy evaluation at Hierarchical Level II (HL-II) includes both the

generation and transmission facilities in an assessment of the ability of the composite system to deliver energy to the bulk load points. This analysis is usually termed as composite system reliability evaluation or bulk power system reliability evaluation. Adequacy evaluation at Hierarchical Level III (HL-III) is an overall assessment that includes all three functional segments.

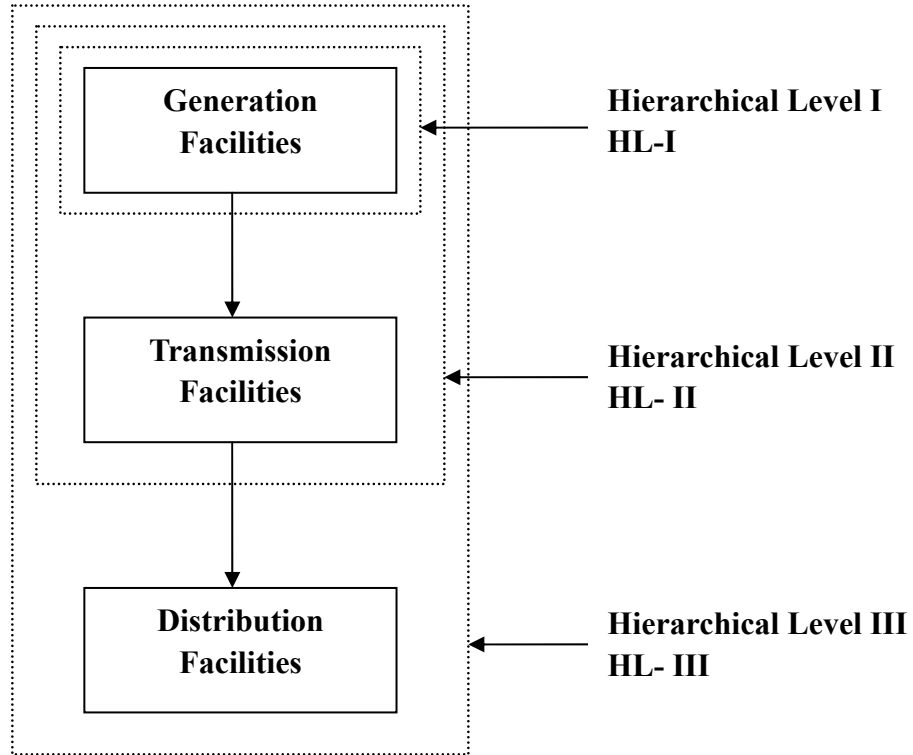


Figure 1.2: Hierarchical levels.

The research work described in this thesis is conducted at the HL-I level, and is focused on the adequacy benefits associated with incorporating wind power and energy storage facilities in a traditional power generating system.

## 1.2 Wind Energy and Power System Reliability

There has been a rapid growth of renewable energy sources in power systems

due to environmental concerns in energy generation from the conventional sources. Growing demand for electrical energy and the concerns associated with limited reserves of fossil fuels such as coal, oil, and natural gas are also responsible for the development and increase in renewable energy utilization.

Wind energy is one of the fastest growing renewable energy sources. Figure 1.3 shows the total wind capacity installed around the world from 1980 to 2008. A total of 120,791 MW of wind capacity has been installed throughout the world [2] by the year 2008. The cost of energy from wind has dropped to the point that in some sites it is nearly competitive with conventional sources. The current total installed wind capacity in Canada is 2,577 MW, which is about 1 % of Canada's total electricity demand [3]. Saskatchewan currently has 171.2 MW of installed wind capacity, with the completion of the 150 MW centennial wind project in 2006 [3].

The World Energy Council has estimated that wind energy capacity worldwide may total as high as 474,000 MW by the year 2020 [4]. In Canada, Ontario, Nova Scotia and Prince Edward Island have committed to generate 10%, 5% and 15% respectively of the total electricity production from renewable energy sources by the year 2010 [3]. Many countries around the world are implementing different policies to promote the growth of renewable energy. The Renewable Portfolio Standard (RPS) is a policy that requires those who sell electricity to have a certain percentage of renewable power in their mix [5]. In the USA, 13 states have written the RPS into state law to increase the percentage of renewable power to 10%-20% before the year 2010. Renewable energy policies, such as the Fixed Feed-in-Tariffs in Germany, Denmark, and Spain [6], and Renewable Obligation in the UK [7], have driven the development of wind power in these countries.

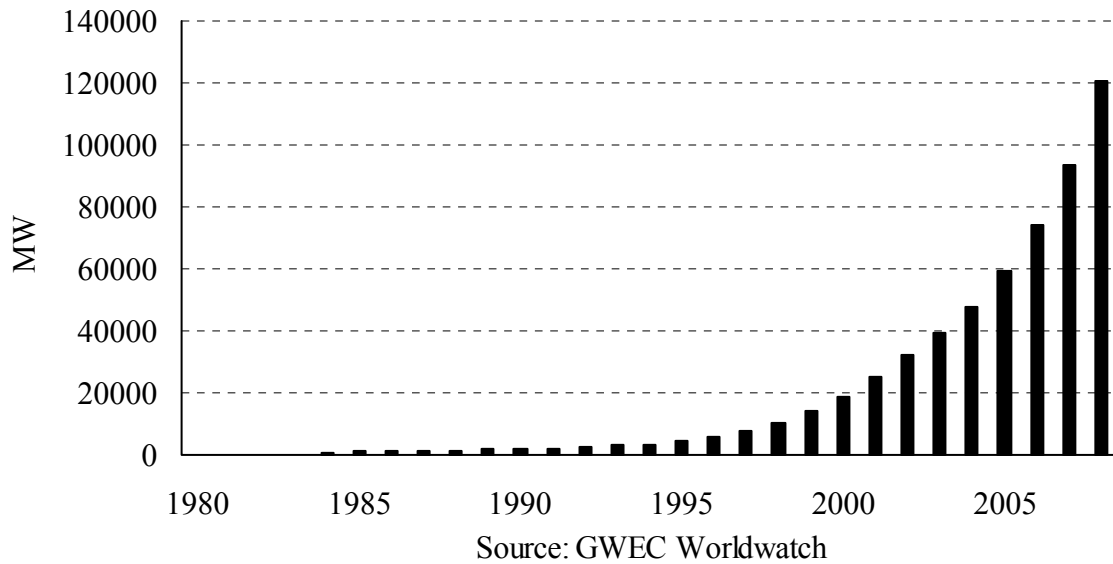


Figure 1.3: World wind electricity-generating capacity, 1980-2008.

It is important to develop comprehensive reliability evaluation techniques as wind power penetration levels in traditional power systems continue to increase. Conventional generating units (CGU) are capable of generating rated power during normal operation. Reliability evaluation techniques for these units are well established, and are routinely used in reliability evaluation and capacity planning of electric power utilities. This is not the case with wind energy sources, the power output of which fluctuate randomly with time depending on the wind variability at the wind farm site. The reliability evaluation of power systems including wind energy conversion systems (WECS) is, therefore, relatively complex.

Wind power studies require accurate models to forecast wind speed variation at the wind farm locations of interest and appropriate models for wind turbine generators (WTG). Wind speed distributions are often characterized by Weibull distributions in system evaluation using analytical methods. The methods using Weibull distributions [8] have previously been used to estimate wind speed data in wind power studies. These techniques cannot recognize the chronology in wind speed variation at a geographic

location. Historical hourly data for the wind farm site collected over a significant period of time are normally required to obtain the shaping parameters. Reference [9] presents an algorithm to simulate the hourly wind speed using a time series auto regressive and moving average (ARMA) model. The method requires actual hourly wind speed data collected over a long period of time for the particular geographic location in order to construct a wind speed simulation model for the specific site. This model can reflect the true statistic characteristics of wind speed for the wind site.

The power output characteristics of WTG are quite different from those of conventional generating units. Conventional generating units are capable of producing rated power outputs at all times except when they undergo partial or complete failures. The WTG design characteristics and the available wind speed affect the electric power output of a normally operational WTG unit. The wind speed characteristics, however, have a major impact on the power output. The relationship between the wind speed and the power output of the WTG is usually provided by the wind turbine manufacturers in the form of a non-linear graph known as the wind power curve [10].

Reliability assessment of generating systems including wind power can be performed using different techniques. Analytical methods evaluate the reliability indices using numerical solutions from mathematical models that represent the power system. Monte Carlo simulation (MCS) techniques provide a different approach to estimate the indices by simulating the actual process and random behavior of the system.

There has been considerable research activity in the area of power system reliability including wind energy in the past several years. A WTG unit has been modeled as a multi-state unit to recognize the intermittent nature of wind power in reliability evaluation of power systems including wind energy using analytical techniques in [8, 10-14]. A procedure to incorporate the WTG power curve in

determining the impact of wind generation on system reliability is presented in [10]. Reference [11] presents an algorithm to derive a probabilistic WTG model, and the application of this model to determine the annual energy output of a grid connected wind farm. Reference [12] presents a technique to obtain multi-state power output models of WTG units for reliability evaluation. Reference [13] provides a simplified wind power generation model with reasonable accuracy for reliability evaluation. This model can be used to generate the wind speed probability distributions for multiple wind sites if their annual mean and standard deviation of wind speed data are known. The simplified wind power model presented in [13] is extended to include the effect of wind power delivery system in [14]. Large wind penetrations will require large investments in wind facilities. It becomes very important to consider the capacity credit of WECS. Conventionally, wind is considered as a source of energy, but not a source of capacity. References [15] and [16] have considered the issue of calculating the capacity credit of WECS. The WECS capacity credit is approximated by the average wind power in reference [17] for relatively low wind power penetration levels.

The inherent complexities with site-specific wind variations, WTG characteristics, and their impact on the overall system performance make it very difficult to develop an accurate analytical model for WECS. MCS methods estimate the reliability indices by simulating the actual process and random behavior of the system. MCS can theoretically take into account virtually all aspects and contingencies inherent in the planning, design and operation of a power system [1]. There has been a growing interest and an increasing trend in applying MCS approaches to power system reliability analysis in the last decade due to the rapid development in high speed computation tools.

There are generally two types of MCS techniques for power system reliability evaluation. One is designated as the sequential and the other as the non-sequential approach. Sequential simulation can fully take into account the chronological behavior

of the system, while the non-sequential method involves non-chronological system state considerations. The sequential technique, therefore, provides more accurate frequency and duration assessments than the non-sequential method [18].

Chronological simulation methods for the reliability evaluation of electric power systems containing non-conventional energy sources are presented in [19-26]. ARMA models are used in conjunction with a MCS method in the reliability evaluation of power systems including wind energy in [19-24]. The sequential MCS technique can incorporate the chronological characteristics of wind, load profiles and the chronological transition states of all the components within a system. Sequential simulation can, therefore, provide realistic and more accurate results than analytical methods when considering a large number of system variables in the assessment of wind power.

### **1.3 Reliability Considerations in Generating Systems Containing Wind Power and Energy Storage**

Conventional generating units are usually quite reliable and are operated without the use of energy storage facilities. The power output from WTG can not be expected to continuously satisfy the scheduled energy demand due to the rapid fluctuations of wind speed. Large scale integration of wind power in an electric grid can produce large power fluctuations, and result in a high risk in providing a continuous power supply [27]. This risk can be reduced by storing energy and using it during low wind or no wind periods.

The value of bulk energy storage combined with operating reserve provided from conventional generation is investigated in [28]. Reference [29] presents an approximate technique for the reliability evaluation of power systems including WECS and energy storage. The relationship between the amount of energy storage and the loss of power supply probability is also investigated. A probabilistic method for the calculation of

reliability indices of a stand alone wind energy system in parallel with a storage battery is presented in [30]. A general probabilistic model of a WECS containing WTG units and battery storage is presented in [31]. In reference [31], wind speed is assumed to have a Weibull distribution, and a bi-directional flow of power in and out of the battery is considered. Reference [32] presents a technique utilizing Monte Carlo simulation for the reliability evaluation of generating systems including wind, and energy storage. This method incorporates an energy storage model appropriate for sequential simulation, and considers the chronological random nature of wind speed. There is a need to develop reliability evaluation models for energy storage considering energy storage operating constraints and the coordination between wind farm and energy storage.

#### **1.4 Power Systems including Wind and Hydro Power Generation**

System operators responsible for integrating large wind farms have concerns about the system's ability to absorb available wind energy and simultaneously maintain system reliability. The amount of wind energy that can be absorbed by an electric power system can be greatly limited if the available conventional units are not able to respond quickly to the changes created by wind power fluctuations. This problem can be better addressed if wind energy can be stored and utilized where needed. Hydro power stations with a reservoir have an ability to change their power output quickly and act as an energy storage facility to store water during high wind periods, and increase output when wind power goes down.

The coordination between wind farm and hydro power stations has been explored in [33-38]. Most researchers agree that the value of wind and hydropower can be mutually enhanced by working together to produce a stable supply of electricity [33]. A planning algorithm is presented in [34] for a multi-reservoir hydropower system coordinated with wind power. The long term economic viability of the operation of a



wind farm cooperating with two water reservoirs, involving a micro-hydroelectric power plant and a water pump station is investigated in [35]. An hourly discretized optimization algorithm to identify the optimum daily operational strategy to be followed by both wind turbines and hydro generation pumping equipment is described in [36]. Wind power is interconnected to the grid and the hydro power is used as a backup option to compensate for the wind power fluctuations in a context of a global energy balance in [37]. Economic benefits for the integrated operation of large scale wind power plants with existing hydropower plants are investigated in [38]. Little research work has investigated the reliability benefit of using wind power in conjunction with hydro plants in large power systems.

### **1.5 Research Objectives**

The rapid growth of wind power in electric power systems, and the implementation of policies that have established significantly high wind power penetration targets have led to serious concerns on the reliability of power systems. The fluctuating characteristic of WTG power output makes the utilization of energy storage important in generating systems including WECS. System operators responsible for integrating large wind farms have concerns about the system's ability to absorb available wind energy and simultaneously maintain reliability. The amount of wind energy that can be absorbed by an electric power system can be greatly limited if the available conventional units are not able to respond quickly to the changes created by wind power fluctuations. Energy storage can be used to smooth out the wind power fluctuations to maintain system stability, and also improve the continuity of power supply. Hydro power stations with a reservoir have an ability to change their power output quickly and act as an energy storage facility to store water during high wind periods, and increase output when wind power goes down.

The scope of this research work is concentrated on the development of HL-I adequacy evaluation models and techniques for generating systems including wind energy and energy storage. The main objectives described in this thesis are to investigate: (1) Reliability benefit of utilizing wind power and energy storage facilities in electric power supply. (2) Reliability impact from coordination between wind power and existed hydro power. The objectives of this research work have been completed by focusing on the following tasks:

1. Development of adequacy assessment techniques for power systems including wind power and energy storage
2. Application of wind energy and storage models
3. Modelling and development of adequacy evaluation techniques for wind hydro systems
4. Application of wind and hydro models for reliability studies

New battery technologies, such as the Vanadium Redox Battery (VRB) [39], are being considered and successfully tested for large scale on-grid applications of wind energy. It is important to investigate the possible impacts of energy storage on the reliability of relatively large systems that include significant amounts of wind power capacity. Reference [32] presents techniques and models for reliability study of small isolated power systems including wind and energy storage. An important contribution in this thesis is the extension of these techniques to include important operating constraints that exist in real life systems. The proposed methodology incorporates models to recognize the impacts of an energy storage facility and its control by different system participants. The newly developed models also include provisions to limit the wind energy dispatch to a fixed percentage of the system load in order to consider system operating constraints when the wind power penetration level is relatively high.

The illustration of important results from the application of the proposed energy storage model in adequacy evaluation of a generating system considering wind power and energy storage is another useful contribution in this thesis. The method used to operate the energy storage facility may have significant impacts on the system reliability and on the efficiency of wind energy utilization in a power system. Different operating strategies for wind farm and energy storage are proposed and compared by evaluating the reliability benefit from energy storage and the amount of wind energy that can be stored. Acceptable wind farm and energy storage operation strategies suitable for system operators and wind farm owners are illustrated, and valuable information is provided for power system reliability evaluation, planning, and decision making. The energy storage model development and application for capacity adequacy evaluation of generating systems containing wind power is the basic objective of this research.

Wind farms with large installed capacities will continue to be connected to major power systems in the near future. As wind is an intermittently changing energy source, grid connected conventional generation can largely guarantee a backup energy source in situations where wind availability is insufficient. However, at high wind penetration, the reliability of the overall system is greatly affected and generation facilities with energy storage capability can be very useful in maintaining the necessary level of system reliability. Hydro power can be combined with wind energy and properly operated to smooth out wind power fluctuations. An important objective of the research described in this thesis is to develop appropriate models and techniques for reliability evaluation of power systems containing wind power in coordination with hydro power.

Reference [40] presents a hydropower model to evaluate the reliability of a hydro-thermal reliability test system (HT-RTS) obtained by modifying the IEEE-RTS [41] in which six 50 MW generating units are considered as hydro units sharing a common reservoir. A major contribution in this thesis is the modification of the hydro

models and development of new models to incorporate wind power for quantitative assessment of reliability and renewable resource utilization in a power system. A methodology for an energy limited hydro plant and wind farm coordination is developed in the work described in this thesis using a Monte Carlo simulation technique considering the chronological variation in the wind, water and the energy demand. The IEEE four-state model [42] is widely used in estimating unavailability parameters for peaking units. An important contribution in this thesis is the application of the four-state model to represent intermittently operated hydro units, which are used for peaking and for wind power coordination, in a sequential simulation to incorporate the chronological impact of wind/hydro coordination and reservoir energy considerations. The proposed model for hydro units is used to examine the actual reliability benefit from WTG units coordinated with energy-limited hydro units. The impact on the overall system adequacy of different factors, such as the number of hydro units coordinated with wind power, wind penetration level, wind farm geographical location, system load level, wind-hydro coordination strategy, water in-flow and reservoir volume, etc are investigated in this research work.

## **1.6 Outline of the Thesis**

Appropriate models and techniques required to conduct reliability evaluation of electric power systems containing wind power and different types of energy storage facilities are established in this thesis. A wide range of case studies are presented to illustrate the application of the proposed models and methodologies in practical system analyses. The contributions of this research work are presented in this thesis in six chapters. An overview of the contents in each chapter is presented below.

Chapter 1 introduces the basic concepts of power system reliability evaluation. The application of wind power in modern electric power systems, and the basic methods

used in power system reliability assessment are briefly introduced. The emergence of potential power system reliability problems with the increase in wind power penetration is highlighted. A brief review of the available literature on reliability assessment of power systems containing wind power and energy storage is presented. This chapter also outlines the objectives and scope of the thesis.

Chapter 2 reviews the basic reliability concepts and techniques for generating system adequacy evaluation. Basic generation models, load models and risk models for probabilistic methods are introduced. Direct analytical techniques and Monte Carlo simulation methods widely used in probabilistic power system reliability evaluation are introduced in this chapter.

Chapter 3 presents the mathematical models required for the adequacy evaluation of generating systems including wind energy and energy storage using the sequential Monte Carlo simulation method. The wind speed model and WTG power generation model are presented at the beginning of the chapter. A time series energy storage model considering its charging/discharging characteristics is then developed and presented. Models to represent hydro power plants are introduced and integrated in the simulation process developed for reliability evaluation of generating systems considering the coordination between wind power and energy limited hydro units. The system reliability indices, energy storage related indices and hydro utilization related indices are also presented in this chapter.

Chapter 4 describes the proposed model for energy storage and its application to a test system. Possible strategies for wind farm operation and energy storage are presented and compared by evaluating the reliability benefit from energy storage and the amount of wind energy that can be stored. A wide range of studies considering variations in key factors, such as wind farm location, wind penetration level, energy storage

capacity, energy storage operating constraints, and wind energy dispatch restrictions are conducted. Operating strategies useful to system operators and wind farm owners are presented, and the benefits from their applications are illustrated.

Chapter 5 presents the application of the adequacy evaluation technique developed considering the coordinated operation of wind power and hydro power. The studies conducted to investigate the impact of energy limited hydro units and the wind power dispatch restrictions on system adequacy are presented at the beginning of the chapter. A wide range of sensitivity studies are also conducted to assess the reliability benefit from the coordination between wind power and hydro units. Important parameters that affect the system adequacy, such as the number of hydro units coordinated with wind power output, water inflow and reservoir volume, system load level, wind power penetration level, wind-hydro coordination strategy, starting failure of hydro units, and initial water volume in the reservoir are examined in this chapter.

Finally, Chapter 6 summarizes the thesis and highlights the conclusions.

## 2. BASIC CONCEPTS AND TECHNIQUES FOR GENERATING SYSTEM ADEQUACY ASSESSMENT

### 2.1 Introduction

The primary concern in adequacy evaluation at the HL-I level is to assess the capacity of the generating facilities to satisfy the total system load demand. In an HL-I adequacy study, the reliability of the transmission system and its ability to deliver the generated energy to the customer load point are normally not considered. The calculated indices reflect the ability of the generating facilities to meet the system load requirement. The basic system representation in an HL-I study is shown in Figure 2.1 [1], where the total generation system and total system load are directly connected.

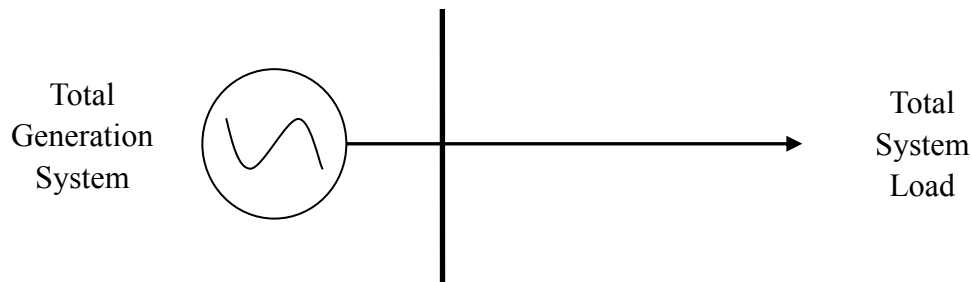


Figure 2.1: System model for HL- I adequacy evaluation.

The basic task in an HL-I adequacy evaluation is to determine the required generating capacity to satisfy the load requirements considering the uncertainty in load variation, generating unit failures and repairs, and allowing for periodic maintenance. The generating capacity in excess of the peak demand, called the capacity reserve, is required to ensure against excessive load curtailment situations. An extremely high

reserve can provide a very high level of system reliability, but at a very high investment cost. On the other hand, a low reserve, although cheaper, may not provide acceptable system reliability. Different techniques are used by electric power utilities to estimate the appropriate reserve required to maintain an acceptable level of system reliability. The two main reliability methods are the deterministic and the probabilistic methods.

The earliest techniques used to determine the required level of capacity reserve were deterministic methods. The common deterministic approaches [43] include:

(1) Capacity Reserve Margin (CRM)

The capacity reserve margin is the excess generation capacity over the peak system demand. A reserve margin equal to a fixed percentage of the total installed capacity is required in this approach to avoid load loss due to the uncertainty with the load growth, or generating unit failures. The percentage value is chosen based on past experience. This method is easy to understand and apply.

(2) Loss of the Largest Unit (LLU)

A capacity reserve equal to the capacity of the largest unit is required in this approach. This is also known as the “n-1” method, and it attempts to maintain supply continuity in the event of an outage of any generating unit in the system.

(3) Loss of the Largest Unit and a Percent Margin

A combination of the above two methods have also been used in the past. The required capacity reserve is equal to the capacity of the largest unit plus a fixed percentage of either the peak load or the total installed capacity.

Deterministic methods estimate the system adequacy largely on the basis of past experience and personal judgment, and do not recognize the inherent random nature of



generating unit failures and the uncertainty in load variations. Therefore, a deterministic approach is unable to recognize and reflect the actual system risk. Probabilistic methods, on the other hand, are capable of recognizing the inherent risk in component failures and load variations. There has been a shift from deterministic methods to probabilistic methods in adequacy evaluation of power systems for capacity planning.

The appropriate system models in probabilistic methods include generation models, load models, and the risk model, and are first introduced in this chapter. The detailed methodologies for different types of probabilistic methods are then presented.

## **2.2 System Modeling in Probabilistic Methods**

The need and benefits of utilizing probabilistic methods have been recognized since the 1930s. However, the lack of relevant data, lack of realistic reliability techniques, limitations of computational resources and misunderstanding of the significance of probabilistic criteria and risk indices have limited the application of such methods in the past [1]. None of these reasons are valid today and, therefore, most modern large power utilities use probabilistic methods in generating capacity adequacy assessment [43].

The basic approach used in the probabilistic adequacy evaluation of an electric power generating system consists of three main parts which are shown in Figure 2.2 [1]. The generation and load models shown in Figure 2.2 are combined to form the risk model. Adequacy evaluation, therefore, consists of the following three steps: (1) Build a generation model based on the operating characteristics of all the generating units in the system. (2) Construct an appropriate load model. (3) Obtain a risk model by combining the generation model with the load model. Appropriate risk indices can be utilized in the risk model to provide a quantitative measure of system reliability. The three models are

described in the following sub-sections.

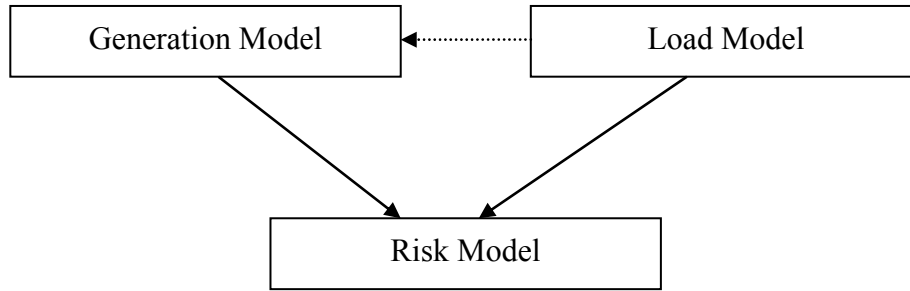


Figure 2.2: Conceptual tasks in generating capacity reliability evaluation.

### 2.2.1 Generation Model

A generating unit in a power system can be represented by a two-state or a multi-state Markov model. A two-state model represents a generating unit that can reside either in the fully functional state, or in the forced out of service state, as shown in Figure 2.3. The generating unit transits between the two states, and the transition rates  $\lambda$  and  $\mu$  are shown in Figure 2.3. Here  $\lambda$  is the failure rate and  $\mu$  is the repair rate of the generating unit. The mean time to failure (MTTF) is the average time a unit spends in the “Up” state. The failure rate  $\lambda$  is equal to the reciprocal of the MTTF, and can be calculated for a generating unit using (2.1). The mean time to repair (MTTR) is the average time taken to repair a unit. The repair rate  $\mu$  is equal to the reciprocal of the MTTR, and can be calculated for a generating unit using (2.2).

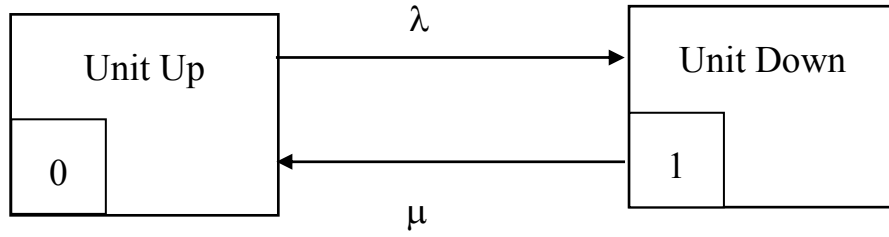


Figure 2.3: Two-state model for a generating unit.

$$\lambda = \frac{1}{MTTF} = \frac{\text{number of failures of a component in the given period of time}}{\text{total period of time the component was operating}} \quad (2.1)$$

$$\mu = \frac{1}{MTTR} = \frac{\text{number of repairs of a component in the given period of time}}{\text{total period of time the component was being repaired}} \quad (2.2)$$

The probability of finding a unit on forced outage at some distant time in the future is known as the unavailability (U). This term is conventionally known as the generating unit forced outage rate (FOR), and is a key reliability parameter in power system reliability studies [1]. Equation (2.3) can be used to obtain the unavailability or the FOR of a generating unit if the unit failure rate  $\lambda$  and the repair rate  $\mu$  are known. Similarly, the availability (A) of the generating unit can be obtained using (2.4). Equations (2.3) and (2.4) are obtained from the two-state Markov model shown in Figure 2.3. The generating unit FOR is usually calculated from the unit operational data using (2.5) [1].

$$U = \frac{\lambda}{\lambda + \mu} \quad (2.3)$$

$$A = 1 - U = \frac{\mu}{\lambda + \mu} \quad (2.4)$$

$$FOR = \frac{\sum[down\_time]}{\sum[down\_time] + \sum[up\_time]} \quad (2.5)$$

A generating unit can reside in a number of other derated states where it operates with a reduced capacity in addition to being in the fully rated and failed states. The simplest model that incorporates derating is shown in Figure 2.4. Figure 2.4 shows a three-state Markov model with a single derated state in addition to the fully available state and the totally failed state.

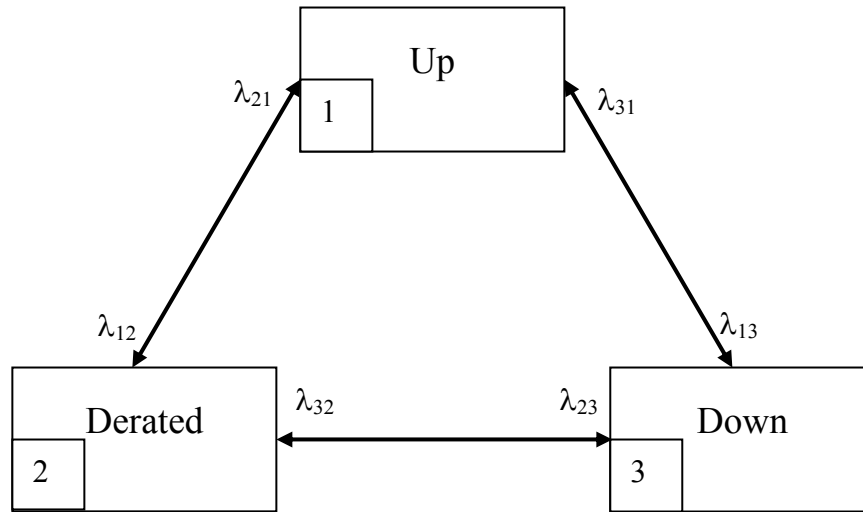
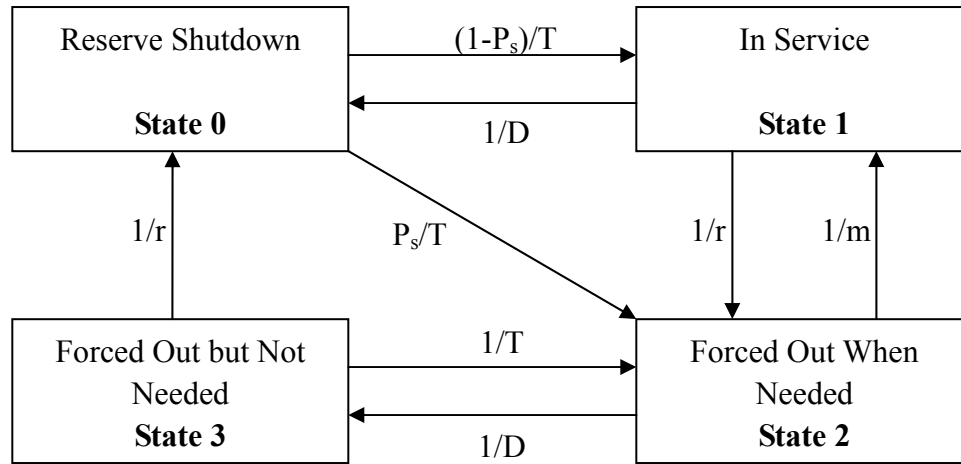


Figure 2.4: Three-state model for a generating unit.

Base loaded units have relatively long operating cycles, and the conventional two-state model in Figure 2.3 or three-state model in Figure 2.4 is a good representation for them. Peak loaded units operate for relatively short periods since they are frequently started and stopped due to economy shutdowns. The IEEE Subcommittee on the Application of Probability Methods proposed a four-state model for peaking units [42].

This model includes the reserve shutdown and forced out but not needed states, and is shown in Figure 2.5. Hydro units in power systems have the ability to be started quickly and provide rated power output, and therefore, are often used as peaking units. The four-state model shown in Figure 2.5 is a good representation for hydro units if they are used as peaking units, or are started and stopped frequently in response to system conditions, and operating constraints.



$m$  = Mean time to failure (MTTF)

$r$  = Mean time to repair (MTTR)

$T$  = Average reserve shutdown time between periods of need

$D$  = Average in service time per occasion of demand

$P_s$  = Probability of starting failure

Figure 2.5: IEEE 4-state model for a peaking unit.

### 2.2.2 Load Model

There are different types of load models that can be used to represent the system energy demand over a specific period of time. The simplest load model is to use a fixed

load for the entire period under study, and in these situations the system peak load is usually taken as the fixed load.

The daily peak load variation curve (DPLVC) and the load duration curve (LDC) are widely used load models in adequacy evaluation of generation systems. The DPLVC is created by arranging the individual daily peak load data, usually collected over a period of one year, in descending order. The LDC is created when the individual hourly peak loads are used, and in this case the area under the curve represents the total energy demand for the system in the given period [1]. The LDC provides a more complete representation of the actual system load demand than the DPLVC. A sample load duration curve is shown in Figure 2.6.

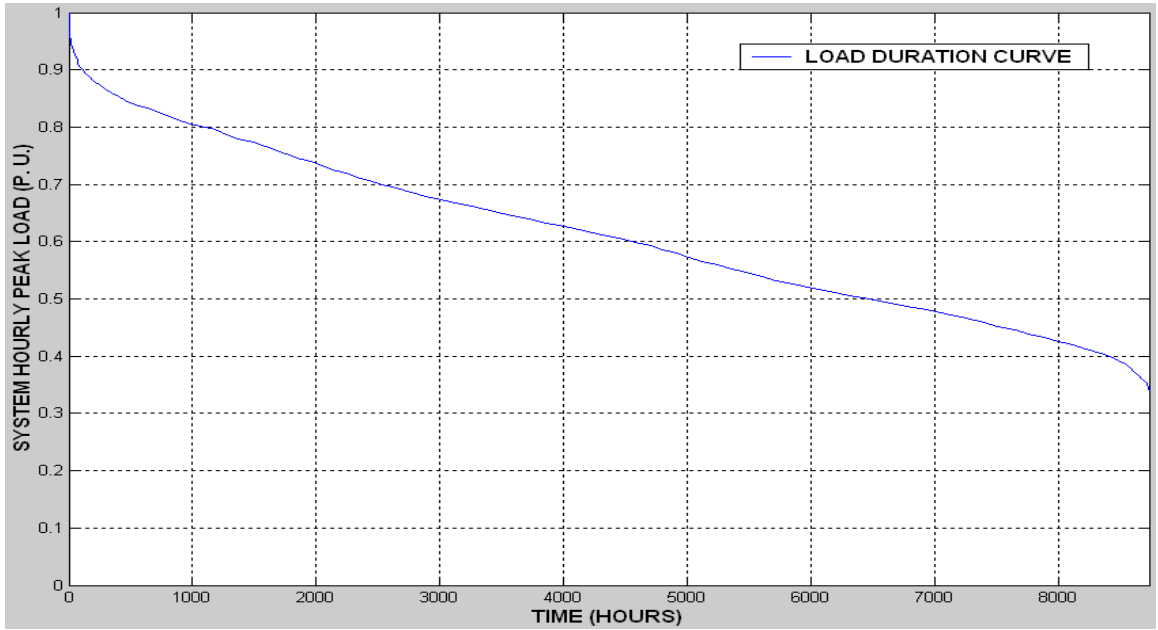


Figure 2.6: A sample load duration curve.

The IEEE-RTS is a published test system that is widely used in reliability studies. The hourly load data for this system is provided in Appendix A. A chronological load

model can be obtained from the available hourly data. The load  $L(t)$  for hour  $t$  can be determined applying (2.6).

$$L(t) = L_y \times P_w \times P_d \times P_h(t) \quad (2.6)$$

In equation (2.6),  $L_y$  is the annual peak load,  $P_w$  is the percentage of weekly load in terms of the annual peak,  $P_d$  is the percentage of daily load in terms of the weekly peak load and  $P_h(t)$  is the percentage of hourly load in terms of the daily peak. Once the annual peak load, weekly percentage, daily percentage and 24-hour load profile are determined, the annual hourly load model can be developed from (2.6). Figure 2.7 shows the chronological hourly load model for the IEEE-RTS which has an annual peak load of 2850 MW. The y-axis of Figure 2.7 can also be represented in per unit of the annual peak load, and the resulting load model is often used in studies considering different peak load scenarios. This load model has been used in all the simulation analyses in this thesis.

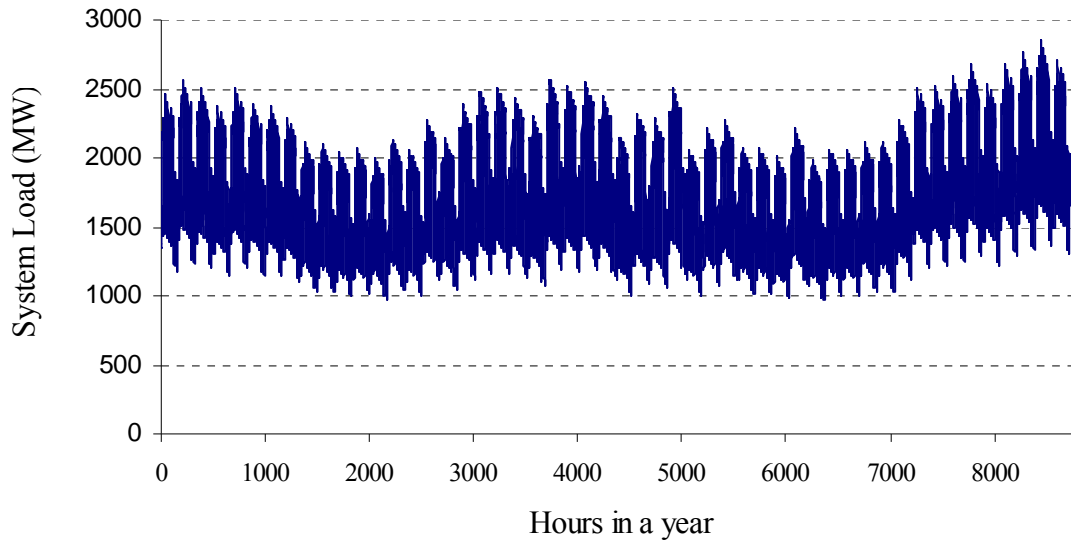


Figure 2.7: Chronological hourly load model for the IEEE-RTS.

### **2.2.3 System Risk Model**

The system risk model is obtained by combining the generation model with the load model. The risk model thus obtained can provide the system risk indices, such as loss of load expectation (LOLE) and loss of energy expectation (LOEE). The LOLE and LOEE are the most widely used adequacy indices. The LOLE is the expected number of hours or days in a year that the total system generation will not be able to satisfy the system demand. The LOEE is the expected energy that will not be supplied by the generating system due to those occasions when the load demand exceeds the available capacity.

## **2.3 Probabilistic Adequacy Evaluation Methods**

There are generally two fundamental approaches used to calculate the risk indices in a probabilistic evaluation, the analytical method and the simulation method commonly known as Monte Carlo Simulation (MCS) [1]. Analytical techniques use mathematical and statistical models to represent the system elements. The system risk indices are obtained by solving mathematical models. Monte Carlo Simulation, on the other hand, simulates the actual process and the random behavior of the system. The reliability indices are obtained by observing the simulated operating history of the system. There are both advantages and disadvantages in each approach. The selection of the proper approach should be based on the desired type of evaluation and the particular system problems.

### **2.3.1 Analytical Techniques**

Analytical assessment of generating capacity adequacy can provide information



on the likelihood that the generation will be unable to serve the system load. The basic generation model in an analytical technique is a capacity outage probability table (COPT). The COPT is arranged in the form of an array of capacity levels and their associated probabilities of existence. A recursive technique can be utilized to construct the COPT by adding a two-state or a multi-state generating unit in the COPT one at a time in a loop process until all the units in the system have been considered.

A generating unit with a capacity of C MW is considered to be either fully available (Up) or totally out of service state (Down) in a two-state model as shown in Figure 2.3. The cumulative probability of a capacity outage state of X MW, after adding the unit with a FOR of U, is given by (2.7).

$$P(X) = (1 - U)P'(X) + (U)P'(X - C) \quad (2.7)$$

where,  $P'(X)$  and  $P(X)$  denote the cumulative probabilities of a capacity outage level of X MW before and after the unit of capacity C is added respectively. Equation (2.7) is initialized by setting  $P'(X) = 1.0$  for  $X \leq 0$  and  $P'(X) = 0$  otherwise [1].

If a generating system contains generating units with derated states as shown in Figure 2.4, a recursive technique using (2.8) can be used to construct the COPT. (2.8) reduces to (2.7) when the number of unit states n is equal to 2.

$$P(X) = \sum_{i=1}^n p_i P'(X - C_i) \quad (2.8)$$

where,

n = the number of unit states,

$C_i$  = capacity of the outage state  $i$  for the unit being added,  
 $p_i$  = probability of existence of the unit state  $i$ .

The COPT can be combined with the appropriate load model, such as the DPLVC or the LDC, to calculate the system LOLE which is the expected number of days or hours in the period that the load exceeds the available generation capacity. Figure 2.8 shows the method of combining the different system capacity states in a generation model with the DPLVC load model.

It can be seen from Figure 2.8 that a capacity outage  $O_k$  will result in a loss of load condition for a time duration  $t_k$ . This outage condition will contribute to the system LOLE by an amount equal to the product of the probability of the existence of the outage  $p_k$  and the corresponding time  $t_k$ , i.e.  $p_k \times t_k$ . Any capacity outages less than the reserve do not contribute to the system LOLE. Equation (2.9) mathematically expresses the system LOLE for a specified period of interest.

$$LOLE = \sum_{k=1}^n p_k \times t_k \quad (2.9)$$

where,

$n$  = the number of capacity outage states in the COPT,

$p_k$  = probability of the existence of the capacity outage  $O_k$ ,

$t_k$  = the time for which loss of load will occur due to the outage  $O_k$ .

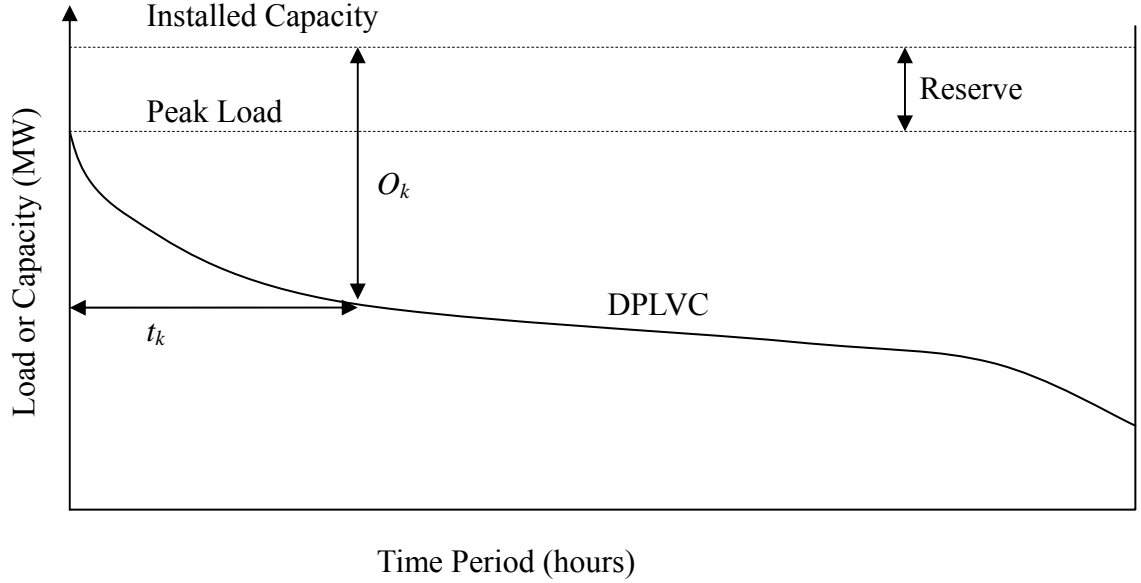


Figure 2.8: Loss of load method.

The  $p_k$  values in (2.9) are the individual probabilities of the corresponding capacity outage states and can be obtained from the COPT. If the cumulative probabilities are used, (2.9) should be modified as shown in (2.10).

$$LOLE = \sum_{k=1}^n P_k \times (t_k - t_{k-1}) \quad (2.10)$$

where,  $P_k$  = the cumulative outage probability for capacity outage  $O_k$ .

LOLE is measured in days per year if the load characteristic in Figure 2.8 is the DPLVC for a period of one year. If a LDC is used, the LOLE is in hours per year. If the time  $t_k$  is a per unit value of the total period considered, the index calculated by (2.9) or (2.10) is called the Loss of Load Probability (LOLP).

The area under the LDC is the total system energy demand. The energy based risk indices can be obtained if the COPT is combined with the LDC load model. The

loss of energy indices obtained using this approach are the LOEE or its normalized values. Figure 2.9 shows that any outage of generating capacity which exceeds the reserve can result in a curtailment of the system load. The energy curtailment is given by the shaded area in Figure 2.9.

If  $O_k$  is the magnitude of the capacity outage,  $p_k$  is the probability of the capacity outage, and  $E_k$  is the energy curtailment by the outage  $O_k$ , the total expected energy curtailment or LOEE can be calculated using (2.11).

$$LOEE = \sum_{k=1}^n p_k \times E_k \quad (2.11)$$

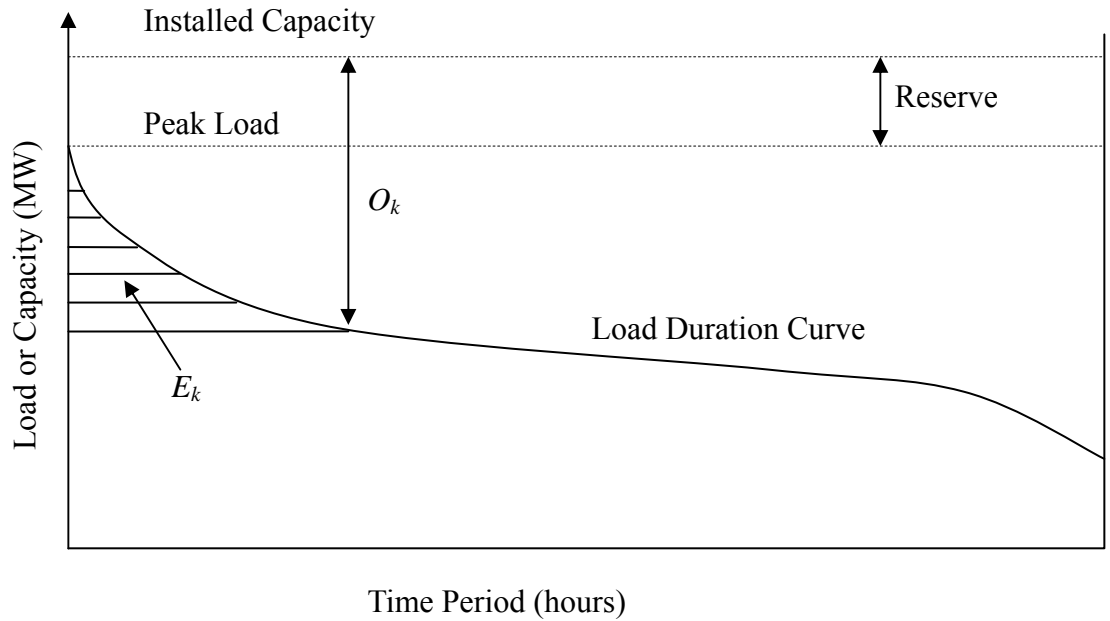


Figure 2.9: Loss of energy method.

Other analytical evaluation techniques include the load modification method and the frequency and duration approach. The load modification method is based on the

concept of determining the equivalent load model seen by the remaining units when each unit is placed sequentially in service. If the generating system is energy limited, such as a hydro plant with limited storage, the process includes the modification of the equivalent load model by the generating unit based on the energy limitations [44]. The frequency and duration method uses Markov models to represent the generating units and the system load. Additional data such as the generating unit and load state transition rates are required for the frequency and duration calculations. The basic concepts for this method are presented in [45], and its detailed application in adequacy evaluation can be found in [1].

The system under study is represented by a mathematical model in an analytical method. Once the mathematical model is derived, these methods are usually simple to apply and the results are easily reproduced. The mathematical models representing practical systems are often simplified as power systems in real life are very complex. The system model in an analytical approach can be over simplified if the system includes highly variable energy sources such as wind power and energy limited hydro power, and the coordination of different types of energy sources to satisfy the varying load. The results thus obtained can be inaccurate. The MCS methods are more appropriate in the evaluation of these types of complex systems.

### **2.3.2 Monte Carlo Simulation Method**

The primary task of this thesis is to develop generating capacity adequacy evaluation models and methods for systems containing wind power and energy storage. The analytical techniques presented in previous section have been well developed for power systems with conventional generating units. The analytical techniques can not easily consider the chronology of the random events, and the correlation between the load, the wind power and the storage charging/discharging condition, which are

important in reliability assessment. Stochastic simulation, on the other hand, is a practical technique for systems that contain a large number of time dependent random variables.

The main disadvantage of the simulation methods is that the computation time involved in the simulation is usually extensive. The rapid development of computer technology has made this much less of a problem in recent years.

Stochastic simulation methods used in power system reliability evaluation are commonly known as Monte Carlo simulation. They can be broadly classified into one of two categories, namely state sampling and sequential methods [18].

#### **2.3.2.1 State Sampling Method**

The state sampling method uses random selection of time intervals to simulate the system operation. In each simulation interval, the status of each generating unit can be described by a uniform distribution between  $[0, 1]$ , and the system available capacity can be obtained by summing the individual capacity of each available generating unit. Another uniform random number is generated to determine the system load level using the DPLVC or LDC. The total available system capacity is compared with the system load to determine the occurrence of a loss of load situation. The simulation process continues until a specified stopping rule indicates that the simulation has successfully converged.

The simulation process does not move chronologically in the non-sequential state sampling method, and the system behavior at each time interval is considered to be independent. The proper adoption of a non-sequential or sequential approach depends on whether one basic interval has an effect on the next interval, and whether the effect has

an impact on the reliability indices being evaluated.

It is important to recognize the chronology of events when evaluating a power system that includes non-conventional generation such as wind power and energy storage facilities, which are time dependent and correlated. The state sampling method is, therefore, not suitable for the evaluation of these types of system. The sequential simulation approach that recognizes the chronology of events in time is therefore used in the research described in this thesis.

### **2.3.2.2 Sequential Monte Carlo Simulation Method**

The sequential MCS approach simulates the basic intervals in chronological or sequential order, recognizing the fact that the system state in a give time interval is correlated with that in the previous and the following time intervals. In this approach, the system capacity model is the available generating capacity obtained by combining the operating history of each generating unit. Uniform random numbers generated by a random number generator are utilized to simulate the operating states and their durations for each generating unit in the system. The system capacity model is then superimposed on the chronological load model to form the system risk model.

The main parameters used to create an operational history for each individual unit are usually the generating unit MTTF and MTTR [1]. These parameters can be used in conjunction with random numbers between  $[0, 1]$  to produce a state history consisting of a series of random up and down times called state residence times for each generating unit in the system. The state residence time is sampled from its probability distribution. In this thesis, the relevant distributions are assumed to be exponential. The operating history of a generating unit modeled as a two-state unit is shown in Figure 2.10.

If the state residence time is represented by an exponentially distributed random variable  $t$ , the corresponding probability density function is given by (2.12) [18],

$$f(t) = xe^{-xt} \quad (2.12)$$

where  $x$  is the reciprocal of the mean value of the distribution. The cumulative probability distribution function is given by (2.13).

$$F(t) = 1 - e^{-xt} \quad (2.13)$$

The inverse transform method [18] is utilized and the random variable  $t$  can be obtained using (2.14).

$$t = -\frac{1}{x} \ln(1 - u) \quad (2.14)$$

where  $u$  is a uniformly distributed random number between  $[0, 1]$ . Since  $1-u$  is distributed uniformly in the same way as  $u$  in the interval  $[0, 1]$ , the random variable  $t$  can be obtained using (2.15).

$$t = -\frac{1}{x} \ln(u) \quad (2.15)$$

The variable  $x$  in (2.15) is the failure rate ( $\lambda$ ) of the generating unit when it is in the up state, and the repair rate ( $\mu$ ) in the down state when the two-state model shown in Figure 2.3 is considered.



The basic overall sequential simulation methodology for reliability evaluation of generating systems can be briefly described in the following five steps:

Step 1: Specify the initial state of each generating unit. Generally, it is assumed that all units are initially in the success or the “up” state.

Step 2: Generate the operating history for each generating unit. The operating history of each unit is in the form of chronological up-down-up operating cycles. The duration in each state is calculated using (2.15). This step is illustrated in Figure 2.10.

Step 3: Obtain the system available capacity by combining the operating cycles of all the generating units in the system. The chronological state transition processes for a sample generating system with two units are shown in Figure 2.11.

Step 4: Superimpose the system available capacity obtained in Step 3 on the chronological load model to construct the system available margin model. This step is illustrated in Figure 2.12.

Step 5: Estimate the desired reliability indices by observing the margin model constructed in Step 4 over a long time period.

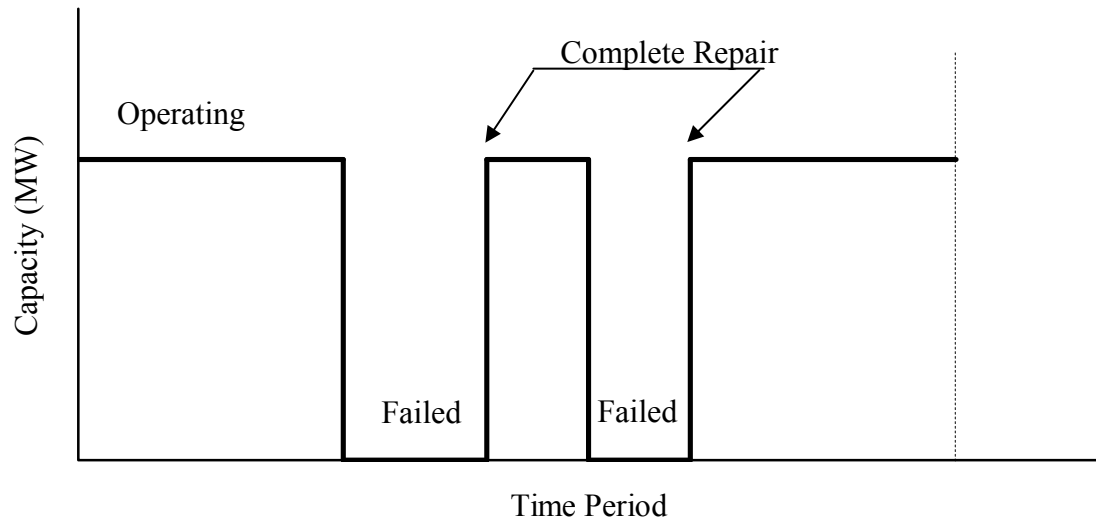


Figure 2.10: Operating history of a conventional generating unit.

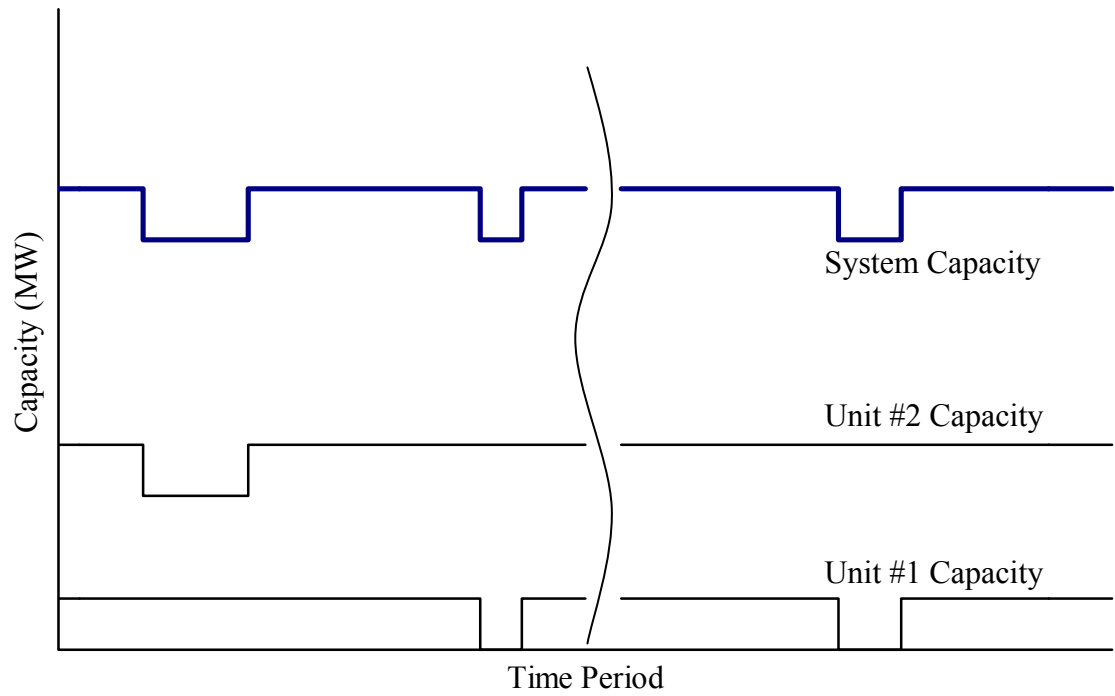


Figure 2.11: Operating history of individual generating units and the capacity states of an entire system.

The load model in sequential MCS is usually a chronological hourly load model, which is shown in Figure 2.7. The load is usually modeled in one hour time steps, although smaller steps can be used. The desired adequacy indices can be determined from the risk model obtained by superimposing the generation model on the load models as shown in Figure 2.12. This model provides the chronological variation of the system reserve margin. The available margin at a specific point in time is the difference between the available capacity and the load at that instance. A negative margin indicates that an outage has occurred.

Normally the time reference in a sequential Monte Carlo simulation is a year, and most indices are therefore annual indices. The total number of load curtailments, the loss of load duration and the energy not supplied at each load curtailment are recorded during the simulation. This is illustrated in Figure 2.12. The LOLE, LOEE and the LOLF can then be calculated using (2.16 – 2.18).

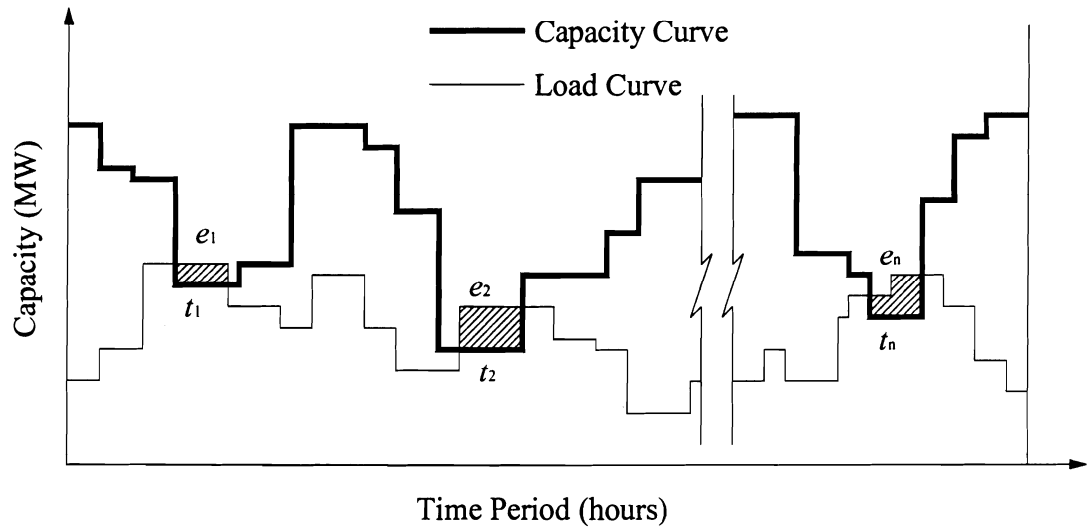


Figure 2.12: Superimposition of capacity states and the chronological load model.

Estimates of the reliability indices for a number of sample years ( $N$ ) can be obtained using the following equations.

(1) Loss of load expectation (hours/year)

$$LOLE = \frac{1}{N} \sum_{i=1}^n t_i \quad (2.16)$$

where:

$t_i$  = loss of load duration in load curtailment  $i$ .

$N$  = total number of simulated years.

$n$  = number of load curtailments.

(2) Loss of energy expectation (MWh/year)

$$LOEE = \frac{1}{N} \sum_{i=1}^n e_i \quad (2.17)$$

where

$e_i$  = energy not supplied in load curtailment  $i$ .

(3) Loss of load frequency (Occs/year)

$$LOLF = \frac{n}{N} \quad (2.18)$$

The LOLE, LOEE, and LOLF indices provide an overall indication of the ability of the generating system to satisfy the total system load. Other indices [18], such as the expected duration of interruptions and the expected loss of energy of interruptions, can

also be calculated if required.

### 2.3.2.3 Simulation Convergence

MCS is a fluctuating convergence process. As the simulation continues, the estimated indices will approach their “real” values. The simulation should be terminated when the estimated reliability indices obtain a specified degree of confidence. The objective of a stopping rule or a convergence criterion is to provide a compromise between the accuracy and the computation time [18].

The coefficient of variation is generally used as the convergence criterion in MCS. The coefficient of variation of an index is defined as

$$\alpha = \sigma / E(x) \quad (2.19)$$

where  $E(x)$  is the estimated expected value of the index, and  $\sigma$  is the standard deviation of the estimated expectation. The mathematical expressions for  $E(x)$  and  $\sigma$  are shown in (2.20) and (2.21).

$$E(x) = \frac{1}{N} \sum_{i=1}^N x_i \quad (2.20)$$

$$\sigma(E(x)) = \left[ \frac{1}{N(N-1)} \sum_{i=1}^N (x_i - E(x))^2 \right]^{\frac{1}{2}} \quad (2.21)$$

where,

$x_i$  = observed value of  $x$  in year  $i$ .

$N$ = total number of simulated years.

The stopping rule applied in the studies presented in this thesis uses the coefficient of variation of the LOEE index. The simulation pauses at a specified number of sample years, and the coefficient of variation  $\alpha$  is checked to see it is within the acceptable tolerance. The simulation process is terminated when  $\alpha < \epsilon$ , where  $\epsilon$  is the maximum error allowed.

Not all indices converge at the same rate. A number of studies [18] indicate that the coefficient of variation for the LOEE index has the lowest convergence speed compared to other indices, and therefore, is taken as the base index to check for convergence in this study. Figure 2.13 shows the convergence process of the LOEE index for the IEEE-RTS.

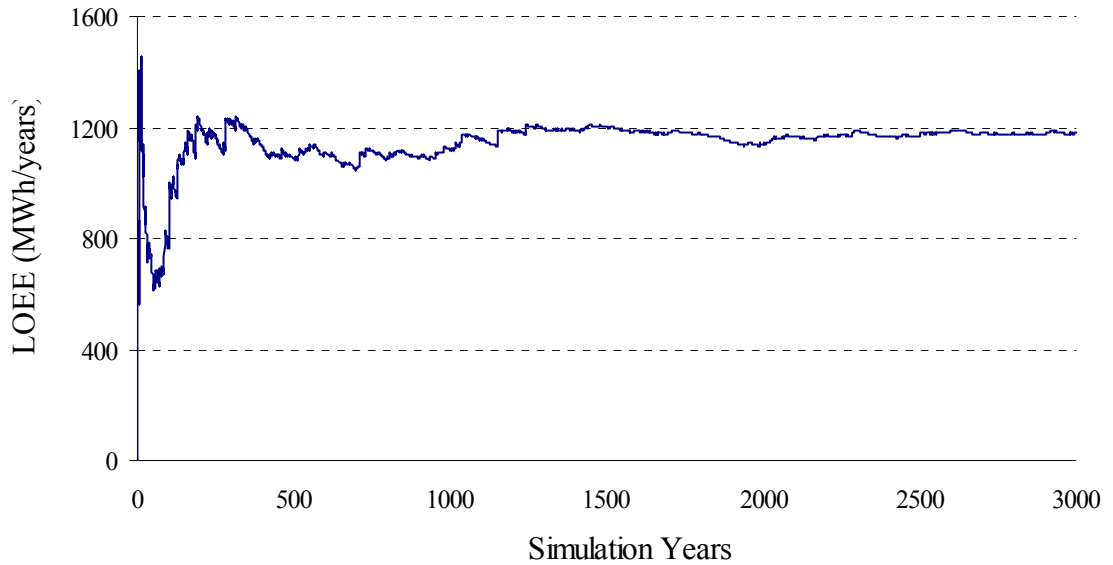


Figure 2.13: Convergence of the LOEE.

Figure 2.13 shows that the system LOEE index greatly fluctuates at the beginning of the simulation, and becomes more stable as the number of simulated yearly

samples is increased.

A random number generator requires an initial seed. The effect of the initial seed on the convergence of the reliability index LOEE is shown in Figure 2.14. It is shown in Figure 2.14 that the fluctuations in the results generated by different random number seeds can eventually stabilize at different values. A good seed can drive the simulation to converge quickly at the correct value, and a bad seed can lead to non-convergence. In this thesis, simulation results using different initial seeds are compared with the standard analytical results for conventional systems such as the RBTS [46] and the IEEE-RTS. In this way, a suitable seed is chosen for the simulation studies presented later in this thesis.

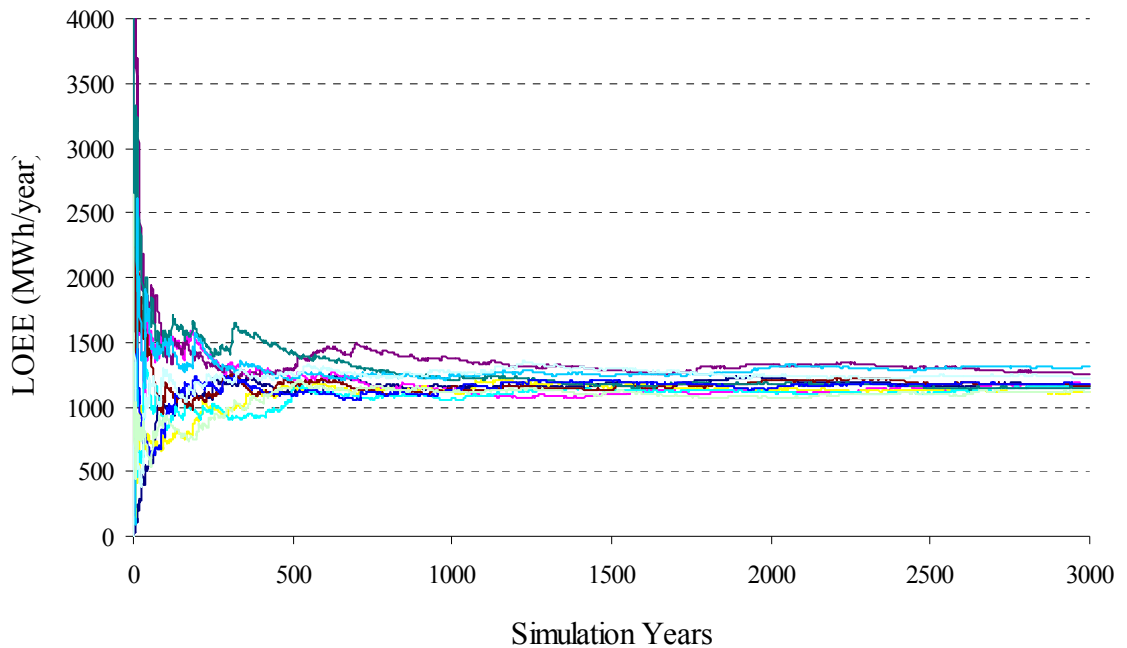


Figure 2.14: Convergence with different initial seeds.

## 2.4 Summary

The basic models and techniques for generating system adequacy evaluation are

briefly described in this chapter.

There are two broad categories of adequacy evaluation methods used in power system planning: the deterministic methods and the probabilistic methods. Although deterministic methods are easy to apply, they cannot recognize the random system behavior, and therefore, cannot provide a consistent measure of system risk. Probabilistic methods have therefore replaced deterministic methods in adequacy evaluation at the HL-I level. There are a large number of random variables and uncertainties associated with wind power and energy storage, and probabilistic methods are required for adequacy evaluation of these types of system.

The different generation models, load models and risk models that are used in basic probabilistic methods for HL-I adequacy evaluation are described. Probabilistic methods include direct analytical techniques and MCS techniques. The evaluation methodologies for both techniques are described. There are advantages and disadvantages in both techniques and the right technique should be chosen for a particular application. The sequential MCS method can recognize the chronology and the correlation between subsequent events, which is very important in the assessment of power systems with wind energy and energy storage. This method is therefore used in the research described in the following chapters. The two widely used probabilistic reliability indices LOLE and the LOEE are discussed in detailed and are used in the following chapters in this thesis.



### **3. MODELS FOR ADEQUACY ASSESSMENT OF GENERATING SYSTEMS INCLUDING WIND POWER AND ENERGY STORAGE**

#### **3.1 Introduction**

Enhanced public awareness of the environment has led to widespread wind power growth in order to reduce greenhouse gas emissions and natural habitat disturbances associated with conventional energy generation. As noted earlier, many countries have implemented or are in the process of implementing policies to promote renewable energy. Large scale integration of wind power in an electric grid may result in large power fluctuations due to the intermittence of wind speed, and result in a high risk in providing a continuous power supply. This risk can be reduced by storing wind energy and using it during low wind or no wind periods. The amount of wind energy that can be utilized by an electric power system can be greatly limited if the available conventional units are not able to respond quickly to the changes created by wind power fluctuations. Hydro power stations with reservoirs have the ability to change the generated power output quickly and also act as energy storage facilities.

The development of suitable modeling techniques and methodologies for reliability evaluation of power systems including wind power and energy storage facilities become more important as wind power penetration in traditional power systems continues to increase significantly. Both analytical and simulation methods have been utilized in adequacy assessment of power systems containing wind power and energy storage. A realistic evaluation approach should be able to recognize the chronological

variation in wind speed and its influence on the power system performance. Sequential Monte Carlo simulation is used in this research to incorporate such considerations in an adequacy assessment of a generating system including wind energy and energy storage. The simulation technique is based on using hourly random events to mimic the operational history of a generating system, taking account of the failure and repair characteristics of the generating units in the system, and the chronological nature and state of wind speeds and energy storage.

Time Series Auto-Regressive and Moving Average (ARMA) models for different wind regimes are presented and utilized to simulate the hourly wind speed. The power output from a WTG unit is simulated using a relationship between the power output and the simulated wind speed. A time series energy storage model considering its charging/discharging characteristics is developed, and an operating strategy for wind farms and energy storage is presented. Models for energy limited hydro units and coordination strategy between wind power and hydro units are also introduced in this chapter.

### **3.2 Models for Wind Energy Conversion Systems**

The methodology for modeling WECS includes two parts: wind speed data simulation, and WECS power generation model derivation. The first part recognizes the random variation of the wind. This randomness must be included in an appropriate model to reflect the chronological and auto-correlation characteristics at a particular geographic location. The second step considers the non-linear relationship between the WTG power output and the wind velocity. This relationship can be determined using the WTG operational parameters and power curve modeling techniques.

### 3.2.1 Wind Speed Model

The sequential simulation of WECS involves the generation of hourly wind speed over a sufficiently long period of time for a given site. The wind speed varies in time and by site, and at a specific hour is related to the wind speeds of previous hours. The simulation of wind speed has been the subject of a number of publications [9, 47, 48], and is used to study the performance, planning and reliability of WECS or mixed power systems containing wind energy. Wind speed modeled as a random variable with a Weibull distribution, and a simple auto-regressive (AR) model is presented in [48] for simulating the main statistical characteristics of wind speed. These models, however, underestimate the high-order auto-correlation of the wind speed, and are therefore considered to be incomplete and inadequate to represent the wind resources [9].

It has been shown that any stationary stochastic system can be approximated as closely as required by an ARMA model of order (n, n-1) [49]. Reference [9] provides an approach for fitting time series wind speed models. Time series ARMA wind speed models developed using this approach can reproduce the high-order auto-correlation, the seasonal and diurnal distribution of the actual wind speed and therefore can be used in reliability studies of power systems including WECS [9].

Wind speeds for a selected wind farm site are simulated using a site-specific ARMA model, which is mathematically expressed in (3.1).

$$y_t = \sum_{i=1}^n \phi_i y_{t-i} + \alpha_t - \sum_{j=1}^{n-1} \theta_j \alpha_{t-j} \quad (3.1)$$

$y_t$  is the time series value at time  $t$ ,  $\phi_i$  ( $i = 1, 2, 3 \dots n$ ) and  $\theta_j$  ( $j=1, 2, 3 \dots n-1$ ) are the auto regressive and moving average parameters of the model respectively.  $\alpha_t$  is a normal white noise process with zero mean and a variance of  $\sigma_a^2$  (i.e.  $\alpha_t \in \text{NID}(0, \sigma_a^2)$ , where NID denotes Normally Independently Distributed). A nonlinear least square method is used to estimate the values of  $n$ ,  $\phi_i$ ,  $\theta_j$  and  $\sigma_a^2$  for the ARMA ( $n, n-1$ ) [50].  $\alpha_t$  is recursively calculated from initial guess values of each parameter and the known  $y_t$  values as described in [50]. The sum of squares of  $\alpha_t$ 's is calculated, and the least square method is used to minimize the residual sum of the squares. Using the Marquart procedure [49], a point in the parameter space giving the smaller sum of squares of  $\alpha_t$ 's will be reached. It starts a new iteration with this point as initial values, and the iterations are continued until specified tolerances are reached.

Historical hourly wind speed data collected over 15 years by Environment Canada for two different sites: Swift Current and North Battleford in the Province of Saskatchewan, Canada are used to obtain the respective ARMA models. The data was recorded at a height of 10m. Swift Current has an average wind speed of 20 km/hour and lies in the southern part of the province. It is home to one of the large wind farms in Canada. North Battleford lies to the north and has a relatively poor wind resource. The average wind speed at this site is 15 km/hour. The time series wind speed ARMA models [9, 13] for the Swift Current and North Battleford locations are shown in (3.2) and (3.3) respectively.

$$y_t = 0.8782 y_{t-1} - 0.0066 y_{t-2} + 0.0265 y_{t-3} + \alpha_t - 0.2162 \alpha_{t-1} + 0.0091 \alpha_{t-2} \quad (3.2)$$

$$\alpha_t \in \text{NID}(0, 0.55792^2)$$

$$y_t = 1.7901y_{t-1} - 0.9087y_{t-2} + 0.0948y_{t-3} + \alpha_t - 1.0929\alpha_{t-1} + 0.2892\alpha_{t-2} \quad (3.3)$$

$$\alpha_t \in NID(0, 0.474762^2)$$

The wind speed  $SW_t$  at any given time  $t$  for the two sites can be simulated using (3.4).

$$SW_t = \mu_t + \sigma_t \cdot y_t \quad (3.4)$$

where  $\mu_t$  and  $\sigma_t$  are the historical hourly mean wind speed and the standard deviation of wind speed respectively for the wind sites. Figure 3.1 and Figure 3.2 show the  $\mu_t$  and  $\sigma_t$  for 8760 hours in a year for the Swift Current wind site. Figure 3.3 and Figure 3.4 show the  $\mu_t$  and  $\sigma_t$  for 8760 hours in a year for the North Battleford wind site.

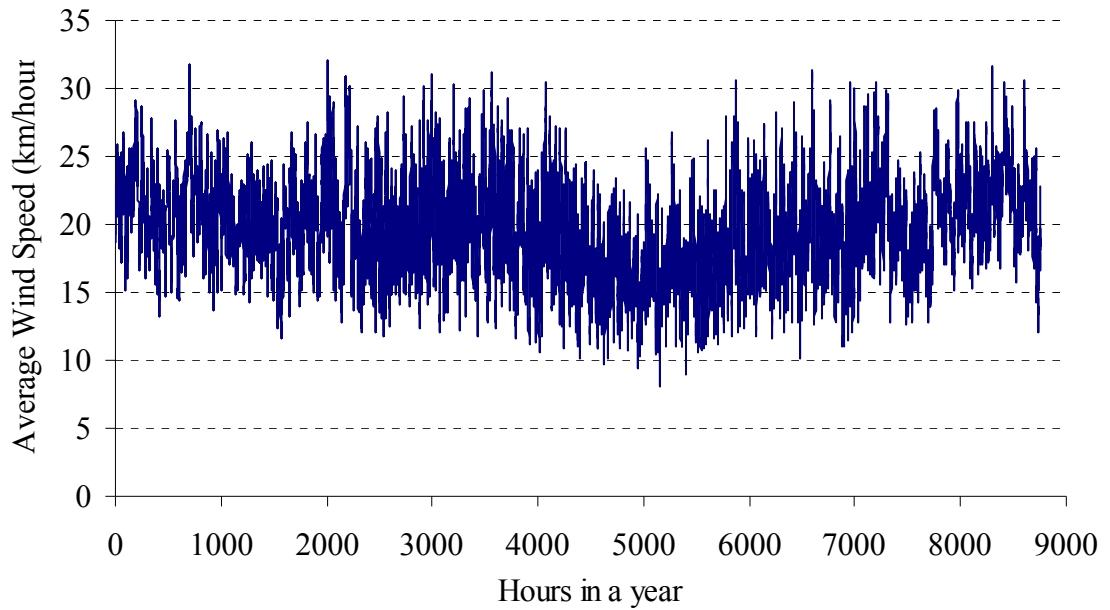


Figure 3.1: Hourly average wind speed for the Swift Current wind site.

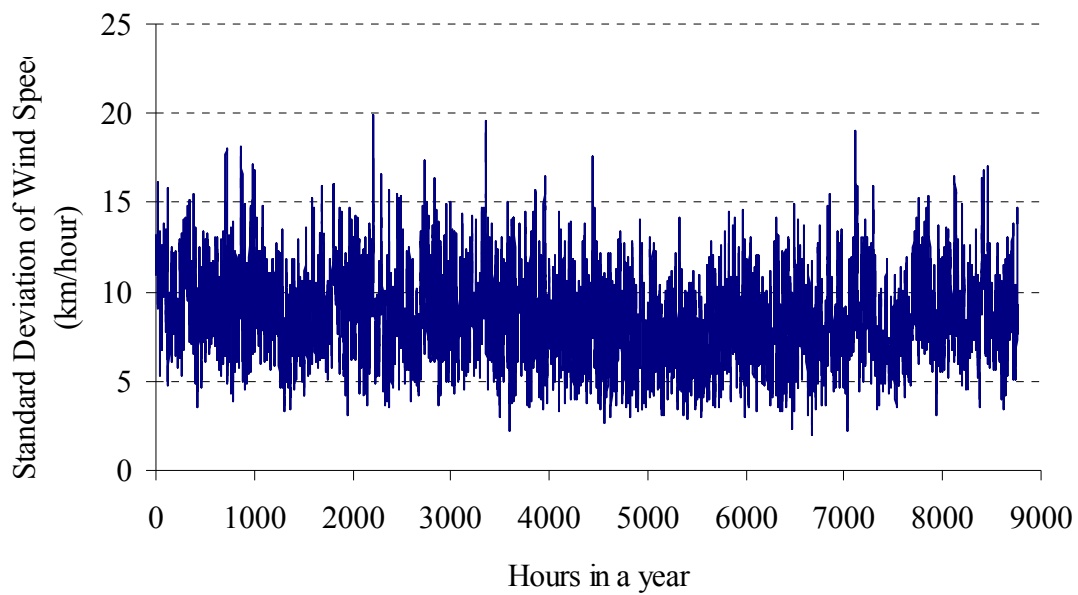


Figure 3.2: Hourly standard deviation of wind speed for the Swift Current wind site.

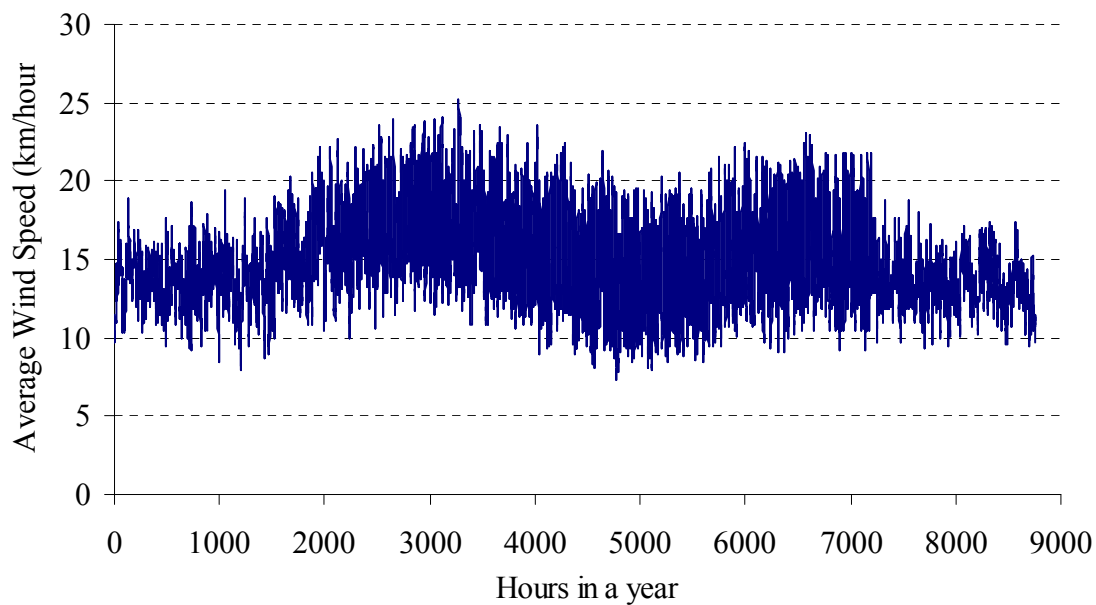


Figure 3.3: Hourly average wind speed for the North Battleford wind site.

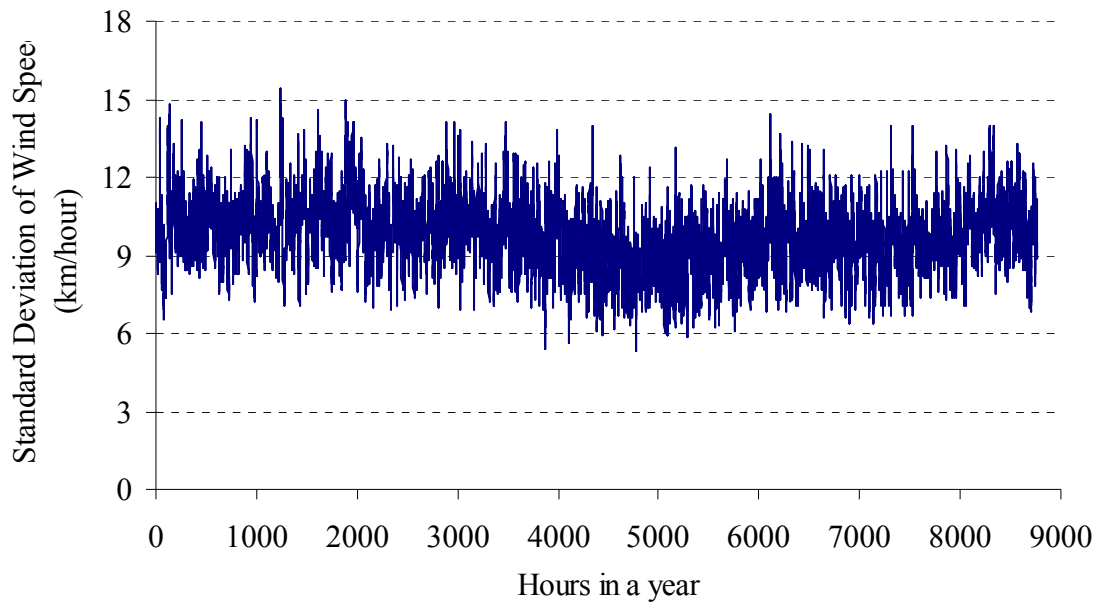


Figure 3.4: Hourly standard deviation of wind speed for the North Battleford wind site.

Figure 3.5 to 3.7 show the simulated hourly wind speeds for a day, a month and a year respectively for Swift Current. It can be seen from these figures that the hourly wind speeds are distributed around the average value of 20 km/hour. The time series ARMA models expressed in (3.2) and (3.3) provide a valid representation of the wind regime, which includes the correlation between the wind speeds of successive hours. The ARMA model, the known historical mean wind speed and standard deviation of wind speed data for a particular geographic location can be used to simulate wind speeds at the location.

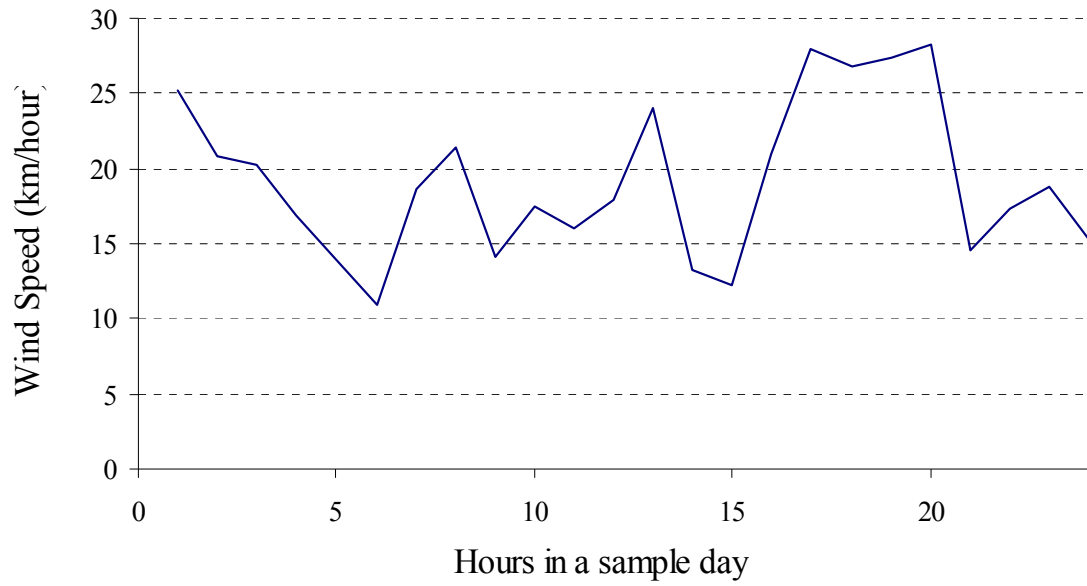


Figure 3.5: Simulated wind speed for the Swift Current site for a sample day.

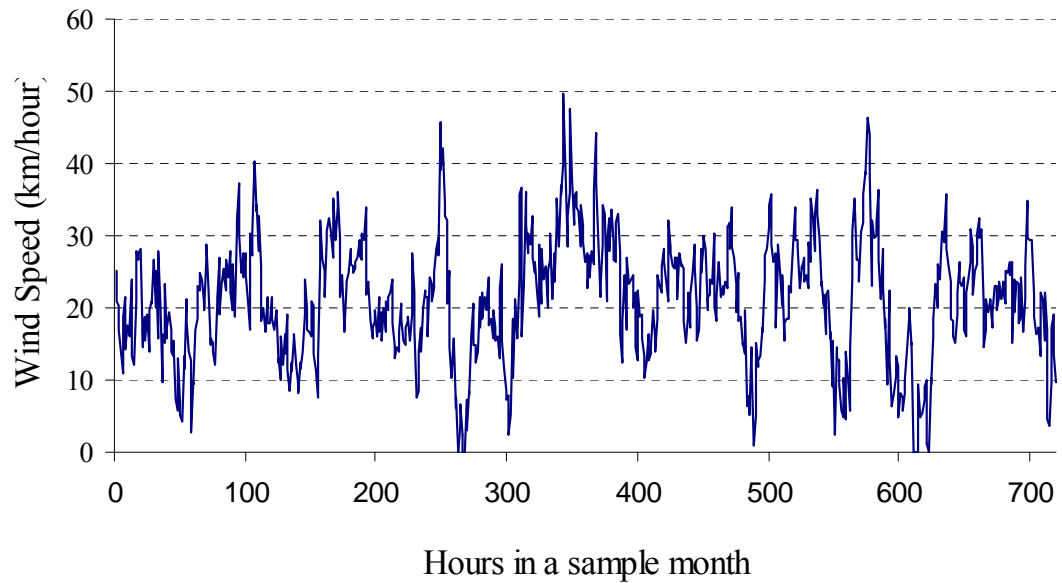


Figure 3.6: Simulated wind speed for the Swift Current site for a sample month.



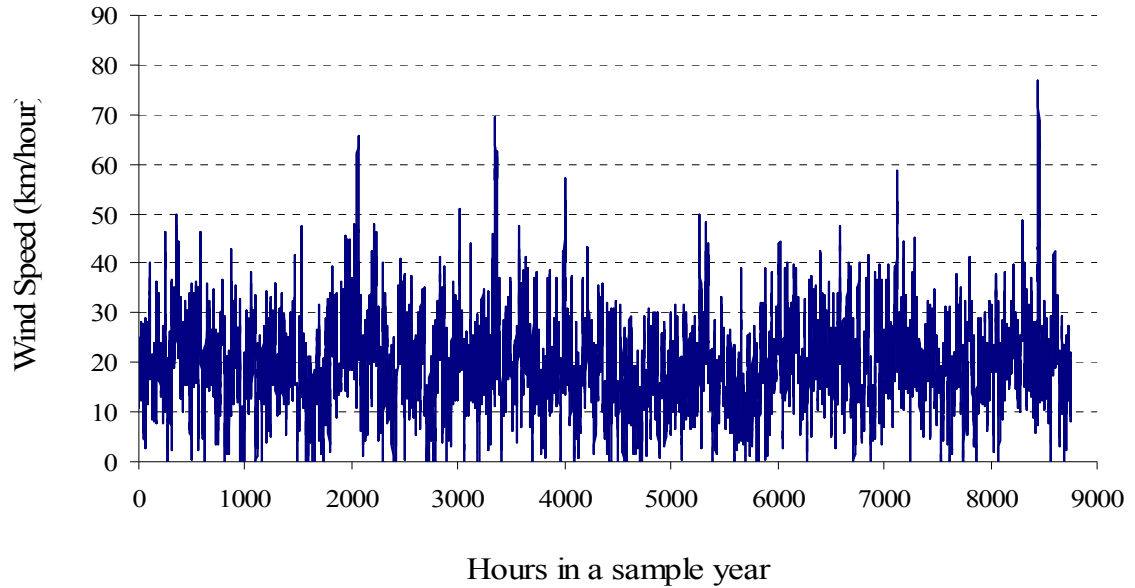


Figure 3.7: Simulated wind speed for the Swift Current site for a sample year.

### 3.2.2 Wind Turbine Generator Model

The power output characteristics of WTG are quite different from those of conventional generating units. Conventional generating units are capable of producing their rated power outputs at all times except when they undergo partial or complete failures. The performance characteristics and the efficiency of the generator affect the electric power output of a WTG in the up state. The wind speed characteristics, however, have a major impact on the power output. There is a non-linear relationship between the power output of the WTG and the wind speed as shown by the “Power Curve” in Fig. 3.8. This relationship is described by the operational parameters of the WTG. The important parameters are the cut-in wind speed, the rated wind speed, and the cut-out wind speed. A WTG starts to generate power at the cut-in wind speed. It generates its rated power when the wind speed is between the rated wind speed and the cut-out wind speed. WTG units are shut down for safety reasons when the wind speed reaches the cut-out wind speed. The power curve is expressed mathematically by (3.5) [10], which can be used to obtain the hourly power output of a WTG from the simulated hourly wind

speed.

$$P(SW_t) = \begin{cases} 0 & 0 \leq SW_t < V_{ci} \\ (A + B \times SW_t + C \times SW_t^2) \times P_r & V_{ci} \leq SW_t < V_r \\ P_r & V_r \leq SW_t < V_{co} \\ 0 & SW_t \geq V_{co} \end{cases} \quad (3.5)$$

Where  $P_r$ ,  $V_{ci}$ ,  $V_r$  and  $V_{co}$  are the rated power output, the cut-in wind speed, the rated wind speed and the cut-out wind speed of the WTG respectively. The constants A, B, C are determined by  $V_{ci}$ , and  $V_r$  as expressed in (3.6) [10].

$$A = \frac{1}{(V_{ci} - V_r)^2} \left\{ V_{ci}(V_{ci} + V_r) - 4V_{ci}V_r \left[ \frac{V_{ci} + V_r}{2V_r} \right]^3 \right\},$$

$$B = \frac{1}{(V_{ci} - V_r)^2} \left\{ 4(V_{ci} + V_r) \left[ \frac{V_{ci} + V_r}{2V_r} \right]^3 - (3V_{ci} + V_r) \right\}, \quad (3.6)$$

$$C = \frac{1}{(V_{ci} - V_r)^2} \left\{ 2 - 4 \left[ \frac{V_{ci} + V_r}{2V_r} \right]^3 \right\}$$

The cut-in, rated and cut-out wind speed values used in the studies are 14.4, 36, and 80 km/hour respectively [51]. The constants A, B, C for this wind turbine are 0.0311, -0.0215 and 0.0013 respectively. The wind farm considered in the studies consists of identical WTG units, each having a rated power output of 1 MW. Each WTG is exposed to the same wind regime characterized by the geographic location, and provides the same power output within an hourly interval. System simulations for long term adequacy

studies are generally done using hourly time intervals. Wind variations within the interval are not considered. The power outputs of the individual WTG are aggregated to obtain the total wind farm power output at each time interval.

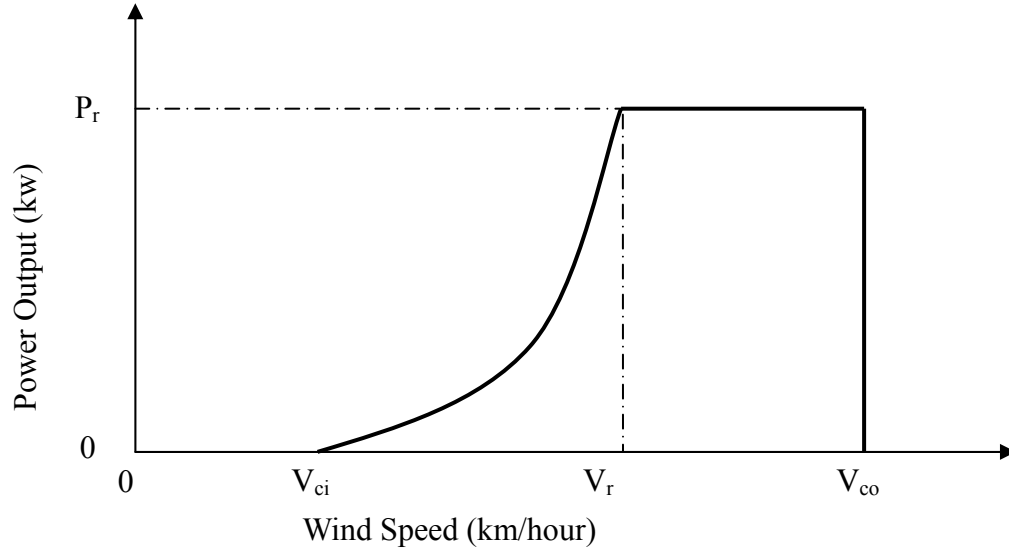


Figure 3.8: Power curve of a typical WTG unit.

Figures 3.9 and 3.10 show the hourly power output from a wind farm with the Swift Current wind regime for a sample month and year respectively. The wind farm has an installed capacity of 300 MW. The wind power output shown in these figures varies greatly from hour to hour.

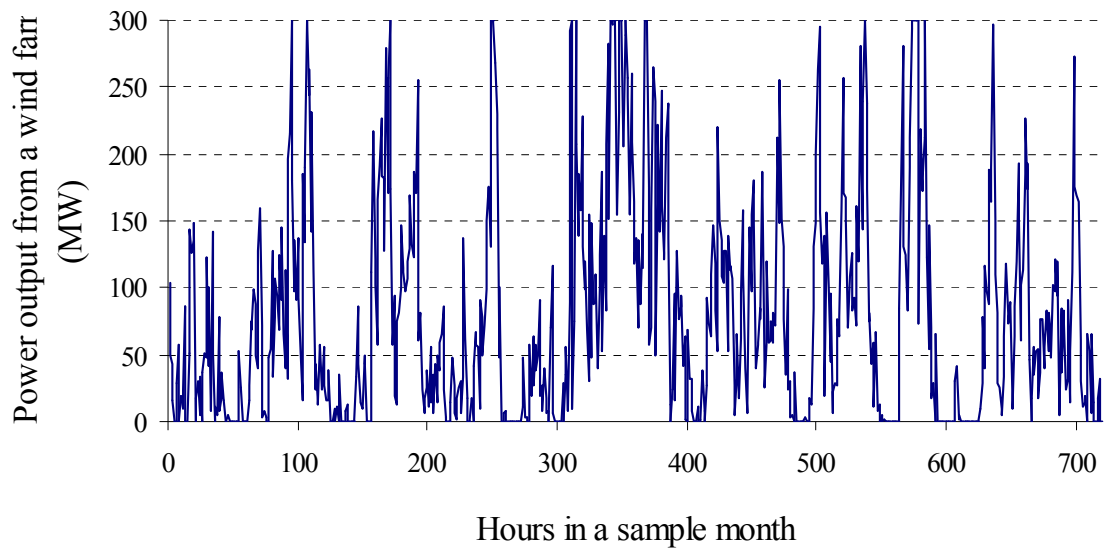


Figure 3.9: Power output from a wind farm in a sample month.

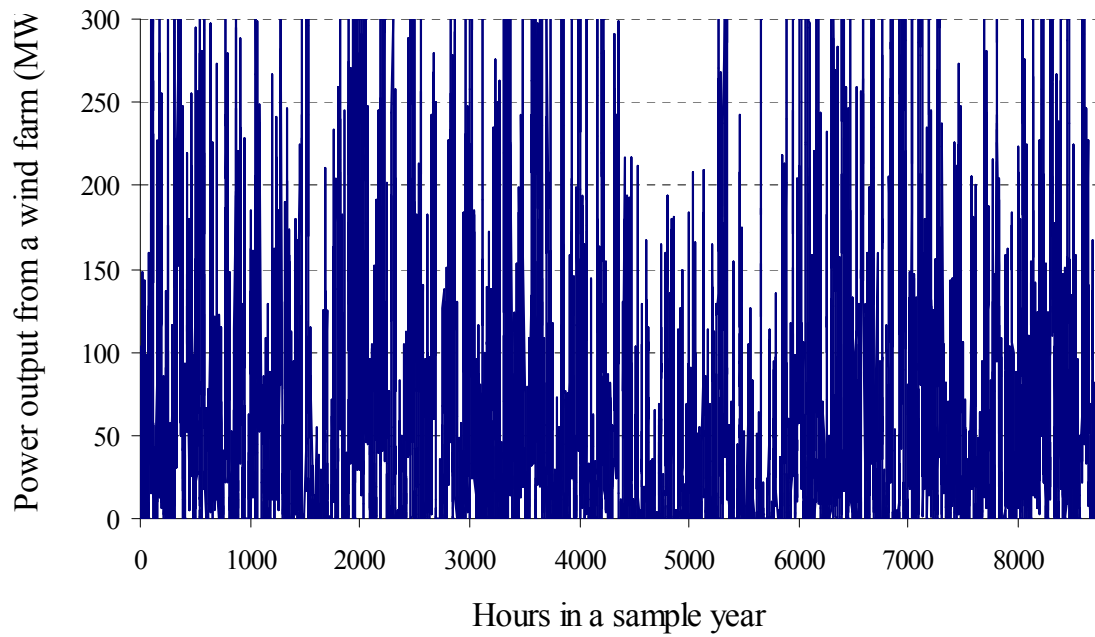


Figure 3.10: Power output from a wind farm in a sample year.

Figure 3.11 shows the probability distribution of the power output from the Swift Current wind farm. The vertical line shows the expected power output, which is

approximately 0.2 p.u. of the rated wind farm output.

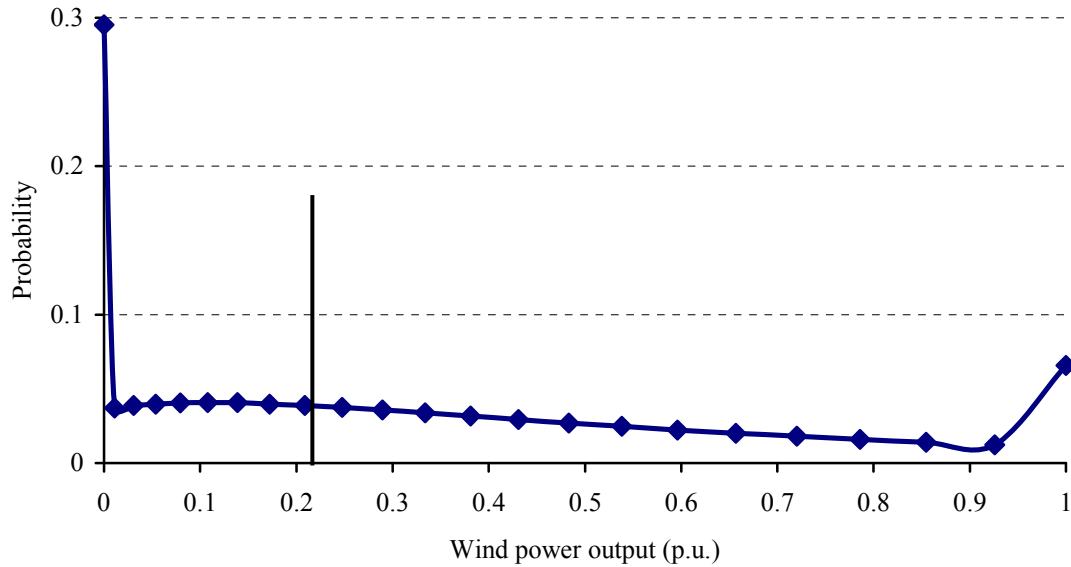


Figure 3.11: Probability distribution of the simulated wind power generation.

### 3.3 Reliability Evaluation Model for Generating Systems Including Wind Power and Energy Storage

Wind penetration expressed as the ratio of the installed wind capacity relative to the system generation capacity in many power systems around the world is rapidly increasing. Many large wind farms have been integrated in power grids in recent years. The power output from WTG units usually fluctuates randomly, and therefore, cannot be counted on to continuously satisfy the system load. Although wind power output at any time is not controllable, the power output from a wind farm can be utilized when needed if energy storage is available.

There are different types of energy storage technologies that can be utilized in power systems to attain improved system performance. Flywheels, superconducting coils, compressed air, deep cycle lead-acid batteries, and pumped storage are some

examples that provide storage capability of different magnitudes, response rates and time scales. New battery technologies, such as the Vanadium Redox Battery (VRB) [39], are being considered and successfully tested for large scale on-grid applications of wind energy. It is important to investigate the possible impacts of energy storage on the reliability of relatively large systems that include significant amounts of wind power capacity.

The basic system model for generating system including wind power and energy storage is shown in Figure 3.12. This model has also been used by other researchers using simulation techniques [32]. The model has been extended in this research work to include the system operating constraints imposed by the chronology of the various system events, the charging and discharging characteristics of the storage facility, generator loading order and the wind power dispatch restriction for system stability. These effects have been incorporated in the simulation process. The storage facility in this model is controlled either by the power system operator or an independent system operator in a de-regulated structure. The stored energy is used to serve the system load when the total system generation fails to meet the system load. Excess energy from the entire generating system is then used to bring the storage facility to a fully charged condition in this model.

The basic purpose of adding energy storage to a wind-conventional generating system is to smooth out the power fluctuations from the WTG units. It is not normally practical to store energy from conventional units for future use. A modified system model for a wind-conventional generating system including energy storage is shown in Figure 3.13. In this case, only energy generated by WTG units is stored for future use. The energy storage facility in this model is located at the wind farm site and is connected to the system through a transmission line. The storage facility in this model can be under the control of either the wind farm owner or the system operator.

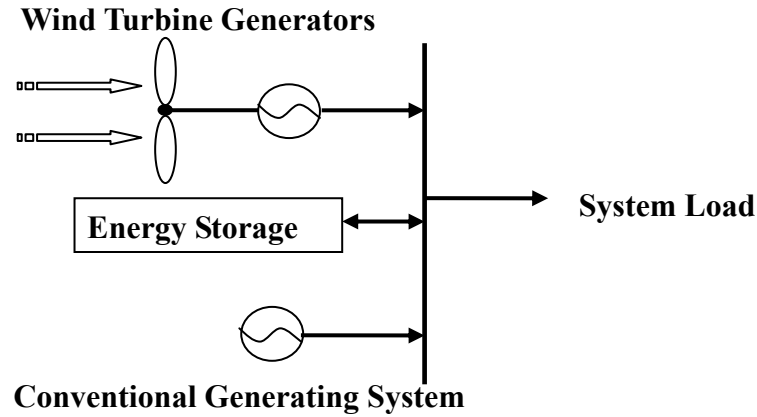


Figure 3.12: Basic model for a wind-conventional generating system including energy storage.

When wind penetrations are relatively low and have insignificant impact on the system performance, wind power has priority in serving the system load. In such situations, all the power generated from the wind farm can be absorbed by the system. The ability of a power system to absorb wind energy is reduced due to stability concerns as the wind penetration increases. Power systems can become unstable if a large share of the system load at any instant is served by the wind. A wind power dispatch restriction ( $X_w$ ) which is a certain percentage of the system load is imposed.

The hourly wind energy dispatch is restricted to  $X_w\%$  of the hourly system load, and the surplus wind energy above  $X_w\%$  of the system load is available for storage. When the sum of the wind power and the conventional power is insufficient to meet the system load, the stored energy is used to supplement the generated energy and supply the system load.

The procedure involved in the simulation process in order to determine the status of the energy storage, the power output from energy storage and the reliability index

calculations are described in the following four steps:

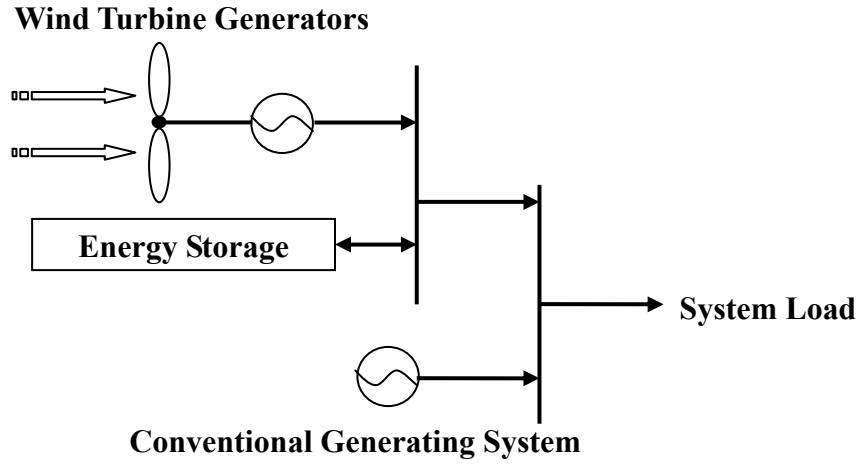


Figure 3.13: Realistic model for a wind-conventional generating system including energy storage.

Step 1: Determine the power output time series  $\{TG_{wi}; i=1,2, \dots, T\}$  from a wind farm using an ARMA wind speed model for the selected wind regime and the power curve. Calculate the power output time series  $\{TG_{ci}; i=1,2,\dots, T\}$  for the conventional generating units.

Step 2: Determine the amount of wind power that can be used to supply the system load directly, and the amount of wind power that is available to be stored in the energy storage. In the simulation process, the surplus wind generation time series  $\{SG_{wi}; i=1,2, \dots, T\}$  and the surplus conventional generation time series  $\{SG_{ci}; i=1,2,\dots, T\}$  can be obtained using (3.7) and (3.8). It should be noted that the surplus generation SG can be either positive or negative values.

$$SG_{wi} = TG_{wi} - X_w \% * L_i \quad (3.7)$$



$$SG_{ci} = TG_{ci} - (1 - X_w\%) * L_i \quad (3.8)$$

The energy storage time series  $\{ES_i; i=1, 2, \dots, T\}$ , and the energy discharged from the energy storage time series  $\{TG_{ei}; i=1, 2, \dots, T\}$  can be obtained using (3.9) and (3.10) respectively.

$$ES_{i+1} = \begin{cases} ES_i + SG_{wi} \times t_i & SG_{wi} \geq 0 \text{ and } SG_{ci} \geq 0 \\ ES_i + SG_{ci} \times t_i & SG_{wi} \geq 0 \text{ and } SG_{ci} < 0 \\ ES_i & SG_{wi} < 0 \text{ and } (SG_{wi} + SG_{ci}) \geq 0 \\ ES_i + (SG_{wi} + SG_{ci}) \times t_i & SG_{wi} < 0 \text{ and } (SG_{wi} + SG_{ci}) < 0 \end{cases} \quad \text{if} \quad (3.9)$$

$$TG_{ei} = \begin{cases} 0 & SG_{wi} \geq 0 \text{ and } SG_{ci} \geq 0 \\ -SG_{ci} \times t_i & SG_{wi} \geq 0 \text{ and } SG_{ci} < 0 \\ 0 & SG_{wi} < 0 \text{ and } (SG_{wi} + SG_{ci}) \geq 0 \\ -(SG_{wi} + SG_{ci}) \times t_i & SG_{wi} < 0 \text{ and } (SG_{wi} + SG_{ci}) < 0 \end{cases} \quad \text{if} \quad (3.10)$$

where  $ES_i$  has maximum ( $ES_M$ ) and minimum ( $ES_m$ ) storage limitations.  $\{L_i; i=1, 2, \dots, T\}$  is the system load time series.  $\{t_i; i=1, \dots, T\}$ , where  $t_i$  is the  $i^{\text{th}}$  time interval and  $T$  is the number of time intervals in a year is a time interval series in a simulated year. In general,  $t_i = 1$  hour and  $T=8736$ , and these values are used in the work presented in this thesis. The minimum energy storage capacity is taken as 20% of its rated capacity for the selected type of storage facility. A linear charging and discharging rate is considered in this model using a 5-hour charging and discharging period. The maximum energy charged and discharged from the energy storage is  $(ES_M - ES_m)/5 \times \Delta T$  in a simulation time interval  $\Delta T$ .

Step 4: Compare the sum of the wind power, the conventional power, and the power output from energy storage with the system load. The Loss of Load ( $LOL_i$ ), Loss

of Energy ( $LOE_i$ ) can be calculated by using (3.11) and (3.12).

$$LOE_i = \begin{cases} 0 & SG_{wi} \geq 0 \text{ and } SG_{ci} \geq 0 \\ TG_{ei} + SG_{ci} \times t_i & SG_{wi} \geq 0 \text{ and } SG_{ci} < 0 \\ 0 & SG_{wi} < 0 \text{ and } (SG_{wi} + SG_{ci}) \geq 0 \\ TG_{ei} + (SG_{wi} + SG_{ci}) \times t_i & SG_{wi} < 0 \text{ and } (SG_{wi} + SG_{ci}) < 0 \end{cases} \quad \text{if} \quad (3.11)$$

$$LOL_i = \begin{cases} t_i & \text{if } LOE_i > 0 \\ 0 & \text{if } LOE_i = 0 \end{cases} \quad (3.12)$$

The reliability indices LOLE and LOEE for a number of sample years (N) can be obtained using (3.13) and (3.14) respectively.

$$LOLE = \frac{1}{N} \sum_{i=1}^{T \times N} LOL_i \quad (3.13)$$

$$LOEE = \frac{1}{N} \sum_{i=1}^{T \times N} LOE_i \quad (3.14)$$

### 3.4 Models for Energy Limited Hydro Plants

Models for energy limited hydro units are presented in this section in order to investigate the reliability benefit from wind power in coordination with hydro units. Hydro units have the ability to quickly adjust their power output in response to system conditions and operating constraints. The IEEE Subcommittee on the Application of Probability Methods proposed a four-state model for peaking units [42]. The four-state model from the IEEE is utilized to represent a hydro unit. Energy limitations of hydro units are also considered in the model development in this research work. The simulation

process used to consider peaking hydro units in reliability evaluation is described in Section 3.4.1. Models for the hydro reservoir, hydro generating units, and water in-flow are presented in Section 3.4.2.

### **3.4.1 Peaking Unit Model**

Reference [40] presents a hydro-thermal Reliability Test System (HT-RTS) obtained by modifying the IEEE-RTS in which six 50 MW generating units are considered as hydro units sharing a common reservoir. In the HT-RTS, all the generating units are regarded as base-loaded units. Base loaded units have relatively long operating cycles, and are represented by the conventional two-state model [1] shown in Figure 2.3. Base loaded hydro units are not be started or stopped in response to variations in the system conditions. In the following studies, a specified number of hydro units in the HT-RTS are modeled as peaking units using the IEEE four-state model shown in Figure 2.5. The model is extended to incorporate energy limitations imposed by the reservoir characteristics.

It is assumed that the peaking loaded units can be started and stopped an unlimited number of times, and they can be quickly started and shut down. The steps to determining the status of peaking units during the simulation are as follows:

Step 1: Calculate the total available capacity from the base loaded units for a simulated year.

Step 2: Superimpose the total capacity generated by the base loaded units on the chronological system load.

Step 3: Determine how many peaking load units in the reserve shut down state

need to be started, or how many peaking load units in the service state need to be shut down at the beginning of each hour.

Step 4: Calculate the in-service duration for the successfully started peaking units and the forced out duration for the unsuccessfully started peaking units.

Step 5: Obtain the total capacity margin by superimposing the total system capacity generated by both the base load units and the peaking load units on the chronological load.

Step 6: Determine the state of each peaking unit in each hour considering the system loss of load situation.

The algorithm for the simulation process of generating systems including base loaded units and peaking loaded units are shown in Figure 3.14.

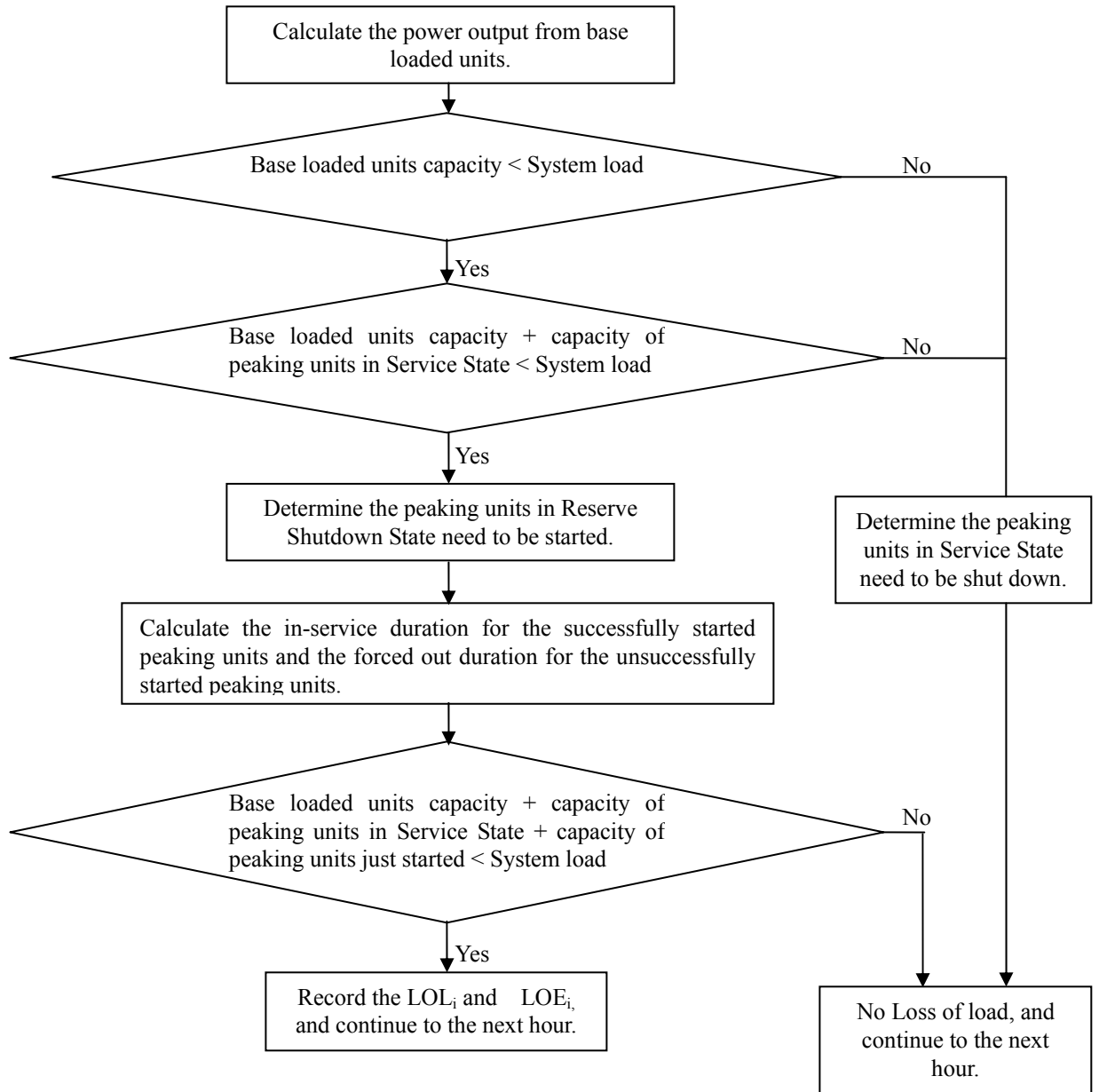


Figure 3.14: Simulation process for a generating system including base-loaded units and peaking units.

### 3.4.2 Energy Limited Hydro Unit Model

Hydro units are modeled using the 4-state model, and energy limitation is incorporated in the model development. The status of the hydro units in each simulated

hour is determined using the method described in Section 3.4.1. After determining the status of the hydro units, the power output from the hydro units in State 1 in Figure 2.5 is determined by the water conditions in the reservoir.

The potential energy in the water stored in a reservoir is transformed into electrical energy by means of hydro turbines and generators. The input energy is associated with water in-flow to the reservoir, and the output energy with the electricity generation. The water in-flow mainly comes from rainfall, which depends on the weather conditions. Three types of weather conditions in a year are considered: wet, dry, and normal. Each type of weather condition has the same probability to be encountered, and it is randomly chosen during a simulation. It is assumed that the water in-flow ( $Z_j$ ,  $j=1, \dots, 13$ ) has a normal distribution, and the value of  $Z_j$  is obtained using the Box and Muller method [52]. In this study, a year is divided into 13 periods, and each period consists of 672 hours with the same weather condition. The mean values of the water in-flow data in each period are shown in Table 3.1, and the standard deviation is 5% of the corresponding mean value.

Table 3.1: Mean value of water in-flow

Period	Wet (Mm <sup>3</sup> )	Dry (Mm <sup>3</sup> )	Normal (Mm <sup>3</sup> )
1	20.5	12.0	12.5
2	34.0	14.5	19.5
3	46.0	23.5	30.0
4	57.0	29.0	42.0
5	31.0	14.0	20.0
6	24.0	11.0	16.0
7	18.0	8.0	12.0
8	12.0	5.0	8.0
9	12.0	5.0	8.0
10	12.0	4.0	7.0
11	18.0	8.0	10.0
12	18.0	10.0	16.0
13	28.0	12.0	18.0

The hourly water in-flow ( $I_i$ ,  $i=1, \dots, 8736$ ) into the reservoir can be obtained using (3.15).

$$I_i = Z_j / 672 \quad (3.15)$$

The water spilled ( $S_i$ ) and water volume of the reservoir ( $V_i$ ) in the  $i$  th hour are calculated at the beginning of this hour using (3.16) to (3.18):

$$V_{pi} = V_{i-1} - R_{i-1} + I_i \quad (3.16)$$

$$S_i = \begin{cases} 0 & \text{if } V_{pi} \leq V_{\max} \\ V_{pi} - V_{\max} & \text{if } V_{pi} > V_{\max} \end{cases} \quad (3.17)$$

$$V_i = \begin{cases} V_{pi} & \text{if } V_{pi} \leq V_{\max} \\ V_{\max} & \text{if } V_{pi} > V_{\max} \end{cases} \quad (3.18)$$

Where:

$V_{pi}$  is volume of the reservoir at  $i$  th hour before the spillage of extra water.

$V_{\max}$  is the maximum reservoir volume.

$R_{i-1}$  is the water utilized to generate electricity during  $(i-1)$  th hour.

$S_i$  is the water spilled during  $i$  th hour.

The net head  $H_i$  of the hydro plant at hour  $i$  is then calculated using the following approximate equation (3.19) when  $V_i$  is greater than the minimum reservoir volume ( $V_{\min}$ ):

$$V_i = c + b \cdot H_i + a \cdot H_i^2 \quad (3.19)$$

Where: a,b,and c are model coefficients.

Peaking hydro units are not in service when the power output from other generating units in the system, such as WTG and thermal units, is sufficient to meet the system load. In this condition, water can be stored in the reservoir. If the power output from other generating units is inadequate, an appropriate number ( $k_a$ ) of hydro units must be run to supply the load. The power output from a hydro unit ( $P_{hi}$ ) can be obtained using (3.20) and (3.21).

$$P_{hi} = g\beta H_i Qs / 10^6 \quad (3.20)$$

$$Q = G\sqrt{2gH_i} \quad (3.21)$$

Where:

$g$  is gravitational constant in  $\text{m/sec}^2$ .

$\beta$  is overall efficiency of the hydro plant.

$Q$  is turbine discharge rate in  $\text{m}^3/\text{sec}$ .

$s$  is specific weight of water in  $10^3 \text{ kg/m}^3$ .

$G$  is opening area of the guide for each hydro turbine in  $\text{m}^2$ .

The water utilized in the  $i$  th hour ( $R_i$ ) can be calculated using (3.22).

$$R_i = 3600k_a Q \quad (3.22)$$

The basic data for the hydro plant and the constraints on the hydro generating units are shown in Table 3.2.



Table 3.2: Hydro plant data

Number of hydro units:		6
Plant efficiency:		0.8 p.u.
Maximum water head (m):		180
Reservoir coefficients:	a	0.00241
	b	0.111
	c	2
Maximum water volume (Mm <sup>3</sup> ):		100
Minimum water volume (Mm <sup>3</sup> ):		5
Initial water volume (Mm <sup>3</sup> ):		80
Maximum discharge rate (m <sup>3</sup> /sec):		53
Minimum discharge rate (m <sup>3</sup> /sec):		10.6
Maximum flow area (m <sup>2</sup> ):		1.1

### 3.5 Coordination between Wind Power and Hydro Units

The reliability evaluation models for a wind farm and an energy limited hydro plant are introduced in Section 3.2 and 3.4 respectively. The detailed simulation process incorporating the coordination between wind and hydro plants is presented in this section. The simulation process for each hour is shown in Figure 3.15.

The method presented considers energy limitations in the hydro reservoir while representing hydro units by the four-state model. Some of the hydro units are assigned to coordinate with wind power to offset the power imbalance due to wind fluctuation, and the rest are assigned as peaking units. The model developed for energy limited peaking hydro units are also used to represent hydro units that are assigned to operate in

coordination with wind power variations. An interactive generation model is developed by incorporating a coordination criterion to determine the wind power output level at which a balance is maintained with the support of hydro units. The coordination criterion is taken to be equal to the long term average power output of the wind farm and is expressed in per unit of the rated wind farm capacity. This value is approximately 0.2 for the Swift Current wind farm. If the power output from the wind farm is less than the coordination criterion, the hydro units assigned to coordinate with wind power are started to provide the required support. These hydro units are stopped when the power output from the wind farm is equal to or greater than the coordination criterion.

The simulation process and the calculation of the reliability indices are described in the following steps:

Step 1: Determine the power output time series  $\{P_{wi}; i=1, 2, \dots, 8736\}$  from the wind farm using the ARMA wind speed model for the selected wind regime and the power curve technique.

Step 2: Calculate the power output time series  $\{P_{bi}; i=1, 2, \dots, 8736\}$  from the conventional generating units represented by the two-state model.

Step 3: The number of hydro units required to coordinate with wind power is  $k$ , where  $k \leq M$ .  $M$  is the total number of hydro units. The coordination criterion ( $F$ ) is a percentage of the rated wind farm capacity ( $C_w$ ). As hydro units can be on forced outage, the number of hydro units ( $k_w$ ) that can be brought in the “In service” state in a time interval is less than or equal to  $k$ . If  $P_{wi} < F \cdot C_w$ , all the hydro units that are assigned to coordinate with wind power are required to provide their support. If  $P_{wi} \geq F \cdot C_w$ , no support from the hydro units is required. The relation between  $k$  and  $k_w$  is shown in (3.23).

$$\begin{cases} k_w \leq k & \text{if } P_{wi} < F \times C_w \\ k_w = 0 & \text{if } P_{wi} \geq F \times C_w \end{cases} \quad (3.23)$$

The power output from a hydro unit that is coordinated with wind power ( $P_{hwi}$ ) is calculated using (3.24).

$$P_{hwi} = \begin{cases} g\beta H_i Q_s / 10^6 & \text{if } P_{wi} < F \times C_w \\ 0 & \text{if } P_{wi} \geq F \times C_w \end{cases} \quad (3.24)$$

Step 4: After determining the number of hydro units required to coordinate with wind power and their total power output, the number of peaking hydro units ( $k_p$ ) and their power output ( $P_{hpi}$ ) is calculated.

The relation between  $k_p$  and  $k_w$  is shown in (3.25). It should be noted that the hydro units that are assigned to coordinate with wind power are still available to reduce the loss of load when  $P_{wi} \geq F \times C_w$ .

$$\begin{cases} k_p \leq M - k_w & \text{if } P_{wi} + k_w \times P_{hwi} + P_{bi} < P_{li} \\ k_p = 0 & \text{if } P_{wi} + k_w \times P_{hwi} + P_{bi} \geq P_{li} \end{cases} \quad (3.25)$$

The power output from a peaking hydro unit  $P_{hpi}$  is calculated using (3.26), and the upper bound for  $P_{hpi}$  is shown in (3.27), since the limited water needs to be saved for future usage.

$$P_{hpi} = \begin{cases} g\beta H_i Q_s / 10^6 & \text{if } P_{wi} + k_w \times P_{hwi} + P_{bi} < P_{li} \\ 0 & \text{if } P_{wi} + k_w \times P_{hwi} + P_{bi} \geq P_{li} \end{cases} \quad (3.26)$$

$$P_{hpi} \leq \frac{(P_{li} - P_{wi} - k_w \times P_{hwi} - P_{bi})}{k_p} \quad (3.27)$$

After calculating the power output from the wind farm, the base units and the hydro units during each time interval, the total system power output ( $P_{gi}$ ) is calculated using (3.28).

$$P_{gi} = P_{wi} + k_w \times P_{hwi} + P_{bi} + k_p \times P_{hpi} \quad (3.28)$$

Step 5:  $P_{gi}$  is compared with the system load ( $P_{li}$ ) for each time interval to determine if a loss of load situation exists. The Loss of Load ( $LOL_i$ ), Loss of Energy ( $LOE_i$ ), and Loss of Load Occurrence ( $LOLO_i$ ) is computed using (3.29), (3.30), and (3.31) respectively.

$$LOL_i = \begin{cases} 0 & \text{if } P_{gi} \geq P_{li} \\ 1 & \text{if } P_{gi} < P_{li} \end{cases} \quad (3.29)$$

$$LOE_i = \begin{cases} 0 & \text{if } P_{gi} \geq P_{li} \\ P_{li} - P_{gi} & \text{if } P_{gi} < P_{li} \end{cases} \quad (3.30)$$

$$LOLO_i = \begin{cases} 0 & \text{if } LOL_i = 0 \\ 0 & \text{if } LOL_i = 1 \text{ and } LOL_{i-1} = 1 \\ 1 & \text{if } LOL_i = 1 \text{ and } LOL_{i-1} = 0 \end{cases} \quad (3.31)$$

The reliability indices LOLE, LOEE, LOLE, Average Water used to produce Electricity (AWE), Average Water Spilled (AWS), and Average Volume of reservoir (AVolume) for a number of sample years (N) can be obtained using (3.32) to (3.37) respectively.

$$LOLE = \frac{1}{N} \sum_{i=1}^{8736 \times N} LOL_i \quad (3.32)$$

$$LOEE = \frac{1}{N} \sum_{i=1}^{8736 \times N} LOE_i \quad (3.33)$$

$$LOLF = \frac{1}{N} \sum_{i=1}^{8736 \times N} LOLO_i \quad (3.34)$$

$$AWE = \frac{1}{N} \sum_{i=1}^{8736 \times N} R_i \quad (3.35)$$

$$AWS = \frac{1}{N} \sum_{i=1}^{8736 \times N} S_i \quad (3.36)$$

$$AVolume = \frac{1}{8736 \times N} \sum_{i=1}^{8736 \times N} V_i \quad (3.37)$$

Where  $R_i$  is the amount of water utilized in each time interval,  $S_i$  is the amount of water spilled in each time interval, and  $V_i$  is the volume of the reservoir at the beginning of each time interval.

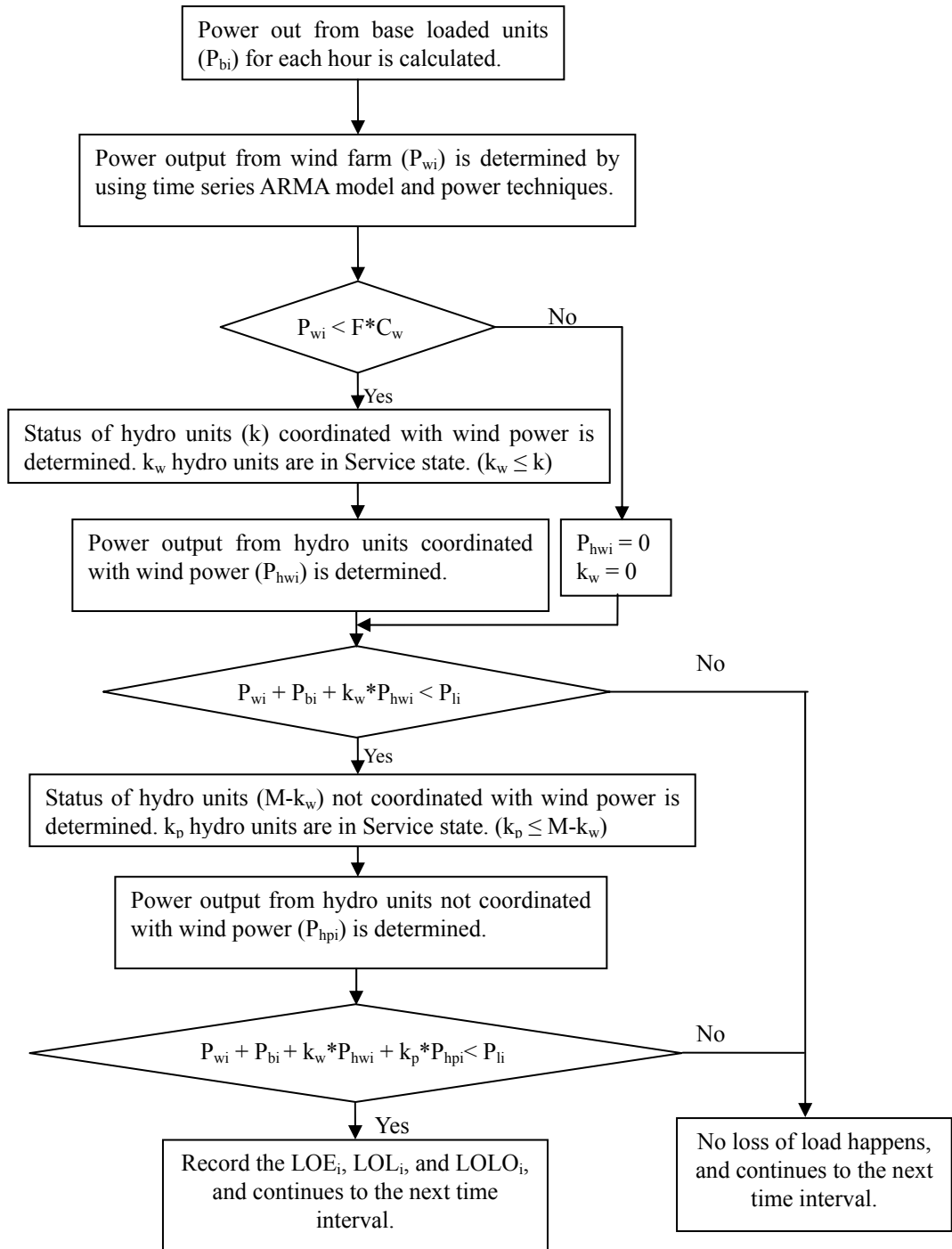


Figure 3.15: Simulation process for a generating system considering the coordination between energy limited hydro units and wind power.

### **3.6 Performance Indices Associated with Reliability Evaluation of Generating Systems Including Wind Power and Energy Storage**

The reliability indices reflect the overall system reliability performance, whereas, the energy indices reflect the wind energy utilization and water utilization in the studies described in this thesis. These indices can be grouped into the following categories.

#### **1. Conventional reliability indices**

The conventional reliability indices are the most widely used indices in capacity adequacy evaluation of large generating systems. These indices include:

Loss of load Expectation (LOLE) in hours/year

Loss of Energy Expectation (LOEE) in MWh/year

Loss of Load Frequency (LOLF) in occs/year

#### **2. Indices associated with wind power and energy storage**

Expected Wind Energy Utilized (EWEU) in MWh/year: expected amount of wind energy that can be directly absorbed by the power system.

Expected Energy Supplied by Wind (EESW) in MWh/year: expected amount of wind energy that can be utilized by the power system including the amount of wind energy stored in energy storage and utilized in the next hours.

Expected Surplus Wind Energy (ESWE) in MWh/year: expected amount of wind energy that can not be directly absorbed by the power system.

Expected Wind Energy Stored in the Battery (EWEB) in MWh/year: expected amount of wind energy that can not be directly absorbed by the power system and can be stored in energy storage.

### 3. Indices associated with hydro power plant

Average Water used to produce Electricity (AWE) in  $\text{Mm}^3/\text{year}$ : average amount of water in a year that can be utilized to generate electric power.

Average Water Spilled (AWS) in  $\text{Mm}^3/\text{year}$ : average amount of water in a year that has to be spilled since there is a maximum limitation of reservoir volume.

Average Water Volume in the reservoir (AVolume) in  $\text{Mm}^3$ : long-term average volume of water in a reservoir.

## 3.7 Summary

The basic models for generating capacity adequacy assessment of power systems including wind power and energy storage are presented in this chapter. A sequential Monte Carlo simulation technique is applied to generate a synthetic operating history of a generating system.

Time series models for wind regimes with different geographic characteristics are used to reproduce the high-order auto-correlation, the seasonal and diurnal distribution of the actual wind speed. Power output from a WTG unit can be computed from the simulated wind speed using the power curve equations.

Large scale integration of wind power in an electric grid can produce large power



fluctuations, and result in a high risk in providing a continuous power supply. This risk can be reduced by using energy storage. A time series energy storage model is developed based on the generation time series and the load time series models. The charging/discharging restriction of energy storage is considered in the model development. A wind power dispatch restriction is introduced to address system stability concerns. The wind energy that can not be directly absorbed by the system is available to be stored in energy storage. All the surplus wind energy can not be stored due to the charging/discharging constraints and the storage capacity limits.

Hydro plants with a reservoir have the ability to adjust their power output quickly and can act as an energy storage facility. Models for a hydro power plant are introduced in this chapter. The hydro units are modeled by incorporating energy limitations in the IEEE four-state model. The hydro reservoir model and the water in-flow model are introduced. The simulation process for the reliability evaluation of generating systems considering coordination between wind power and energy limited hydro units is developed and presented.

The system reliability indices, energy storage related indices and hydro utilization related indices are presented. The application of the introduced models and developed procedures are illustrated in the following chapters.

## **4. ADEQUACY ASSESSMENT OF GENERATING SYSTEMS CONTAINING WIND POWER AND ENERGY STORAGE**

### **4.1 Introduction**

Wind energy sources are intermittent in nature. Even at a site with a high wind power potential, the wind can blow and stop frequently in a short period of time and can be totally absent when it is most needed. It is desirable to use wind energy whenever it is available, and therefore, system operators put wind energy sources at the top of the priority loading order. At low penetration levels, wind power has insignificant impact on the overall system performance, and available wind energy can readily be absorbed by the system. The system performance will be greatly influenced by wind power fluctuations at relatively high penetration levels. The amount of wind energy that can be absorbed by an electric power system at a particular time can be greatly limited if the available conventional units are not able to respond quickly to the changes created by wind power fluctuations. In order to maintain the system stability, wind energy dispatch is usually restricted. Although wind power output at any time is not controllable, it can be made available when needed if the wind energy can be stored in an energy storage facility.

Chapter 3 presents an energy storage model developed in this work that can include the energy storage operating constraints for reliability evaluation using the MCS method. The presented model of energy storage is utilized in this chapter to conduct a series of studies. Due to the stability constraints of a power system, a wind power

dispatch restriction is applied, and the reliability benefit from wind power and energy storage is evaluated. Possible strategies of wind farm operation and energy storage are presented and compared by evaluating the reliability benefit from energy storage and the amount of wind energy that can be stored.

The studies are conducted by adding wind power and energy storage facilities to a small test system known as the Roy Billinton Test System (RBTS) [46]. The results from a wide range of studies considering variations in key factors, such as wind farm location, wind penetration level, energy storage capacity, energy storage operating constraints, and wind energy dispatch restrictions are also presented. An acceptable operating strategy for wind farm and energy storage for system operators and wind farm owners is illustrated, and valuable information is provided.

## **4.2 Reliability Test System**

The RBTS is a basic reliability test system developed at the University of Saskatchewan for educational and research purposes. The RBTS has an installed capacity of 240 MW from 11 conventional generating units. The single line diagram for the RBTS is shown in Figure 4.1. The detailed reliability data for the generating units in the test system is shown in Appendix B. The chronological hourly load model shown in Figure 2.7 is utilized, and the system peak load is 185 MW.

The LOLE is the most widely used generating system reliability index, and the LOEE is an energy based index that provides useful information on the amount of energy curtailed. The LOLE and LOEE indices for the RBTS generating system are 1.09 hours/year, and 9.7 MWh/year respectively.

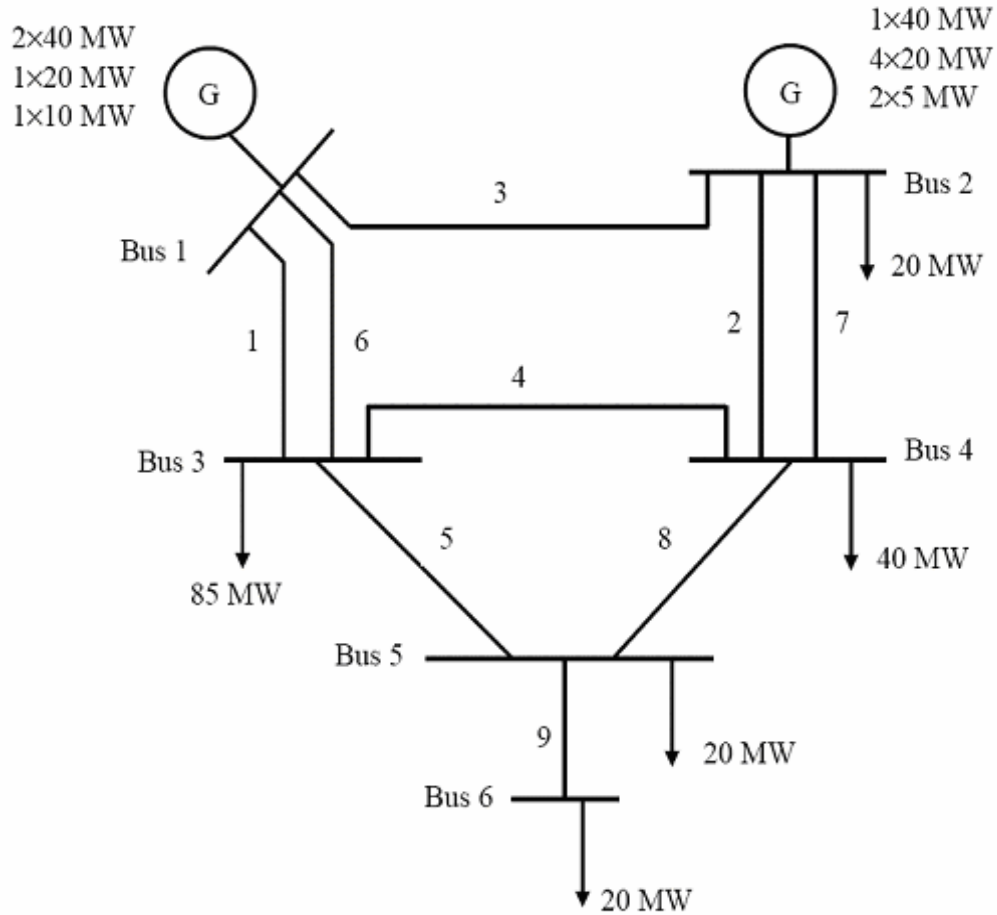


Figure 4.1: Single line diagram of the RBTS.

### 4.3 Impact of Wind Penetration on Wind Energy Utilization and System Reliability

The first study examines the effects of increasing wind penetration on the adequacy of a power system. Different amounts of wind capacity are added to the RBTS, and the resulting system LOLE and LOEE evaluated. Wind data from two different geographic locations, Swift Current and North Battleford, are used.

Figure 4.2 and Figure 4.3 show the relationship between the wind capacity added and the resulting system LOLE and LOEE respectively. The upper curve in Figure 4.2 is

obtained when the wind farm has the North Battleford wind regime. It can be seen that the LOLE decreases with increasing wind penetration. The lower curve in Figure 4.2 is obtained when the wind farm has the Swift Current wind regime. It can be seen that identical WECS located at different sites provide different system reliability benefits. The reliability benefit from the wind farm with the Swift Current data is significantly higher than that obtained from the wind farm with the North Battleford data. Similar effects are observed in terms of the LOEE index in Figure 4.3.

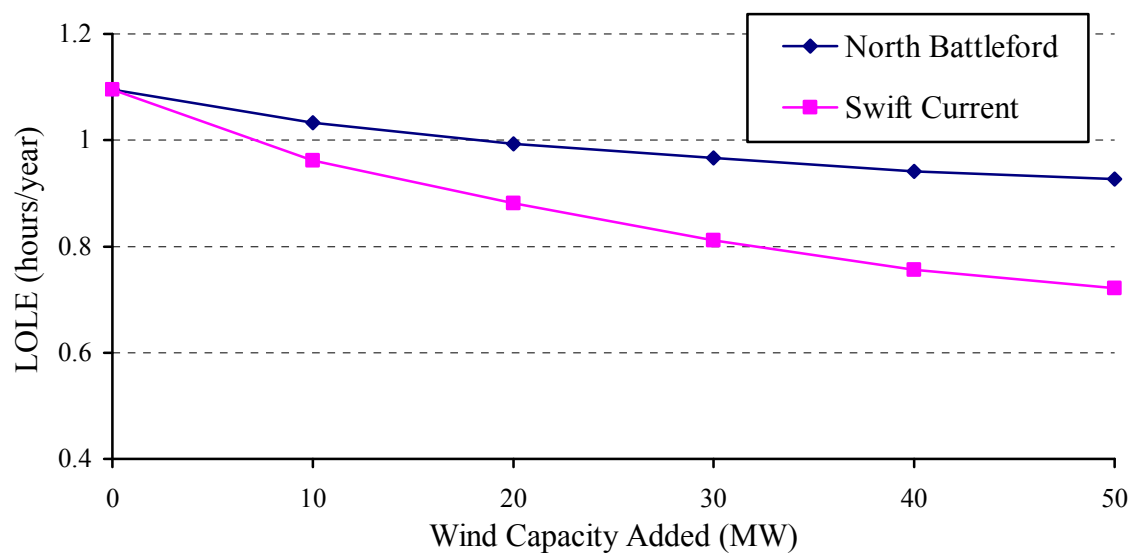


Figure 4.2: LOLE versus wind energy penetration.

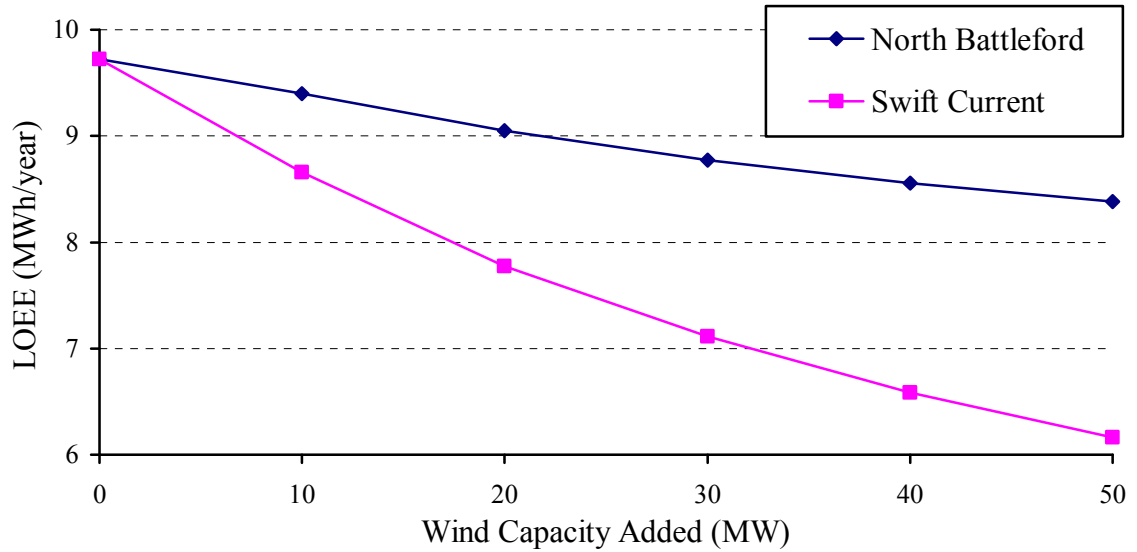


Figure 4.3: LOEE versus wind energy penetration.

This study assumes that the wind power is always first dispatched to serve the load, and all the wind energy can be absorbed by the system. This has been the practice in the past where wind penetration was very small, and therefore, had insignificant impact on system performance.

The minimum hourly load for the RBTS is approximately 63 MW. Based on the above assumption that there are no operating constraints, all the wind energy generated will be used to serve the load if the rated WECS capacity added to the RBTS is less than 63 MW. It is possible to have surplus wind energy only when the rated capacity of WECS is greater than the minimum load. The Expected Surplus Wind Energy (ESWE) depends on the ability of the system to absorb wind, and is calculated during the sequential simulation. Figure 4.4 shows the relationship between the ESWE and the wind capacity added to the RBTS under the assumed conditions. There is no ESWE if the wind capacity added is less than 63 MW. The ESWE increases with increasing wind penetration if the wind capacity is greater than the minimum RBTS load. The ESWE index provides useful information on the potential benefits of wind energy storage.

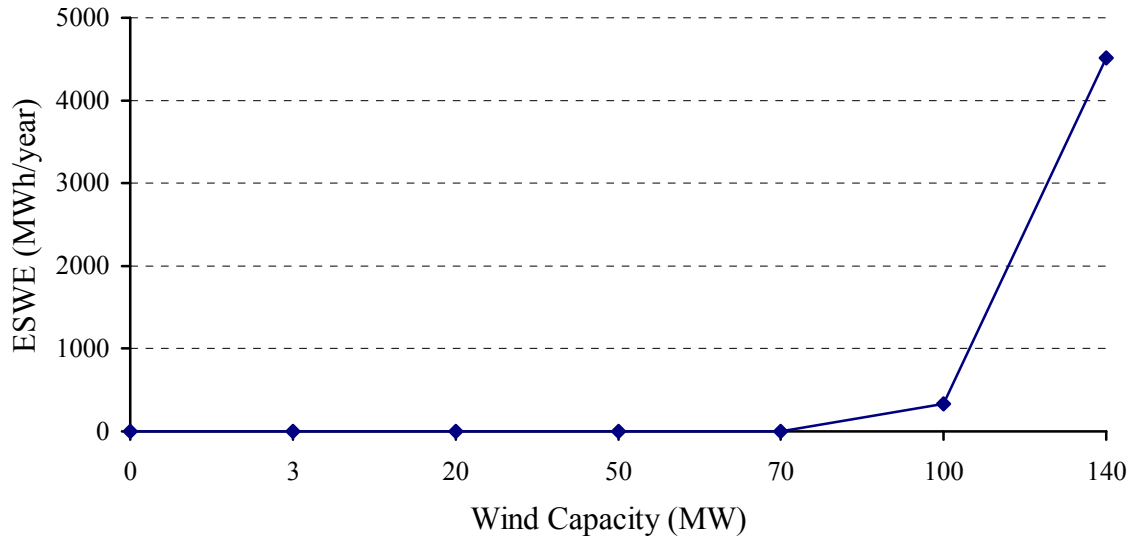


Figure 4.4: ESWE versus wind energy penetration.

Power systems can become unstable if a large share of the system load at any instant is served by the wind power as the wind power penetration level continues to increase. The power output from wind farms is subject to limitations related with the minimum loading levels of the conventional generating units and a dynamic penetration limit in island power systems [53]. If wind power production exceeds the amount that can be absorbed while maintaining adequate reserve and dynamic control of the system, a part of the wind energy produced may need to be cut off [54]. In this study, the wind power dispatch is restricted to a fixed percentage ( $X_w$ ) of the system load considering system operating constraints. The appropriate restriction limit is system dependent and requires a detailed stability analysis for a given system operation and wind condition. Figure 4.5 shows the variation in the ESWE index with increasing wind penetration when the wind dispatch is limited to a fixed percentage of the system load.

The wind power dispatch restrictions depend on the ability of the existing conventional units in the system to respond to the variations in wind power. Figure 4.5

shows that the ESWE is higher for systems with greater restrictions on wind energy usage. The ESWE is 835 MWh/year when 50 MW of wind capacity is added to the RBTS if the wind dispatch is restricted to 40% of the system load. If the restriction is 20%, the ESWE is equal to 12,859 MWh/year when 50 MW of wind capacity is added. If the wind dispatch is limited to 5% of the system load, the ESWE is equal to 5568 MWh/year when 20 MW of wind capacity is added. The wind penetration in this case is 7.7%.

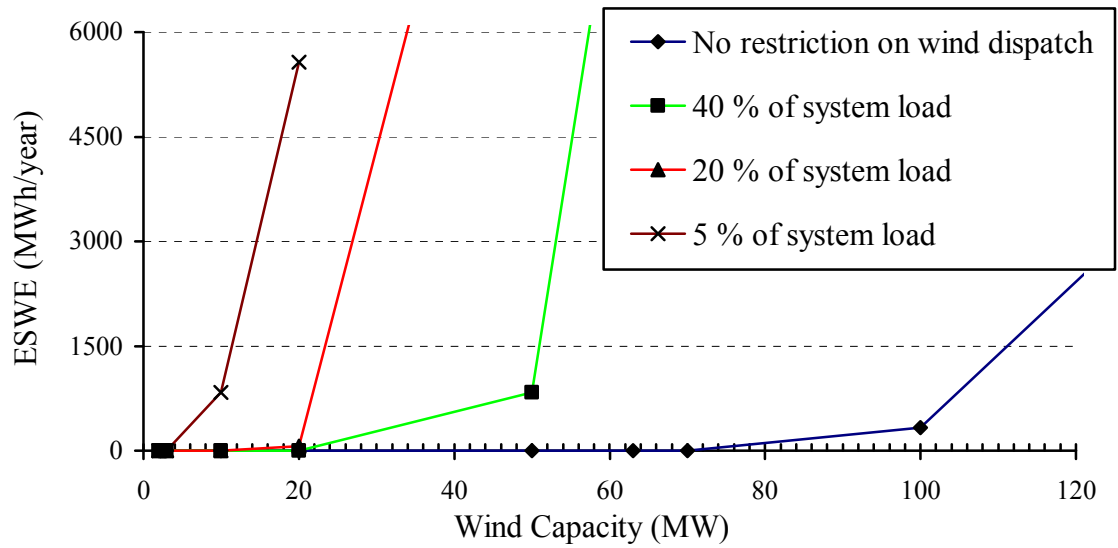


Figure 4.5: ESWE versus wind capacity when wind power dispatch is restricted to a fixed percentage of the system load.

The surplus wind energy shown by the index ESWE is available to be stored in energy storage for future use. The reliability benefits obtained from a combination of wind power and energy storage are analyzed in the following studies and the results are illustrated.

An energy storage facility with a capacity of 10 MWh is added to the power system containing wind power. The surplus wind energy above  $X_w\%$  of the system load



is available for storage. Separate studies are conducted with and without considering the effect of operating constraints associated with the charging and discharging of the energy storage facility. A linear 5-hour charging and discharging period is used in the studies that consider the charging/discharging constraints of energy storage. The detailed energy storage model and the simulation process used in the study are described in Section 3.3.

Figures 4.6 to 4.8 show the effect of energy storage on the system LOLE and LOEE with a wind power dispatch restriction equal to 100%, 40%, and 20% of the system load respectively. It should be noted that there is no restriction on wind energy dispatch in the 100% case, and all available wind energy can be absorbed by the system to supply the load. There are three curves in these figures. The first curve is for the case without energy storage. The second curve is for the case with a 10 MWh energy storage, and its charging/discharging restriction is not considered. The third curve is for the case in which the charging/discharging restriction is considered for the 10 MWh energy storage.

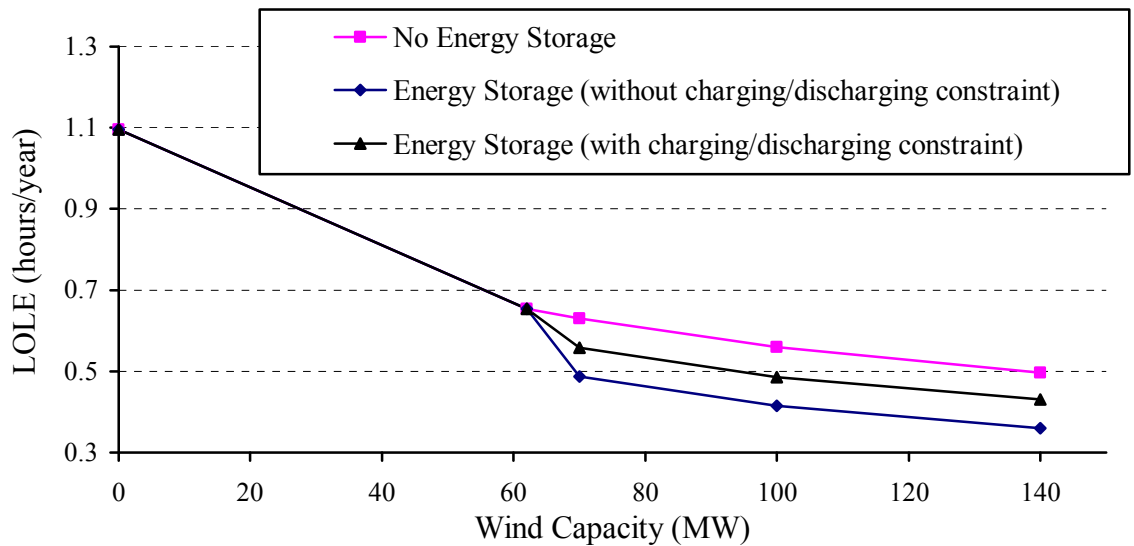


Figure 4.6: Effect of energy storage on system LOLE.

The upper curve in Figure 4.6 shows that the system reliability is improved continuously as wind capacity increases. The incremental reliability benefit however decreases with increasing wind capacity. It is shown in this figure that there is no difference between the three curves when the added wind capacity is less than 63 MW. This is because there is no surplus wind energy available for storage, and the 10 MWh storage facility cannot provide any reliability benefit to the system. There are reliability benefits from the storage facility when the added wind capacity is greater than 63 MW. The increase in system reliability due to energy storage is significantly curtailed when the charging and discharging restrictions of energy storage are considered.

Studies similar to those described and shown in Figure 4.6 were done considering different wind power dispatch restrictions, and the LOLE results are shown in Figure 4.7 and 4.8. The effect of energy storage on the system LOLE with increasing wind penetration is shown in Figure 4.7 considering a wind energy dispatch restriction of 40% of the system load. Figure 4.7 shows that wind energy is available for storage if the installed wind capacity is greater than 25 MW. Figure 4.8 shows the effect of energy storage on the system LOLE when the wind energy dispatch is restricted to 20% of the system load. In this case, wind energy is available for storage if the connected wind farm capacity is greater than 12.5 MW.

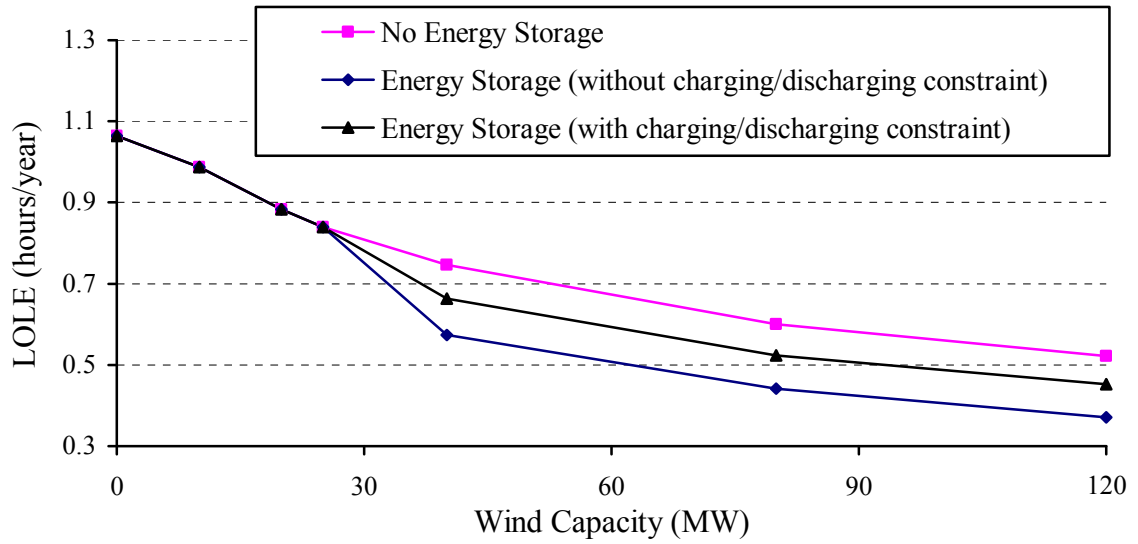


Figure 4.7: Effect of energy storage on LOLE with a wind power dispatch restriction equal to 40%.

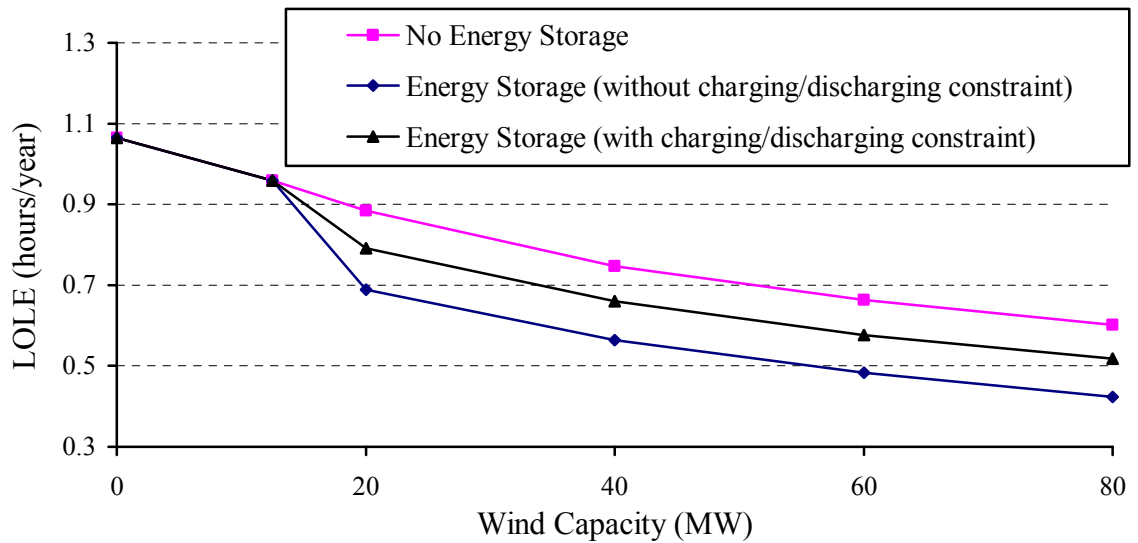


Figure 4.8: Effect of energy storage on LOLE with a wind power dispatch restriction equal to 20%.

#### 4.4 Wind Farm and Energy Storage Operating Strategies

The method used to operate the energy storage facility can have significant

impacts on the system reliability and on the efficiency of wind energy utilization in a power system. The most appropriate operating method, from a system reliability point of view, is to maintain the energy storage facility in its fully charged condition, and use the stored energy to avoid load curtailment situations. This method utilizes the generation and storage model shown in Figure 3.13, and was used to conduct the studies described in Section 4.3. This method, however, does not assist in alleviating power fluctuations from wind generation as the energy storage facility mostly remains in the fully charged state. It would be desirable to have storage space available whenever there is surplus wind energy, and to use stored energy whenever the wind generation drops.

Practically, wind farm operators forecast the wind speed for the next hour, and estimate the power output from the available wind turbines. A commitment is made to the system to provide that amount of power in the next hour. If actual power output is greater than the commitment, the excess energy can be placed in energy storage. If the actual power output is less than the commitment, energy from the storage can be used to meet the commitment. In systems with large wind penetration, the system operator may impose a limit on the wind power that can be absorbed by the system in order to maintain the system stability. The excess wind energy can then be stored.

The energy storage facility could either be operated by the power system operator or a wind farm owner. Three possible operating strategies for wind farm and energy storage are presented as follows in Scenarios 1 to 3. The hourly wind energy dispatch is restricted to  $X_w\%$  of the hourly system load demand in order to maintain system stability in all three scenarios, and the surplus wind energy above  $X_w\%$  of the system load is stored. The energy storage model shown in Figure 3.13 was developed to incorporate the operating strategies described in the three scenarios. The methodology is described in Chapter 3. The MCS approach used in this methodology can be readily modified to incorporate other operating strategies as well.

**Scenario 1:** The energy storage in Scenario 1 is controlled by the independent system operator (ISO). In this operating scenario, the stored energy is used to supply the system load when the sum of the wind power and the conventional power is inadequate to supply the system load.

Energy storage is often controlled by the system operator as indicated in Scenario 1. With large wind penetration, it maybe more appropriate to coordinate the operation of the wind farm and energy storage [39]. This coordination is investigated in Scenario 2 and 3.

**Scenario 2:** If the available wind power is less than  $X_w\%$  of the system load, the stored energy can be used to supply the load. The sum of the wind power and the storage power used cannot exceed the limitation of  $X_w\%$ . In other words, the wind and storage combination is operated to meet a commitment of  $X_w\%$  of the system load. The energy storage time series  $\{ES_i; i=1,2,\dots, T\}$  can be computed using (4.1).

$$ES_{i+1} = ES_i + SG_{wi} \times t_i \quad (4.1)$$

Where  $\{SG_{wi}; i=1,2, \dots, T\}$  is the surplus wind generation time series,  $\{t_i, i=1,\dots, T\}$ , where  $t_i$  is the  $i^{\text{th}}$  time interval and  $T$  is the number of time intervals in a year} is a time interval series in a simulated year.

**Scenario 3:** This is similar to Scenario 2. The difference, however, is that the stored energy can be discharged to serve the load if the available wind power is greater than  $X_w\%$  of the load, and the power from CGU is less than  $(1-X_w)\%$  of load. In this case, the stored energy will also be used to support CGU to avoid load curtailment while

meeting the stability criterion. The energy storage time series  $\{ES_i; i=1,2,\dots,T\}$  can be computed by (4.2).

$$ES_{i+1} = \begin{cases} ES_i + SG_{wi} \times t_i & SG_{wi} \geq 0 \text{ and } SG_{ci} \geq 0 \\ ES_i + SG_{ci} \times t_i & \text{if } SG_{wi} \geq 0 \text{ and } SG_{ci} < 0 \\ ES_i + SG_{wi} \times t_i & SG_{wi} < 0 \end{cases} \quad (4.2)$$

Where  $\{SG_{ci}; i=1,2,\dots,T\}$  is surplus conventional generation time series.

The three operating strategies of wind farm and energy storage are incorporated in the developed model and are applied in the reliability evaluation of a generating system including wind and energy storage in the following section.

#### 4.5 Simulation Results and Analyses

The three operating scenarios for the wind farm and energy storage discussed in Section 4.4 are compared in this section. The relative benefits from energy storage in wind energy utilization and contribution to the overall system reliability are compared in terms of the effects of wind site location, wind penetration level, energy storage operating constraints, energy storage capacity, and wind energy dispatch restrictions. Four quantitative indices are used in the analysis. The first three are the LOLE, LOEE, and the Expected Energy Supplied by Wind (EESW). The EESW as noted earlier is the expected wind energy supplied to the load. When energy storage is added to the system, some of the wind energy is first stored and later supplied to the load. The EESW therefore increases with energy storage. The fourth index is the Expected Wind Energy stored in the Battery (EWEB). The EWEB shows the amount of excess wind energy that can be placed in energy storage during a simulated year. In the figures shown in this section, the charging and discharging restrictions of energy storage are included or not included and the two

conditions are distinguished by (a) and (b) respectively. For example, Scenario 1 (a) indicates that energy storage is in Scenario 1 and the charging and discharging restrictions are not considered.

The following study is conducted on a power system where a wind farm with the Swift Current wind regime and 10 MWh of storage is added to the RBTS. The wind power is restricted to supplying 5% of the system load. The charging and discharging restrictions of energy storage are not considered. The reliability and energy benefits with increasing wind capacity are first evaluated without considering energy storage. The results are compared with cases when an energy storage facility having a maximum capacity of 10 MWh is used to support the power output from the wind farm. The LOLE and EESW respectively are shown in Figure 4.9 and 4.10 for these conditions.

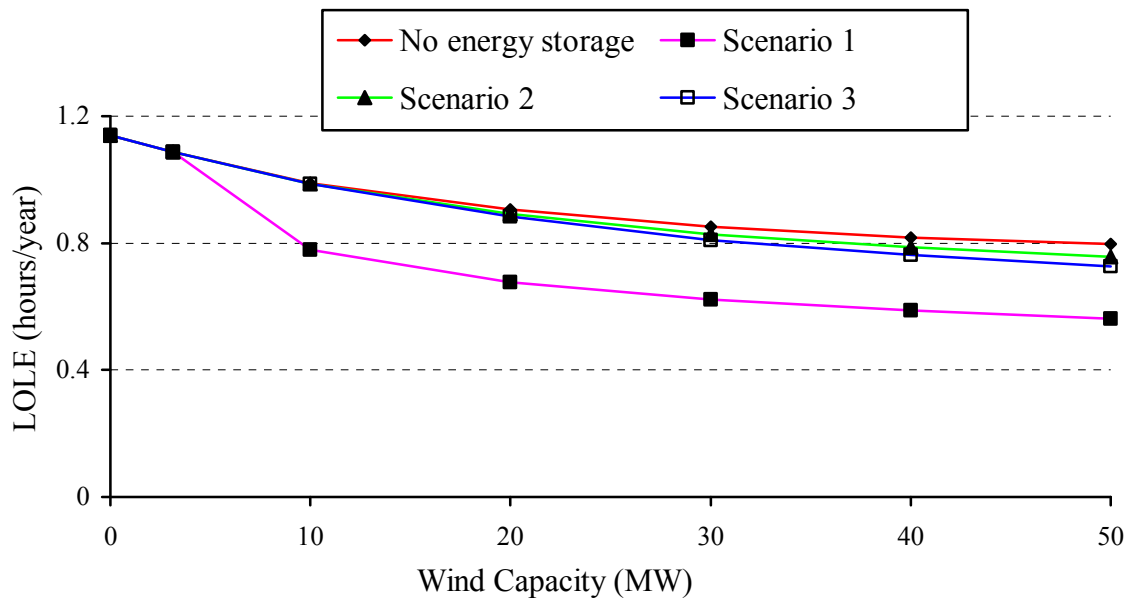


Figure 4.9: LOLE comparison of cases with and without energy storage in different scenarios.

Figure 4.9 shows that the system reliability improves as the added wind capacity

increases, and that energy storage in Scenario 1 can greatly improve the system reliability. The energy storage in Scenarios 2 and 3 improve the system reliability slightly, and the energy storage in Scenario 3 provides higher system reliability benefits than in Scenario 2. As the added wind power increases, the difference in the reliability benefits from added energy storage between Scenarios 2 and 3 increases. It is shown in Figure 4.10 that there is almost no difference between the EESW for the case without energy storage and the case with energy storage in Scenario 1. The utilization of energy storage in Scenario 1 has relatively little effect on the amount of wind energy consumed by the system load. The operating strategies in Scenarios 2 and 3 result in relatively high wind energy consumption by the system. The difference between the energy utilization effects of Scenarios 2 and 3 is small.

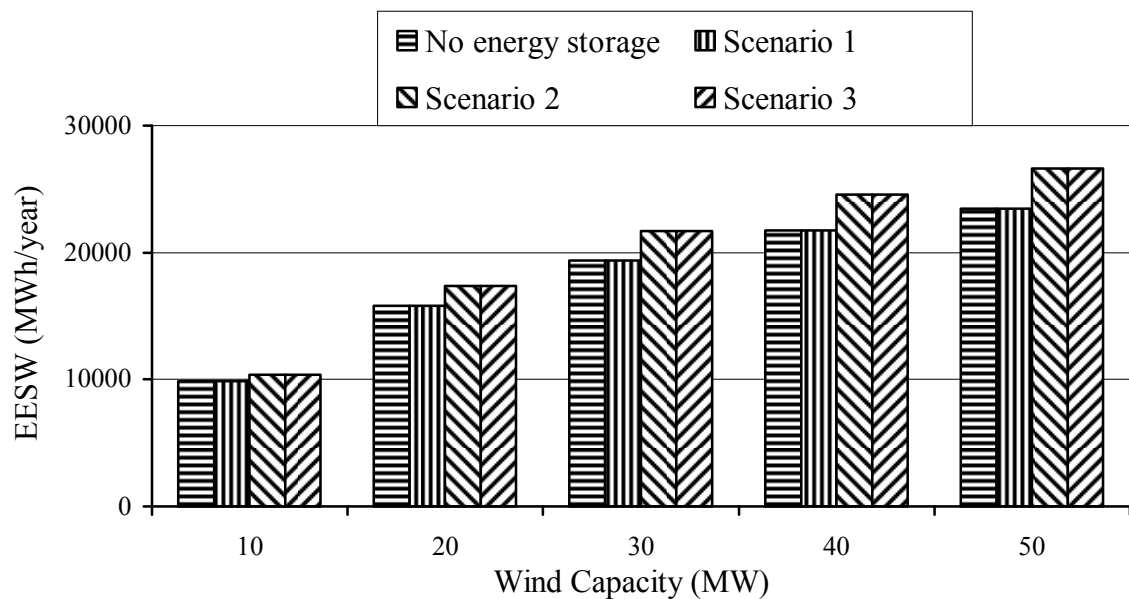


Figure 4.10: EESW comparison of cases with and without energy storage in different scenarios.

The index EESW is the amount of wind energy that can be directly accepted by the power grid. A high EESW value usually means significant reductions in conventional fossil fuel and greenhouse gas emissions.



#### 4.5.1 Effect of Wind Site Location

The following study considers a wind farm connected to the RBTS. Wind data from two different sites, Swift Current and North Battleford, are used. An energy storage facility with a maximum capacity of 10 MWh is used. Wind power is restricted to 5% of the system load. The effect of storage capacity and wind energy dispatch restriction are analyzed in Section 4.5.3 and 4.5.4 separately. The effect of a site-specific wind regime on the system reliability is evaluated in this section. The charging and discharging restrictions of energy storage are not considered. Figure 4.11 shows that greater reliability benefits can be obtained, if energy storage is incorporated in the wind farm with better wind regimes. It should, however, be noted that the North Battleford wind regime using the Scenario 1 operating strategy will provide higher system reliability than the Swift Current wind regime operated using the Scenarios 2 or 3 strategies.

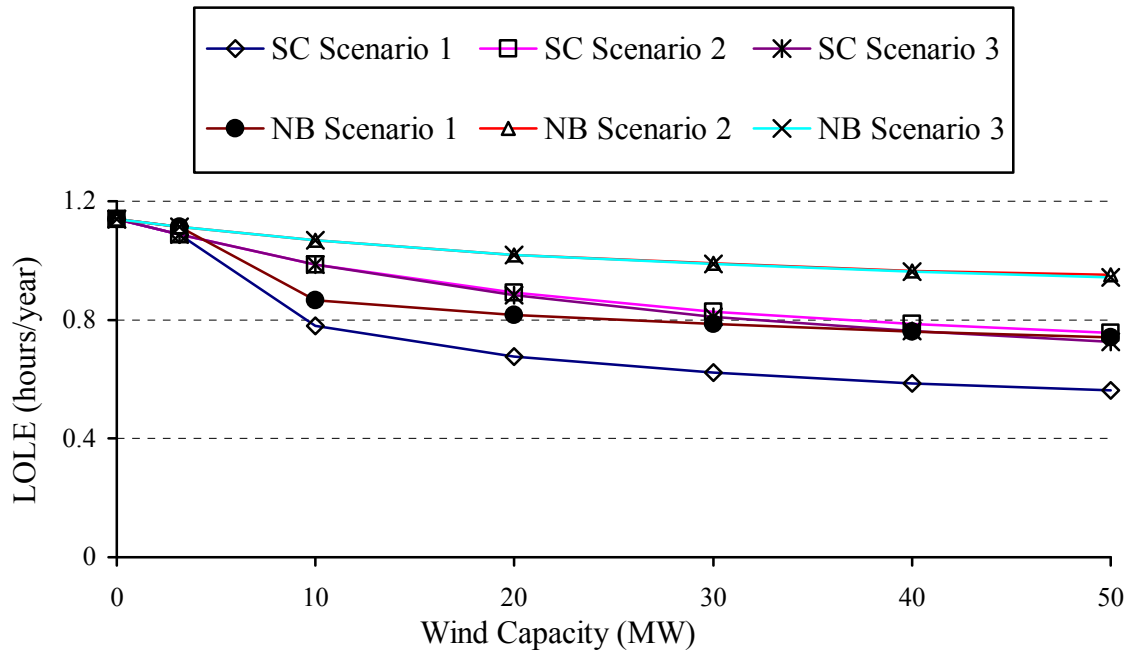


Figure 4.11: Effect of wind farm location on the LOLE. (SC: Swift Current; NB: North Battleford).

Table 4.1 shows that the EWEB increases as the added wind capacity increases. If energy storage is incorporated in the wind farm with better wind regimes, more wind energy can be stored. It can be seen that the EWEB values are very close for the energy storage in Scenarios 2 and 3. This is because the operating strategies for the two scenarios are the same except when a loss of load situation occurs due to inadequate conventional generation, and the probability of this situation is very small. This is the reason why Scenario 3 provides slightly lower LOLE than Scenario 2. The utilization of energy storage during the situation when  $SG_{wi} \geq 0$  and  $SG_{ci} < 0$  in Scenario 3 causes a slight reduction in the wind power that can be stored. Therefore, the EWEB for energy storage in Scenario 3 is slightly less than that for energy storage in Scenario 2 as shown in Table 4.1. Compared with energy storage in Scenarios 2 and 3, the energy storage facility in Scenario 1 receives very small amounts of wind energy during system operation. This energy, however, is only utilized when a loss of load situation occurs, and therefore, results in significant improvement in system reliability. Energy storage in Scenario 1 is almost always maintained at the fully charged condition as the probability of loss of load situation occurring is very small. Energy storage in Scenario 1 is a good addition in regard to improving the system reliability, but it does not provide an active facility for wind energy storage.

Table 4.1: Effect of wind farm location on the EWEB

Wind Capacity (MW)	EWEB (MWh)					
	North Battleford			Swift Current		
	Scenario 1	Scenario 2	Scenario 3	Scenario 1	Scenario 2	Scenario 3
10	0.92	140.51	140.51	0.94	495.91	495.91
20	0.96	712.12	712.1	0.98	1538.05	1538.02
30	0.99	1237.03	1237.00	1.01	2296.19	2296.14
40	1.02	1666.42	1666.39	1.02	2811.03	2810.97
50	1.038	1987.62	1987.58	1.02	3152.33	3152.29

#### 4.5.2 Effect of Charging/discharging of Energy Storage

Different energy storage technologies have different types of charging and discharging characteristics. The following study compares an ideal storage (with no charging/discharging constraints) with a battery type storage that has specific charging/discharging constraints. A wind farm with the Swift Current wind regime and 10 MWh of energy storage are added to the RBTS system in the following studies. The wind power is restricted to supply 5% of the system load. Figure 4.12 shows that the LOLE index decreases as the added wind capacity increases, and the charging and discharging characteristics of energy storage greatly limit the reliability benefit from energy storage in Scenario 1. In Scenarios 2 and 3, the charging and discharging characteristics of energy storage reduce the reliability benefits but the influence is relatively small.

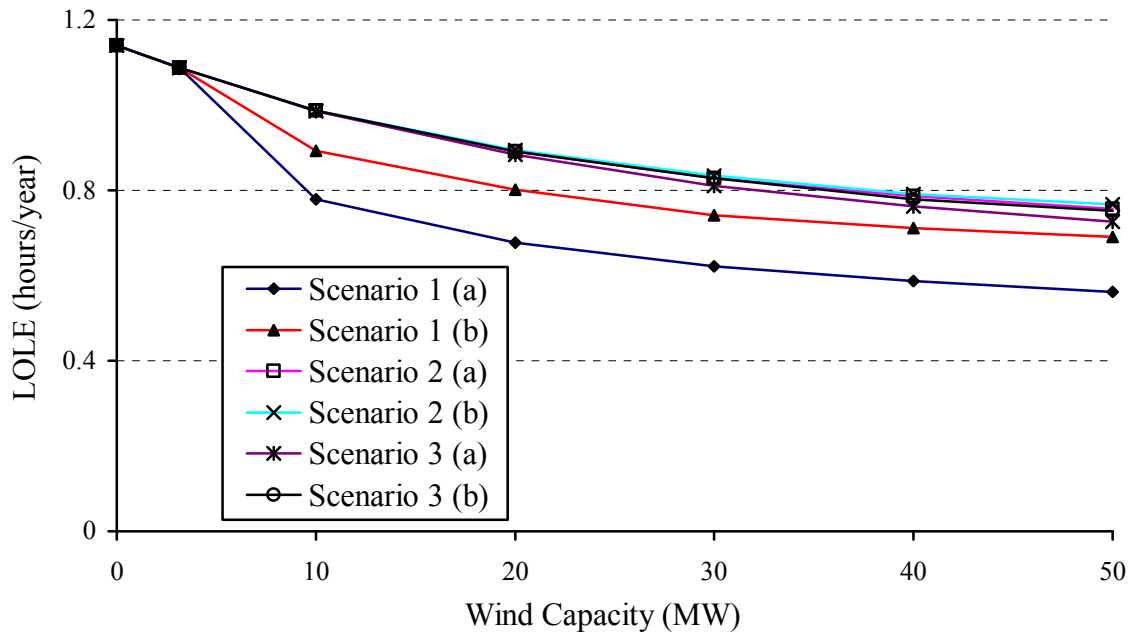


Figure 4.12: Effect of energy storage charging/discharging constraints on the LOLE.

Table 4.2 shows that surplus wind energy can be stored in the energy storage facility as the added wind capacity increases. Similar to the results shown in Table 4.1, the amount of wind energy that can be stored in Scenario 1 is minimal. The charging and discharging characteristics of energy storage reduce the amount of wind energy stored in all three scenarios. The relative restriction in EWEB due to the charging and discharging characteristics increases with wind capacity.

Table 4.2: Effect of energy storage charging/discharging constraints on the EWEB

Wind Capacity (Mw)	EWEB (MWh)					
	Scenario 1 (a)	Scenario 2 (a)	Scenario 3 (a)	Scenario 1 (b)	Scenario 2 (b)	Scenario 3 (b)
10	0.94	495.91	495.91	0.76	385.88	385.87
20	0.98	1538.05	1538.02	0.77	1158.3	1158.27
30	1.01	2296.19	2296.14	0.77	1671.68	1671.64
40	1.02	2811.03	2810.97	0.77	2018.16	2018.12
50	1.02	3152.33	3152.29	0.77	2228.27	2228.25

#### 4.5.3 Effect of Energy Storage Capacity

The effect of the storage capacity on the system reliability and wind energy utilization is analyzed in this section. A wind farm with the Swift Current wind regime is added to the RBTS. The total capacity of the wind farm is 20 MW in the following studies. The wind power is restricted to supply 5% of the system load. Figure 4.13 and Table 4.3 show the variations in the system LOLE and the EWEB with the size of the energy storage capacity added to the system.

The three parallel straight lines in Figure 4.13 show the system LOLE for the original RBTS, the RBTS with wind capacity, and the RBTS with wind capacity restricted to 5% of the system load. The added wind capacity can improve the system reliability, but the reliability benefit is reduced if only 5% of the system load can be served by wind power. As the capacity of the added energy storage increases, the system LOLE continues to decrease. The differences in the reliability benefit from energy storage in Scenarios 2 and 3 are small. The energy storage charging and discharging restrictions greatly affect the reliability benefit from energy storage in Scenario 1, but have little influence on Scenarios 2 and 3.

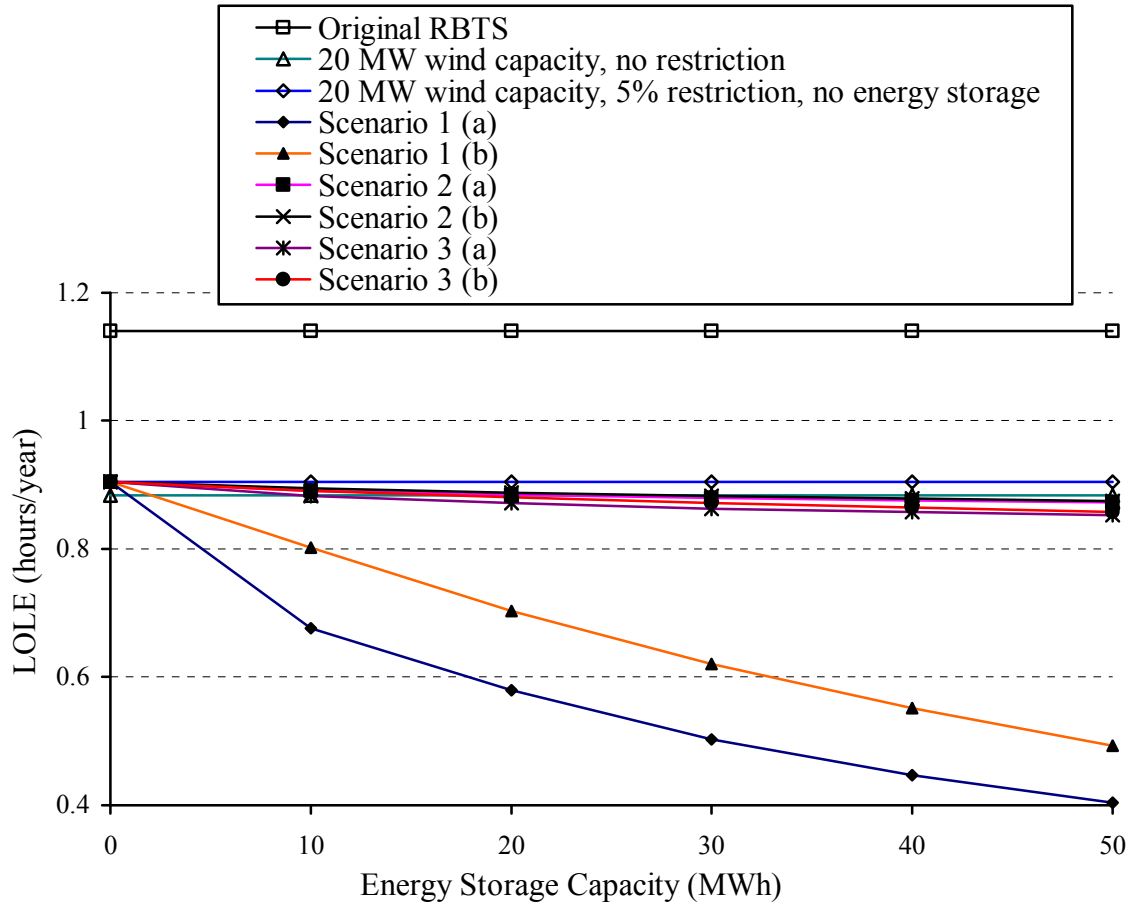


Figure 4.13: Effect of energy storage capacity on the LOLE.

Table 4.3: Effect of energy storage capacity on the EWEB

Energy Storage Capacity (MWh)	EWEB (MWh)					
	Scenario 1 (a)	Scenario 2 (a)	Scenario 3 (a)	Scenario 1 (b)	Scenario 2 (b)	Scenario 3 (b)
10	0.98	1538.05	1538.02	0.77	1158.30	1158.27
20	1.61	2238.42	2238.38	1.41	1946.02	1945.97
30	2.12	2741.02	2740.97	1.94	2523.28	2523.23
40	2.54	3137.15	3137.10	2.40	2966.71	2966.65
50	2.91	3455.82	3455.76	2.80	3324.30	3324.23

Table 4.3 shows that storage capacity has a significant impact on the EWEB for all three scenarios. The EWEB tends to saturate as the energy storage capacity increases since the excess wind energy that can be stored is limited. The difference in the wind energy that can be stored in Scenarios 2 and 3 is small, as explained in Section 4.5.1.

#### **4.5.4 Effect of Wind Power Dispatch Restrictions**

The effect of wind power dispatch restrictions on the reliability benefits from energy storage is analyzed in this section. A wind farm with the SC wind regime is added to the RBTS. The total capacity of the wind farm is 20 MW. An energy storage facility with a capacity of 10 MWh is incorporated in the wind farm. The charging/discharging constraint on energy storage is not considered in the studies described in this section. The analyses in the previous sections show that the differences in reliability benefits from energy storage in Scenario 2 and 3 are very small. The variations in the system LOLE and LOEE with energy storage in different scenarios, as the wind energy dispatch restriction increases, are shown in Figure 4.14 and 4.15 respectively. A 0% wind energy dispatch restriction is obviously not a practical constraint. It is used in the following discussions to initiate the examinations of the effect of increasing dispatch restrictions.

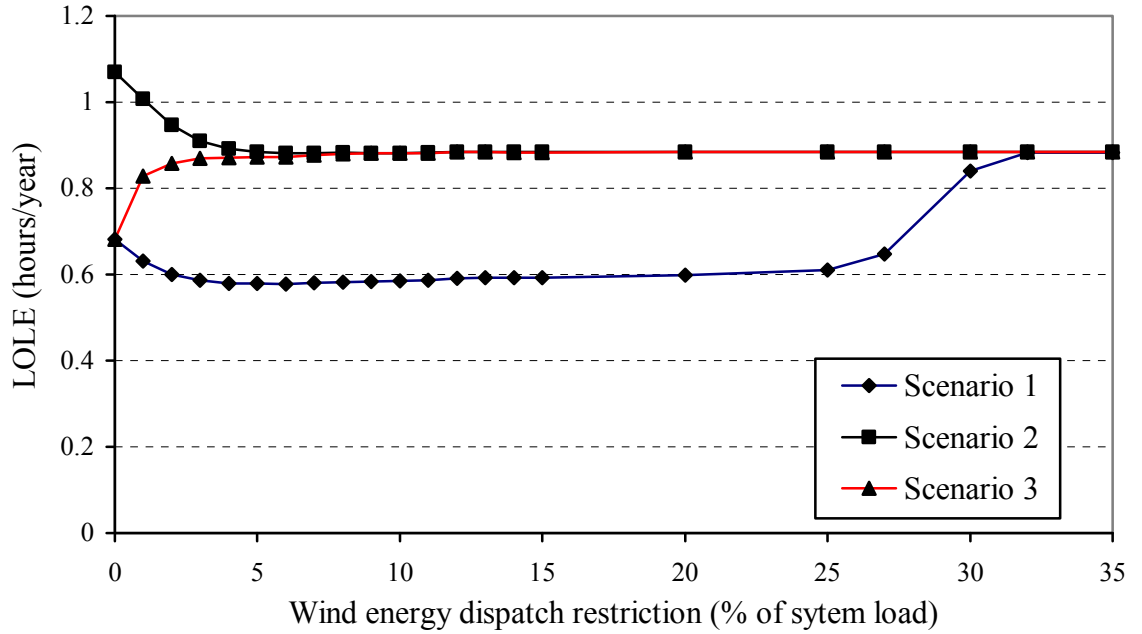


Figure 4.14: Effect of wind energy dispatch restriction on the LOLE.

In Scenario 1, all the wind power is used to charge the energy storage facility when the wind energy dispatch restriction is 0%. As the wind energy dispatch restriction increases from 0%, the LOLE and LOEE decreases as more wind energy can be used to supply the load directly. The LOLE and LOEE reach their minimum values when the wind energy dispatch restriction is approximately 6%. The LOLE and LOEE then begin to increase as less wind power is available to charge the energy storage facility. When the wind energy dispatch restriction reaches 32%, no wind energy can be stored, and the energy storage facility makes no contribution to the system reliability.

In Scenario 2, all the wind power is used to charge energy storage when the wind energy dispatch restriction is 0%. Since energy storage has no opportunity to be used and it is always full, no wind energy can be stored, the wind farm and energy storage have no contribution to the system reliability. The LOLE and LOEE values are the same as those of the original RBTS. As the wind energy dispatch restriction increases from 0% more



wind energy can be used to supply the load directly, the energy in storage can be discharged to supply the load, and the LOLE decreases. The LOLE and LOEE reach their minimum values when the wind energy dispatch restriction is approximately 6%. The minimum values are smaller than those for the RBTS system with 20 MW wind capacity, the SC wind regime and no wind dispatch restriction. The LOLE and LOEE then begin to increase as less wind power is available to charge the energy storage facility. When the wind energy dispatch restriction reaches 12%, there is no reliability benefit from energy storage.

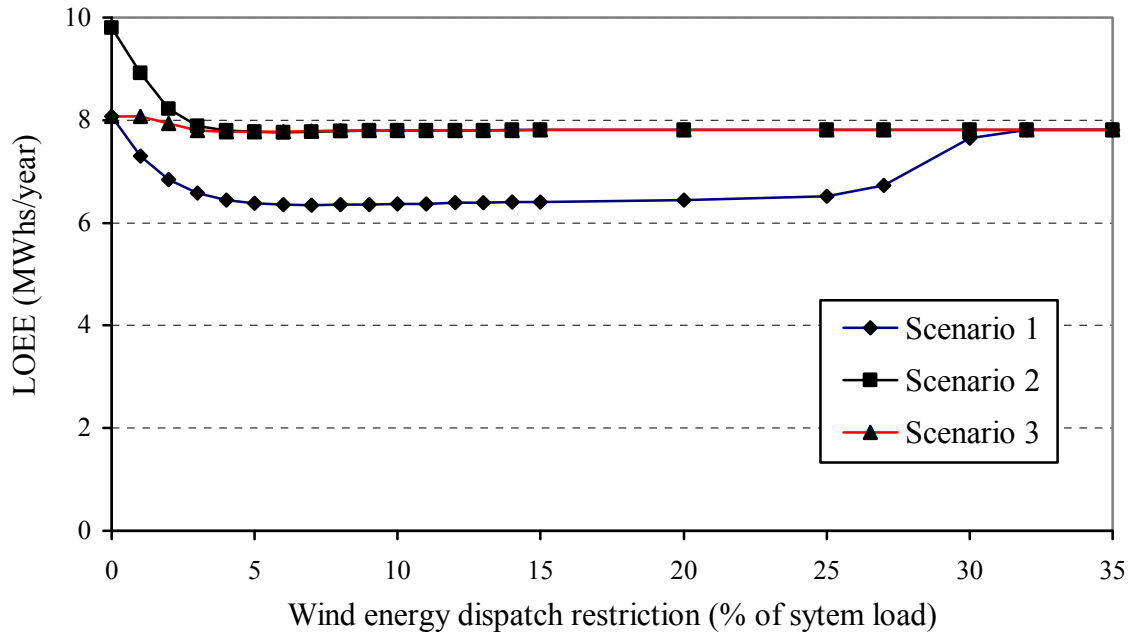


Figure 4.15: Effect of wind energy dispatch restriction on the LOEE.

In Scenario 3, all the wind power is used to charge the energy storage facility when the wind energy dispatch restriction is 0%. The LOLE increases and the LOEE decreases as the wind energy dispatch restriction increases from 0%, since there are fewer situations where the power output from the wind farm exceeds the wind energy dispatch restriction and more wind energy is used to supply the load directly. There is no reliability benefit

from energy storage when the wind energy dispatch restriction reaches 12%.

Figure 4.14 and 4.15 show that the energy storage in Scenarios 1 and 2 provide the maximum reliability benefit when the wind energy dispatch restriction is around 6% of the system load. In Scenario 3, the system LOEE reaches its minimum value when the wind energy dispatch restriction is approximately 6%.

#### **4.6 Summary**

An energy storage facility can be used to smooth the fluctuating nature of wind power, and improve the continuity of power supply from a WECS. A MCS method is utilized in this chapter to recognize the chronological random nature of wind speed in the adequacy evaluation of a generating system including wind power and energy storage.

The system reliability increases with increasing wind penetration in a system. The incremental benefit however decreases. The expected surplus wind energy (ESWE) or the energy that cannot be absorbed by the system increases as the installed wind capacity is increased above the minimum system load in power systems with relatively high wind penetration. The wind power has to be restricted to avoid system stability problems when the wind penetration is relatively high. A wind power dispatch restriction is introduced in terms of a percentage of the system load. When wind power dispatch is restricted to 5% of the system load, there is significant amount of ESWE that cannot be absorbed by the system even when the installed wind capacity is much smaller than the minimum system load. A relatively high ESWE indicates significant benefits from using energy storage to capture and use the surplus wind energy.

An energy storage model for reliability evaluation presented in Chapter 3 is applied in this chapter. The addition of an energy storage facility in a power system can

improve system reliability. The reliability benefit from energy storage is greatly limited by the charging/discharging characteristics of the storage facility.

Three different operating strategies are analyzed and compared in terms of the reliability benefit from energy storage and the amount of surplus wind energy that can be captured and stored for later use. The wind farm and energy storage operating strategy described in Scenario 1 provides higher system reliability than Scenarios 2 and 3. The charging and discharging characteristics of energy storage can greatly affect the reliability benefits from energy storage in Scenario 1, but have negligible effects on the reliability benefits in Scenarios 2 and 3. The reliability benefits from energy storage in all three scenarios are highly dependent on the wind energy dispatch restrictions. Compared with Scenario 2, energy storage in Scenario 3 has more ability to improve the system reliability for a wide range of wind energy dispatch restrictions. The stored energy has more opportunities to discharge in Scenarios 2 and 3 than in Scenario 1. The charging and discharging restrictions on energy storage therefore have a significant influence on the amount of wind energy that can be stored in Scenarios 2 and 3. There is almost no difference between Scenarios 2 and 3 in regard to the wind energy that can be placed in the energy storage facility.

Energy storage in Scenario 3 has the ability to improve the system reliability, and large amounts of surplus wind energy can be stored. The analyses in this chapter show that energy storage in Scenario 3 is a potentially useful option for both power system operators and wind farm owners.

## **5. ADEQUACY EVALUATION CONSIDERING WIND AND HYDRO POWER COORDINATION**

### **5.1 Introduction**

The supply of electrical energy should be adequately planned to meet the system demand, and the supply and demand of electrical energy must always be balanced during system operation. The intermittent nature of wind power makes energy storage facilities important for large scale integration of wind power into power systems. Unlike other conventional power sources, hydro power stations with a reservoir act as an energy storage facility, and also have the ability to change their power output quickly to balance power fluctuations in the system.

A sequential Monte Carlo simulation technique developed to incorporate the coordination of wind power and an energy limited hydro system in a generating capacity adequacy assessment was developed in this work and is presented in Chapter 3. The IEEE four-state model [42] is utilized to model hydro units that are intermittently operated in response to wind generation. An energy limited hydro system model presented in [40] is utilized and modified in the studies, and additional data on hydro plant characteristics, such as water in-flow, reservoir volume, turbine discharge rates are introduced in Chapter 3.

In this chapter, base case studies are first conducted to investigate the impact of energy limited hydro units and the wind power dispatch restriction on the overall system

adequacy. A range of sensitivity studies are conducted to assess the reliability benefit from the coordination between wind power and hydro units. Important parameters that can affect the system adequacy, such as the number of hydro units coordinated with wind power output, water inflow and reservoir volume, system load level, wind power penetration level, wind-hydro coordination strategy, starting failure of hydro units, and initial water volume in the reservoir are all examined in this chapter.

## **5.2 Base Case Studies**

The IEEE-RTS [40] is selected as the test system. The IEEE-RTS has a total of 32 generating units, including 6 hydro units each rated at 50 MW. The detailed generation and reliability data of the test system is presented in Appendix A. The chronological load model shown in Figure 2.7 is used in the studies in this chapter, and the detailed data for this load model are shown in Appendix A. The 6 hydro units in the IEEE-RTS are assumed to be installed in a single hydro plant with a reservoir. Hydro plant data such as water inflow data, reservoir volume limitations, hydro turbine discharge limitations, and reservoir coefficients are shown in Chapter 3.

### **5.2.1 Impact of Energy Limited Hydro Units on System Reliability**

This study is conducted to analyze the results from using different generation models to represent the hydro power units. Three cases are selected with different generation models. In the first case, all the 32 generating units are represented by the two-state model. In the second case, 26 generating units are represented by the two-state model, and the 6 hydro units are represented by the four-state model. Energy limitations of hydro units are not considered in this case, and therefore the power output from these units are determined by the system load condition when the units are in the “In Service” state of the 4-state model. In the third case, the 6 hydro units are represented by the

four-state model, and energy limitations in the hydro reservoir are also considered. The power outputs of the hydro units also depend on the water condition in the reservoir in the third case. The system does not include wind power in this study. The system configurations for the three different cases are shown in Table 5.1.

Table 5.1: System configurations for the cases in Section 5.2.1

Case number	Number of units with a 2-state model	Number of units with a 4-state model	Energy limitation of hydro units is considered? (Yes/No)
1	32	0	
2	26	6	No
3	26	6	Yes

Figure 5.1 to 5.3 show the system reliability indices: LOLE, LOEE, and LOLF for the three cases. It can be seen from these figures that different results are obtained for the reliability indices by using different generation models to represent the hydro units. Representing the 6 hydro units with a 4-state model in Case 2 decreases the exposure to failure for these units, and therefore, results in a higher reliability than in Case 1. The differences in results between Cases 1 and 2 are, however, small. The consideration of water limitations in the reservoir in Case 3 results in lower system reliability than in Cases 1 and 2 due to reduced power outputs from the hydro units. The reliability indices obtained from the model used in Case 3 are significantly higher than those obtained from the simpler models used in Cases 1 and 2. It is therefore important to incorporate energy limitations in the generation model when the hydro units operating strategy is an important aspect of system adequacy evaluation. The generation model developed for Case 3 was therefore is used in the subsequent studies.

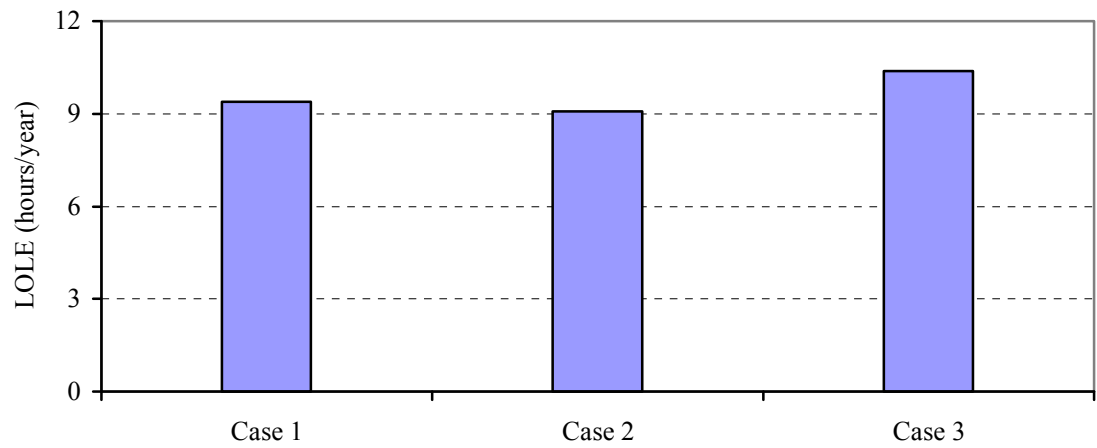


Figure 5.1: Comparison of LOLE for Cases 1, 2 and 3.

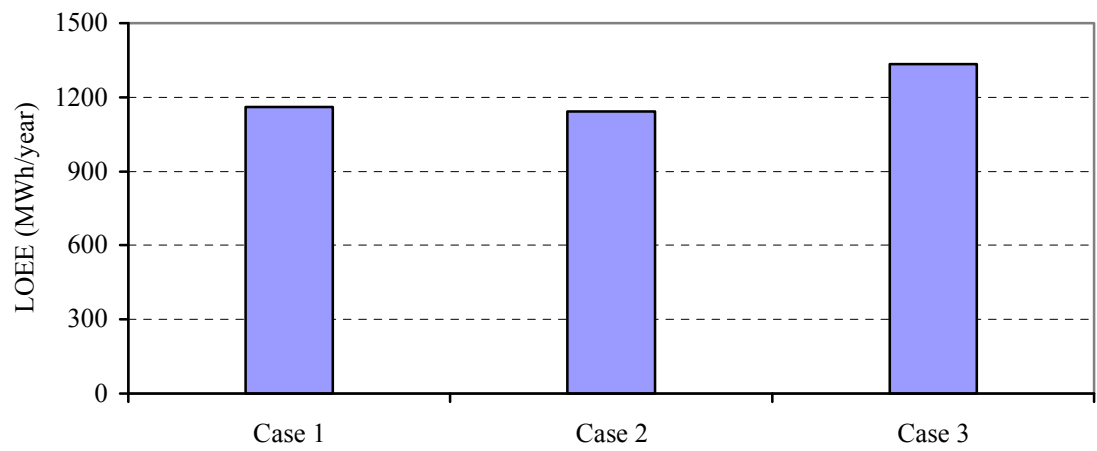


Figure 5.2: Comparison of LOEE for Cases 1, 2 and 3.

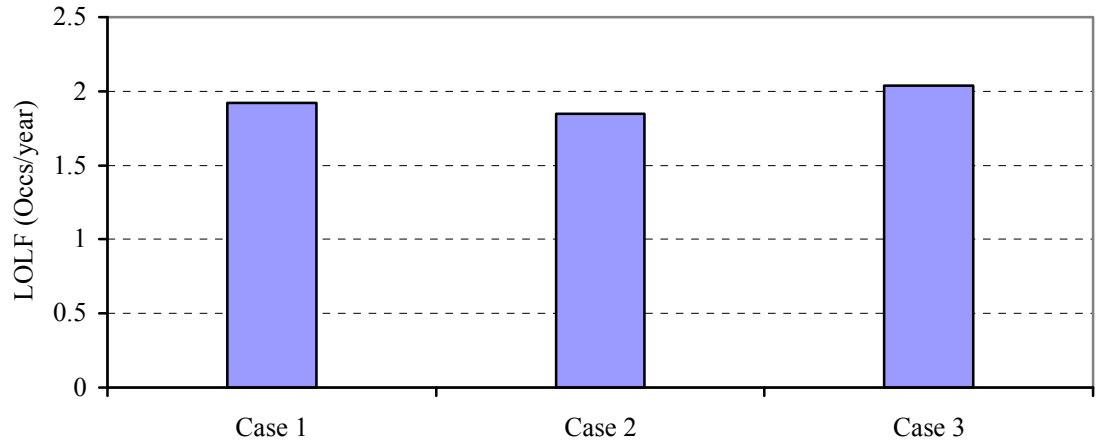


Figure 5.3: Comparison of LOLF for Cases 1, 2 and 3.

### 5.2.2 Impact of Wind Power Dispatch Restriction on System Reliability

Wind penetrations in power systems were relatively small in the past. The impact of wind on system performance is insignificant at relatively low penetrations, and therefore, the system can readily absorb all the power generated from an interconnected wind farm. With increasing wind penetration, the power output from wind farms is subject to limitations in order to maintain adequate reserve and dynamic control of the system [53, 54]. The limitation or restriction on wind power depends on the characteristics of the conventional generating units responsible for providing the necessary regulating reserve for balancing the wind power fluctuations. For example, hydro units respond much faster than thermal units. System operators usually operate selected hydro units in coordination with wind power to enhance the ability of the system to absorb wind power. The wind energy dispatch is restricted to a fixed percentage of the system load in this chapter, if there is no coordination between the interconnected wind farm and the hydro plant. The appropriate restriction limit is system dependent and requires a detailed stability analysis for a given system operation and wind conditions.

The initial study presented in this section investigates the effect of wind power



dispatch restrictions on the benefits obtained from wind power. A wind farm with the Swift Current wind regime is integrated in the IEEE-RTS. Two wind capacity cases are considered: 300 MW and 900 MW, and the corresponding wind penetration levels are 8% and 21% respectively. The Expected Wind Energy Utilized (EWEU) is the average annual wind energy consumed by the system, and is calculated using (5.1) and (5.2) as follows.

$$WEU_i = \begin{cases} P_{wi} & \text{if } P_{wi} \leq X_w P_{li} \\ X_w P_{li} & P_{wi} > X_w P_{li} \end{cases} \quad (5.1)$$

$$EWEU = \frac{1}{N} \sum_{i=1}^{8736 \times N} WEU_i \quad (5.2)$$

Where  $X_w$  is the wind power dispatch restriction in percentage of system load, and  $WEU_i$  is the wind energy utilized in the  $i$  th hour.

A power system can absorb more wind energy as the wind power dispatch restriction ratio  $X_w$  is increased.  $X_w = 100\%$  means that there is no restriction and all the wind power can be absorbed if the wind power output is less than the system load. It is shown in Figure 5.4 to Figure 5.7 that the reliability of the system and the amount of utilized wind energy increases significantly as the wind power dispatch restriction ratio increases. The restriction has a greater influence at high wind penetration. This effect can be seen by comparing the results for the 900 MW wind capacity case with the case with 300 MW of wind capacity.

In the subsequent studies, the wind power dispatch is restricted to 3% of the system load if there is no coordination between the interconnected wind farm and the hydro plant. It is assumed that all the power output from the wind farm can be absorbed

by the system if a number of hydro units are assigned to coordinate with wind power.

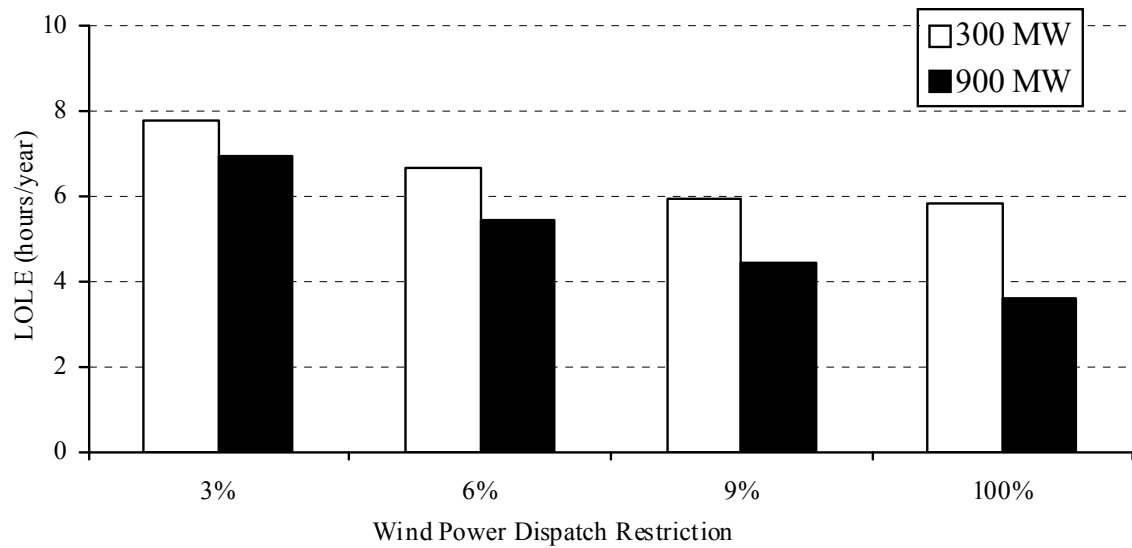


Figure 5.4: Effect of wind power dispatch restriction on the LOLE.

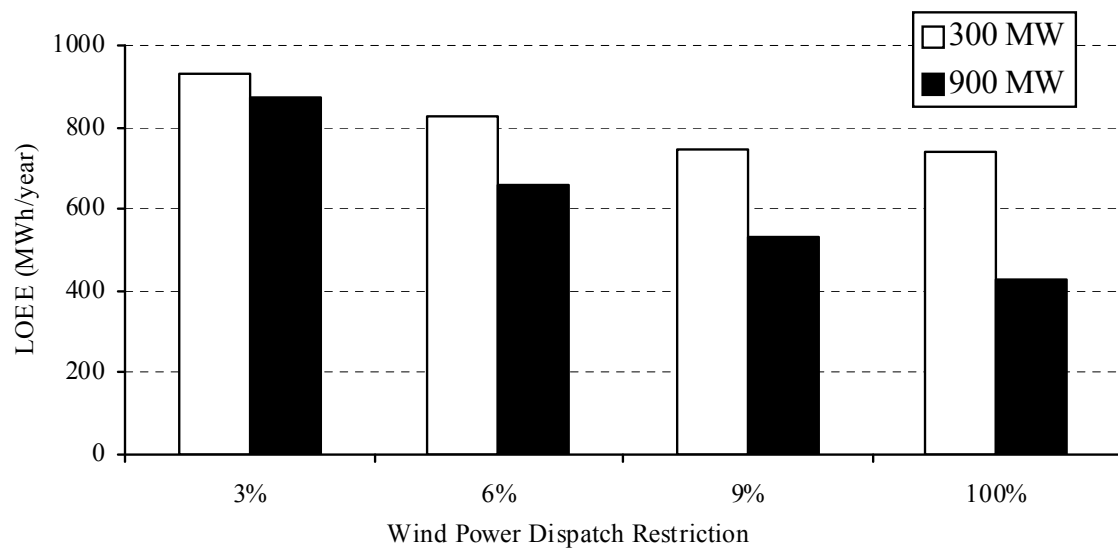


Figure 5.5: Effect of wind power dispatch restriction on the LOEE.

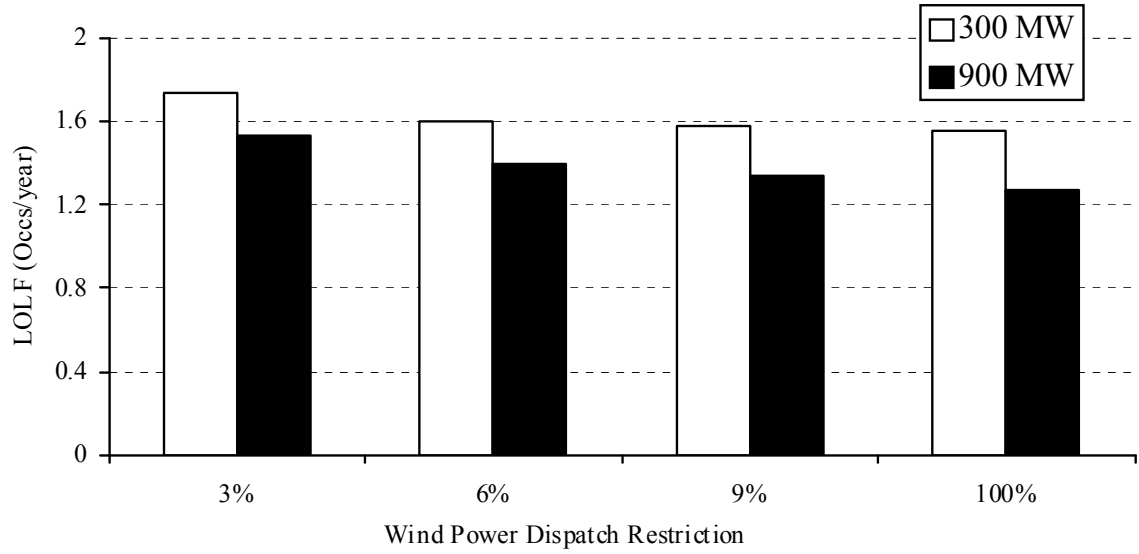


Figure 5.6: Effect of wind power dispatch restriction on the LOLF.

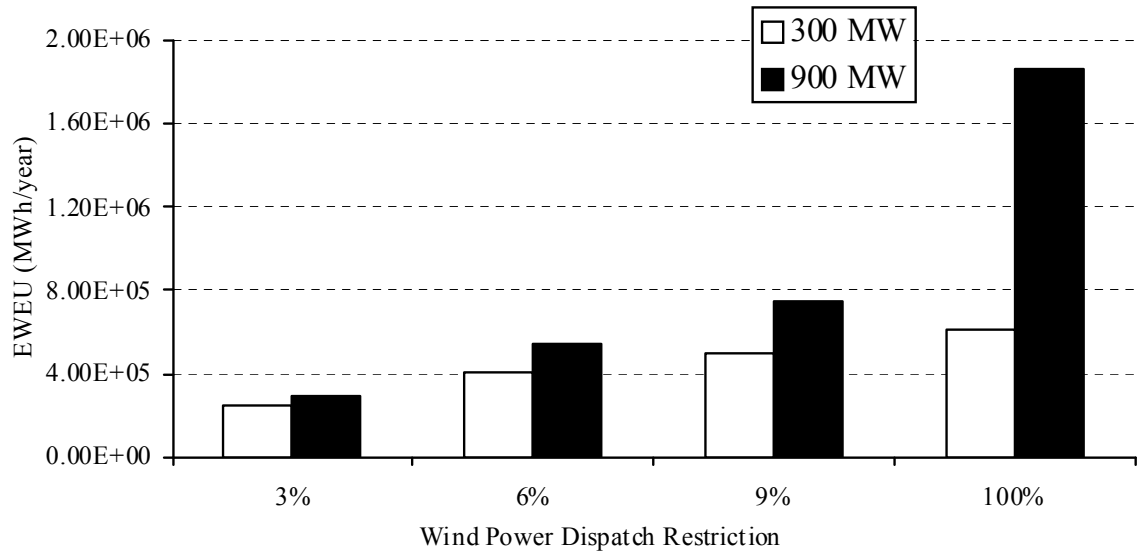


Figure 5.7: Effect of wind power dispatch restriction on the EWEU.

### 5.3 Effect of the Number of Hydro Units Coordinated with Wind Power

A selected number of generating units in the hydro plant are assigned to operate in coordination with the wind power variation, and the rest of the hydro units are assigned as peaking units in this study. The data shown in Tables 3.1 and 3.2 for the

water inflow and reservoir size are utilized. The hydro units coordinated with wind power are started when the wind power output is less than 20% of the rated wind capacity. A wind farm with the Swift Current wind regime is integrated in the IEEE-RTS. The wind farm has a capacity of 300 MW. Figures 5.8 to 5.10 show the effect of the number of hydro units coordinated with wind power on the system reliability indices, such as the LOLE, LOEE, and LOLF. In order to show the impact of the coordination process on system adequacy, hydro unit energy limitations are not considered in the initial part of the study.

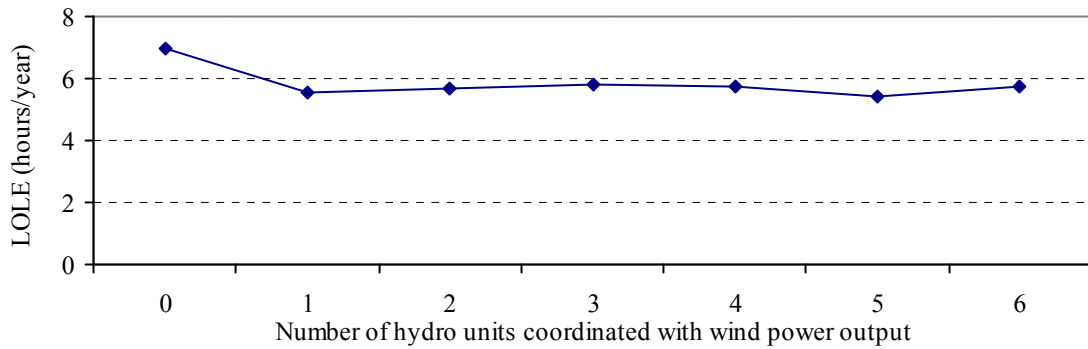


Figure 5.8: Effect of the number of hydro units coordinated with wind power output on the system LOLE when the hydro units not energy limited.

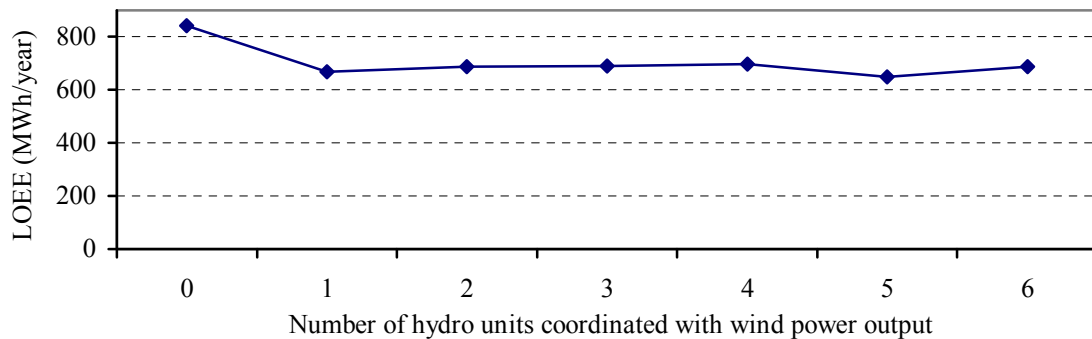


Figure 5.9: Effect of the number of hydro units coordinated with wind power output on the system LOEE when the hydro units are not energy limited.

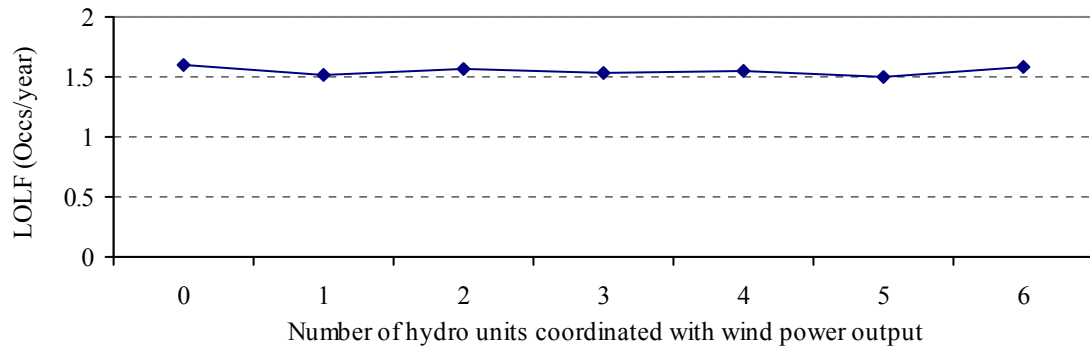


Figure 5.10: Effect of the number of hydro units coordinated with wind power output on the system LOLF when the hydro units are not energy limited.

It is shown in Figures 5.8 to 5.10 that the coordination between wind power and hydro units can increase the overall system adequacy. The reliability indices decrease significantly when the number of hydro units operated in coordination with wind power increases from 0 to 1. There is no restriction on wind power when coordinated with hydro power, and therefore, the benefits from wind increase. The number of hydro units coordinated has little effect on the system adequacy as the number of hydro units coordinated with wind power increases from 1 to 6. This can be seen in Figures 5.8 to 5.10 where the three reliability indices have relatively small variations. The reason is that this study assumes no water limitations during the peak hours when the number of hydro units operating in coordination with wind power is increased.

The amount of energy in a hydro reservoir is limited by its storage capacity. The following study considers hydro unit energy limitations. The effect on the system reliability indices of the number of hydro units coordinated with wind power is shown in Figures 5.11 to 5.13 when hydro unit energy limitations are considered. It is shown that the system adequacy is greatly reduced when the number of hydro units coordinated with wind power increases from 0 to 1. The coordination between wind power and hydro units reduces the level of system adequacy when the data in Tables 3.1 and 3.2 for the

original water inflow and reservoir volume are applied. The number of hydro units coordinated has little effect on the system adequacy as the number of hydro units coordinated with wind power increases from 1 to 6.

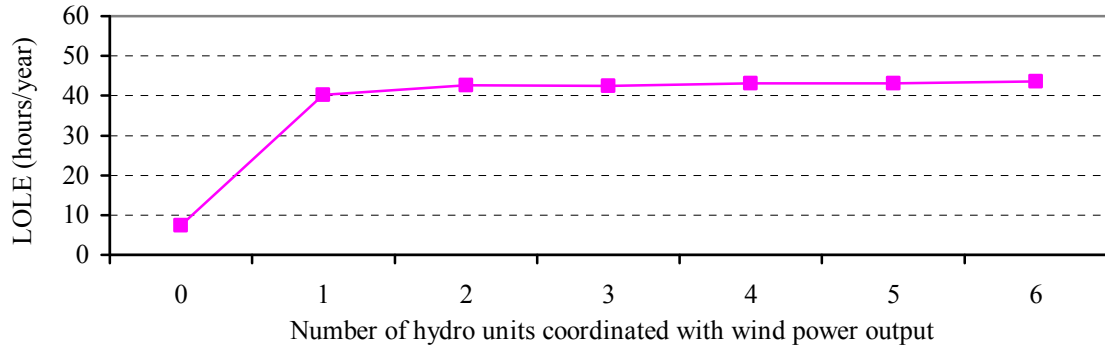


Figure 5.11: Effect of the number of hydro units coordinated with wind power output on the system LOLE when the hydro units are energy limited.

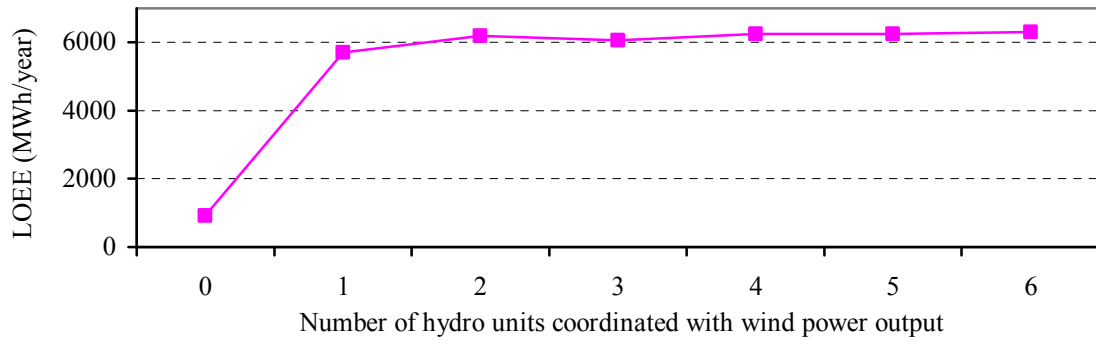


Figure 5.12: Effect of the number of hydro units coordinated with wind power output on the system LOEE when the hydro units are energy limited.

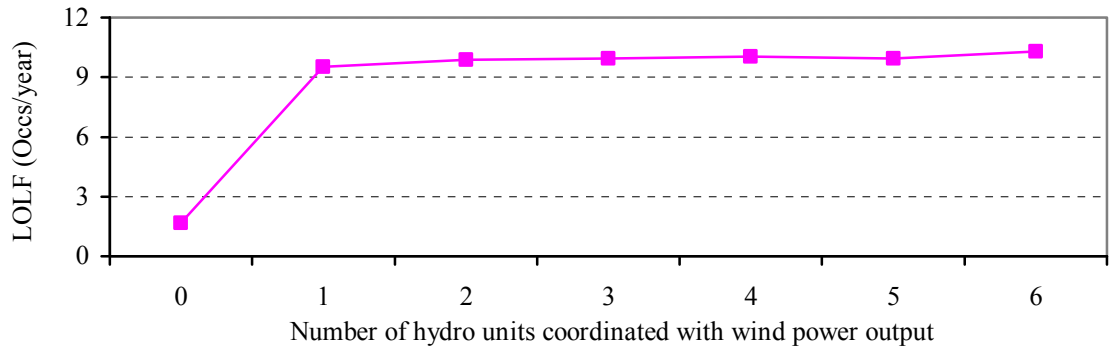


Figure 5.13: Effect of the number of hydro units coordinated with wind power output on the system LOLF when the hydro units are energy limited.

The average water utilized, spilled, and the average water volume in the reservoir can be recorded during the simulation when hydro unit energy limitations are considered. Figures 5.14 to 5.16 show the effect on the AWE, AWS, and AVolume respectively of the number of hydro units coordinated with wind power. When there is no coordination between wind power and hydro units, only a small amount of water is used by the hydro units. Most of the water is spilled, and the reservoir volume is maintained at its maximum level. If there is coordination between wind power and hydro units, the water in the reservoir is used up when the wind power output is less than 20% of wind farm's rated capacity, and no water is available when hydro units are required to reduce the loss of load.

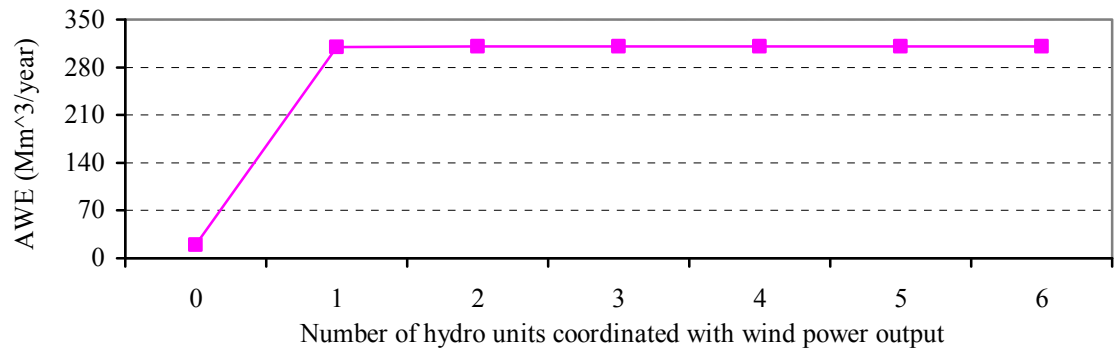


Figure 5.14: Effect of the number of hydro units coordinated with wind power output on the AWE when the hydro units are energy limited.

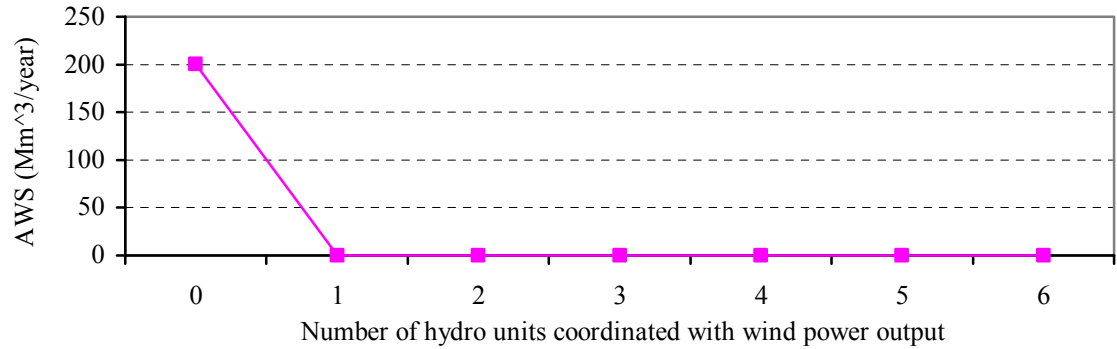


Figure 5.15: Effect of the number of hydro units coordinated with wind power output on the AWS when the hydro units are energy limited.

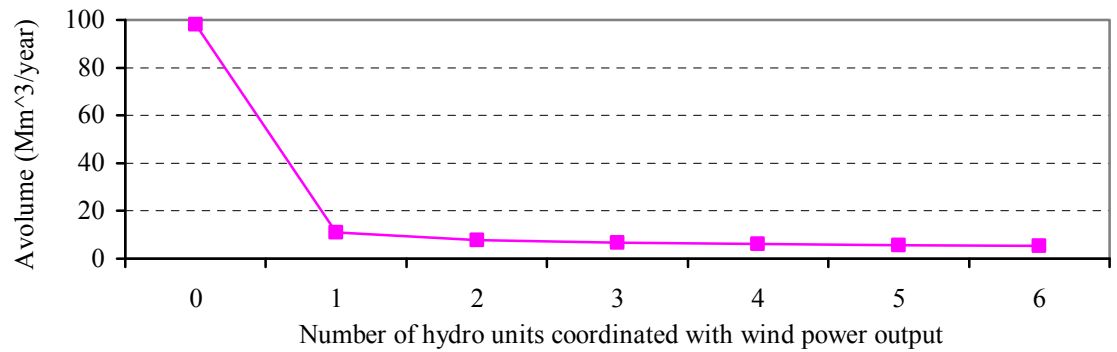


Figure 5.16: Effect of the number of hydro units coordinated with wind power output on the AVolume when the hydro units are energy limited.



Studies in this section show that the original water inflow and reservoir size as shown in Tables 3.1 and 3.2 are comparatively small and inadequate to operate hydro units in coordination with wind power output. In the next section, the water inflow and reservoir size are increased and the effect of the water inflow and reservoir size on the reliability benefit from the coordination between wind power and hydro units is investigated.

#### 5.4 Effect of Water In-flow and Reservoir Volume

The approximate relationship between the water head and the volume of the reservoir is shown in (3.19). The hydro reservoir data used in the studies in the previous section is presented in [40]. The constants  $a$ ,  $b$ , and  $c$  are 0.00241, 0.11100 and 2.00000 respectively. The maximum and the minimum volume of the reservoir are  $100 \text{ Mm}^3$  and  $5 \text{ Mm}^3$  respectively, and the water volume is  $2 \text{ Mm}^3$  when the water head is 0 m. This reservoir is designated as Reservoir A. The water in-flow to this reservoir is  $235 \text{ Mm}^3/\text{year}$ . The relation between the reservoir volume and water head is shown in Table 5.2.

Table 5.2: Relationship between water head and reservoir volume for Reservoir A

Volume ( $\text{Mm}^3$ )	Head (m)
100	180
5	19.1
2	0

The results in Section 5.2 show that the reservoir volume is very small, and therefore, the hydro units have significant energy limitations when they are operated in

coordination with wind variations. The reservoir volume and the water in-flow are increased by a factor of 10 in the following study in order to assess the benefits with increased size of the reservoir. This reservoir is designated as Reservoir B. The increased reservoir water volume and the corresponding water heads are shown in Table 5.3. The reservoir volume data shown in the first column of Table 5.3 are 10 times larger than that of Table 5.2. The corresponding water heads in the second column remain the same in both tables. The depth of the reservoir is not changed since the hydro unit ratings remain the same, and are designed for the particular water head. The water in-flow to Reservoir B is 2350 Mm<sup>3</sup>/year.

Table 5.3: Relationship between water head and reservoir volume for Reservoir B

Volume (Mm <sup>3</sup> )	Head (m)
1000	180
50	19.1
20	0

The new values for the parameters  $a$ ,  $b$ , and  $c$  are obtained by applying the modified relationship between the water head and the reservoir volume in Table 5.3. The new values for the parameters  $a$ ,  $b$ , and  $c$  are shown in (5.3).

$$\begin{cases} a = 0.0241 \\ b = 1.11 \\ c = 20 \end{cases} \quad (5.3)$$

A series of studies were conducted to investigate the reliability benefits from wind power coordinated with hydro units. Data for the wind farm, hydro reservoir, and water inflow for three different cases are shown in Table 5.4. The wind farm capacity is 300 MW in the three cases. Case 1 uses the hydro plant with Reservoir A data. Case 2 uses

Reservoir B in order to explore the effect of increased reservoir volume and water inflow. The water in-flow and reservoir volume for Reservoir B are 10 times greater than that of Reservoir A. In Case 3 the reservoir is very large and the hydro units are not considered to be energy limited.

Table 5.4: Example data for wind farm and hydro plant

Case Number	Wind Capacity (MW)	Reservoir Volume (Mm <sup>3</sup> )	Inflow Water (Mm <sup>3</sup> /year)
Case 1	300	100	235
Case 2	300	1000	2350
Case 3	300	infinite	unlimited

Figures 5.17 to 5.19 show the effect on system reliability as the number of hydro units assigned to operate in coordination with wind power is increased for Cases 1 to 3. The system LOLE, LOEE, and LOLF increase significantly in Case 1 when hydro units are assigned to operate in coordination with wind power fluctuations. As Reservoir A is relatively small, all the available water is used up in balancing wind variation, and no water is available to supply energy during the peak hours. The system adequacy therefore decreases with wind and hydro coordination.

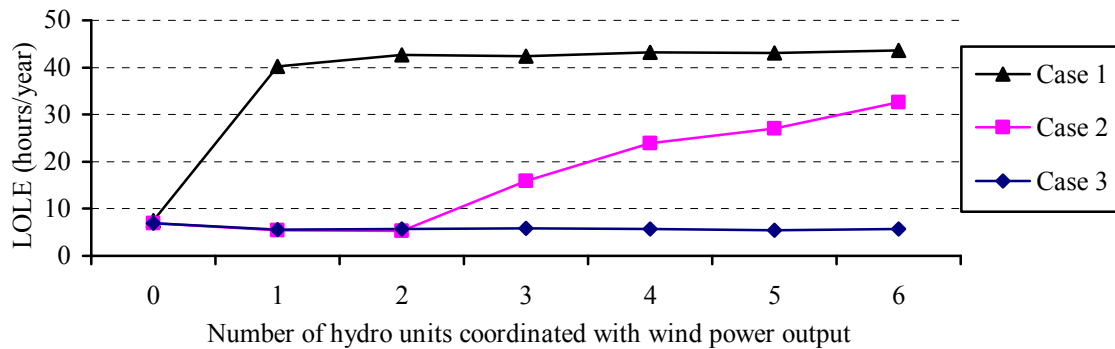


Figure 5.17: Effect of water inflow and reservoir volume on the system LOLE.

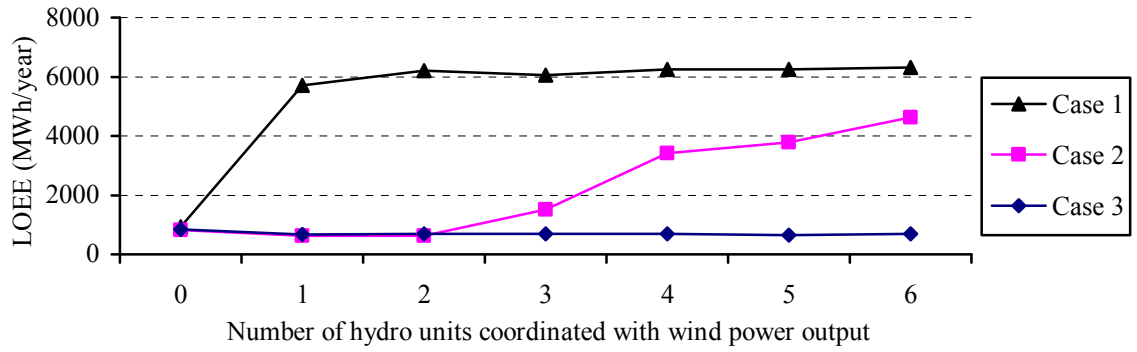


Figure 5.18: Effect of water inflow and reservoir volume on the system LOEE.

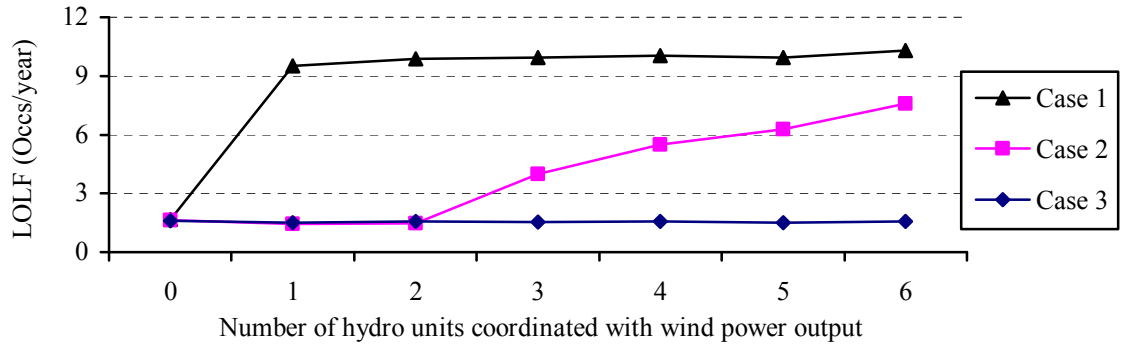


Figure 5.19: Effect of water inflow and reservoir volume on the system LOLF.

The reservoir volume and water inflow are increased in Case 2. The system LOLE, LOEE, and LOLF decrease when the number of coordinated hydro units increases from 0 to 1 for this case. There is no restriction on wind power when coordinated with a hydro unit, and therefore, the benefits from wind are increased. When the number of hydro units coordinated with wind power is 3 or more, the system adequacy begins to decrease as there will be less water available to supply the load during the peak hours.

The system adequacy in Case 3 is the same as in Case 2 when the number of hydro units coordinated with wind power is 0, 1 and 2. The number of hydro units used

for wind power coordination does not influence the system adequacy in this case.

Figure 5.20 to Figure 5.22 respectively show the comparisons of AWE, AWS, and AVolume for Cases 1 and 2 which consider energy limitations in the hydro reservoir. The AWE and AWS indices are represented in percentage of annual water inflow, and the AVolume in percentage of the maximum reservoir volume.

Figure 5.20 shows that only a small amount of water is used in both cases when there is no coordination between wind power and hydro units. In this situation, the hydro units are at the bottom of the priority loading order, and are only brought in service to serve the peak load after all other generating units. All the available water is used in Case 1 if a number of hydro units are assigned to coordinate with wind power. It is noted that the value of AWE is greater than the annual water inflow for Case 1 when the hydro units are coordinated with wind power. The reason is that the initial value of reservoir volume is set to be 80% of its maximum volume at the beginning of each simulated year. The reservoir volume and water inflow are increased by a factor of 10 in Case 2. Figure 5.20 shows that the AWE for Case 2 increases with the number of hydro units coordinated with wind power. Almost all the available water is used up when all 6 hydro units are operated to coordinate with wind power.

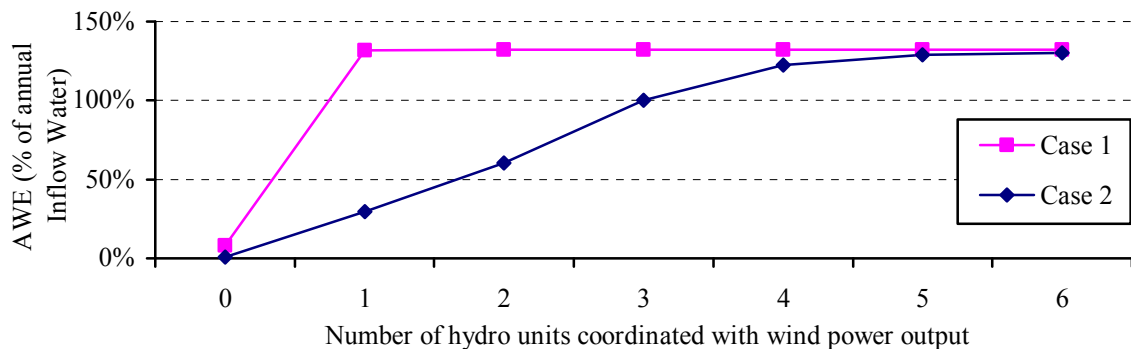


Figure 5.20: Effect of water inflow and reservoir volume on the AWE.

Figure 5.21 shows that there are large differences between cases with different reservoir volumes and water inflows. Figure 5.21 shows that more than 85% of the annual water inflow has to be spilled when there is no coordination between wind power and the hydro units. No water has to be spilled for Case 1 with the relatively small Reservoir A when hydro units are assigned and operated to coordinate with wind power. The AWS continues to decrease with an increasing number of hydro units coordinated with wind power when the reservoir volume and water inflow are increased in Case 2. The AWS is close to zero when all 6 hydro units are coordinated with wind power.

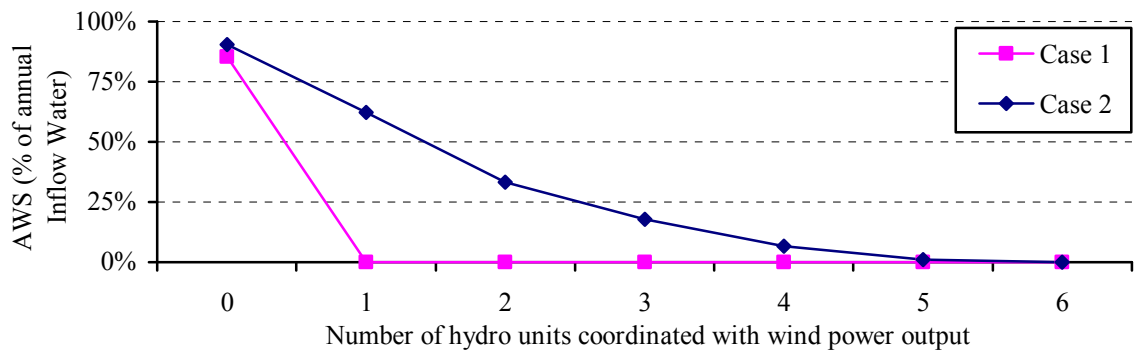


Figure 5.21: Effect of water inflow and reservoir volume on the AWS.

Figure 5.22 shows that the AVolume is close to the maximum volume of the reservoir for both cases when there is no coordination between wind power and the hydro units. The reservoir volume is, however, close to its minimum volume (5% of maximum volume) for Reservoir A when wind power is coordinated with the hydro units in Case 1. The AVolume continues to decrease with increasing number of hydro units coordinated with wind power when the reservoir volume and water inflow are increased in Case 2.

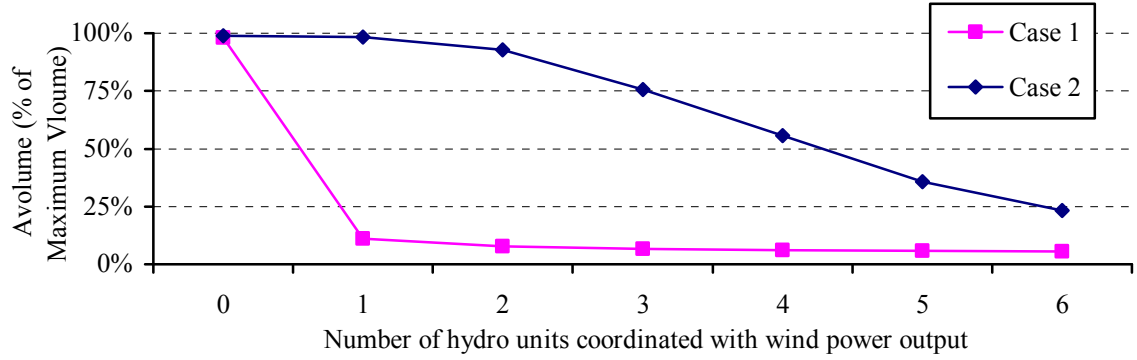


Figure 5.22: Effect of water inflow and reservoir volume on the AVolume.

### 5.5 Effect of Wind Farm Location

This study investigates the effect of wind farm location on the reliability impact of the coordination of wind power and the hydro plant. The base case study presented in this thesis considers a wind farm, with Swift Current (SC) data, connected to the IEEE-RTS. The base case is compared with a case in which North Battleford (NB) wind data is considered. In both the cases, the rated wind capacity is 300 MW, and the corresponding wind penetration level is 8%. The results using Reservoir A data are shown in Figure 5.23 to 5.28.

It is shown in Figure 5.23 to 5.25 that a wind farm located at a site with a better wind regime can provide higher system reliability. The system adequacy is greatly reduced because of the water shortage when a number of hydro units are operated to coordinate with wind power. The differences between the two curves in these figures are increased if the number of hydro units assigned to coordinate with wind power increases from 0 to 1. The reason is that the assigned hydro units for the North Battleford case have to start and operate more frequently and use more water since the power generated by the North Battleford wind farm has a higher probability of not meeting the coordination criterion of 20% of its rated capacity.

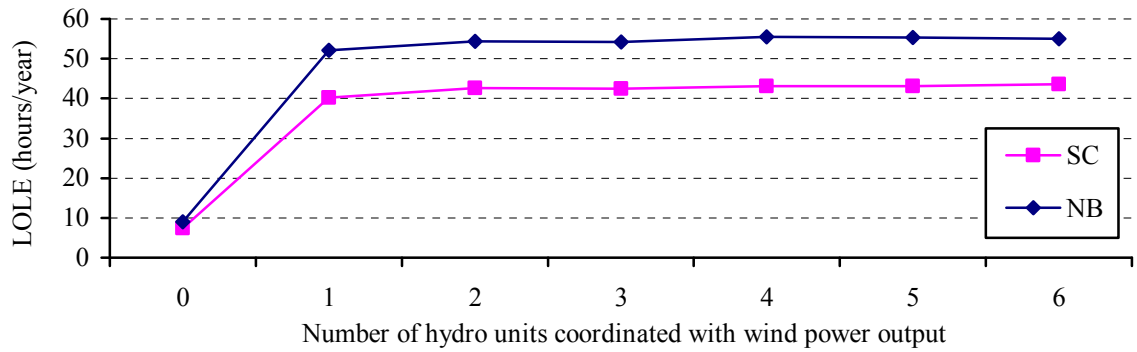


Figure 5.23: Effect of wind farm location on the system LOLE with Reservoir A.

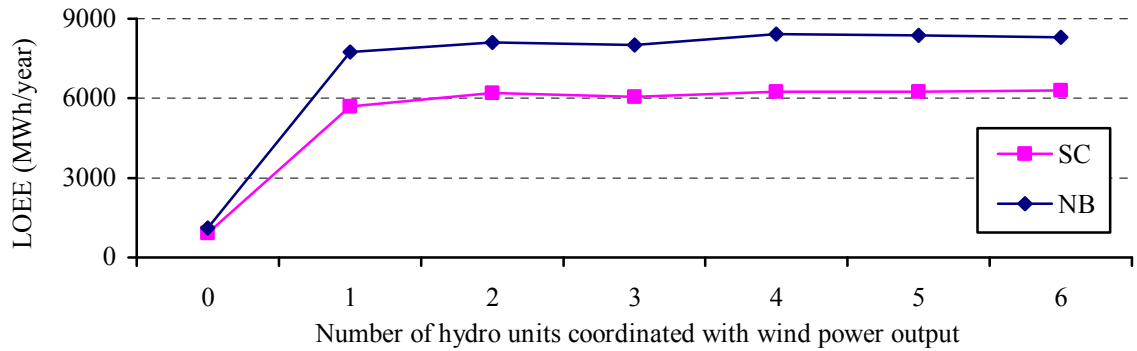


Figure 5.24: Effect of wind farm location on the system LOEE with Reservoir A.

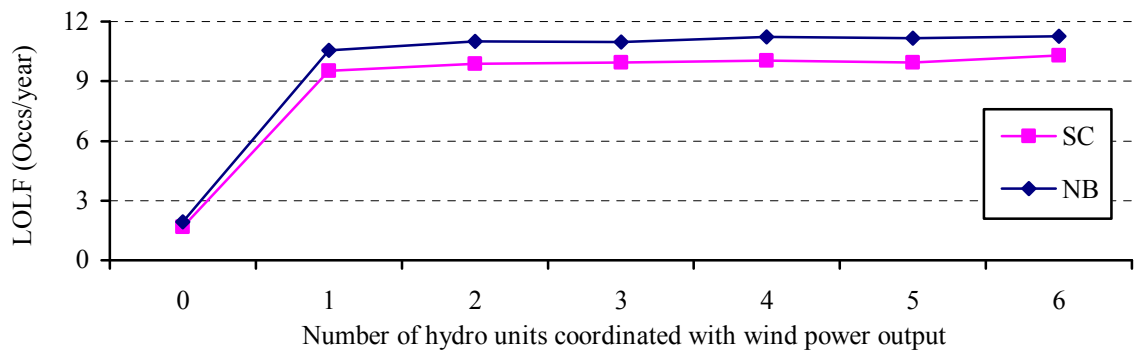


Figure 5.25: Effect of wind farm location on the system LOLF with Reservoir A.

Figure 5.26 to Figure 5.28 respectively show the effect of wind farm location on



the water related indices, i.e. AWE, AWS, and AVolume. The two curves for the two different wind regimes are close together in all the three figures. The amount of water utilized by the hydro units are mainly determined by the number of hydro units assigned to operate in coordination with wind power. The effect of different wind regimes on these indices is very small when Reservoir A data is used in the study.

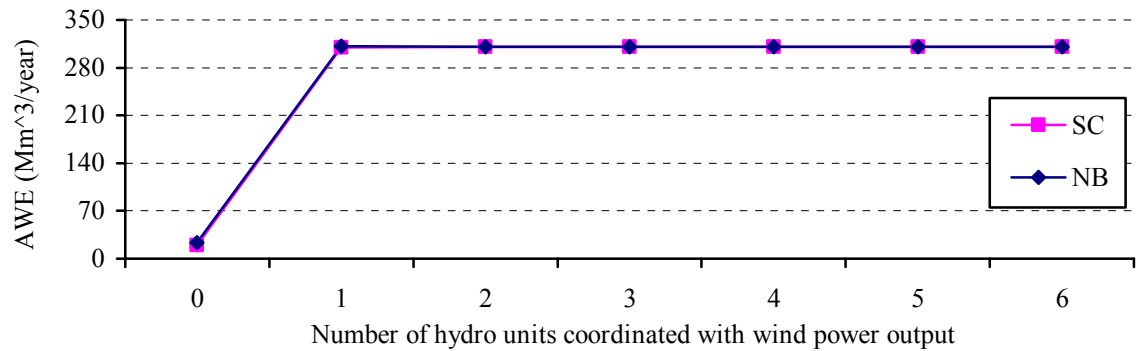


Figure 5.26: Effect of wind farm location on the AWE with Reservoir A.

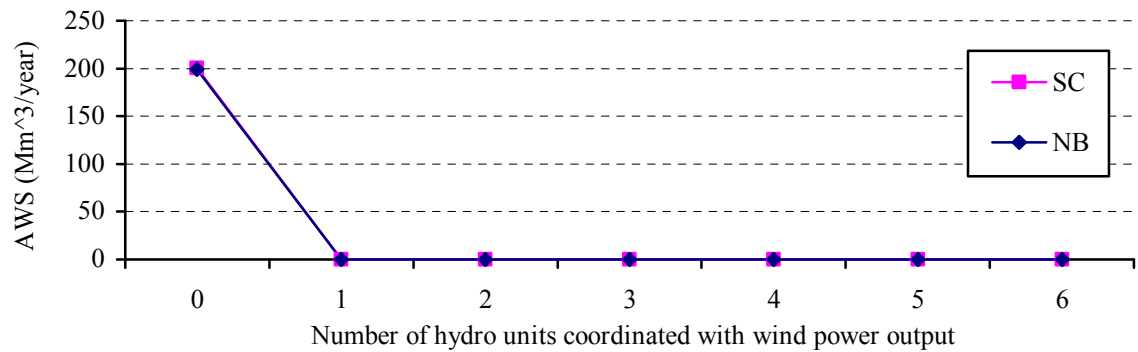


Figure 5.27: Effect of wind farm location on the AWS with Reservoir A.

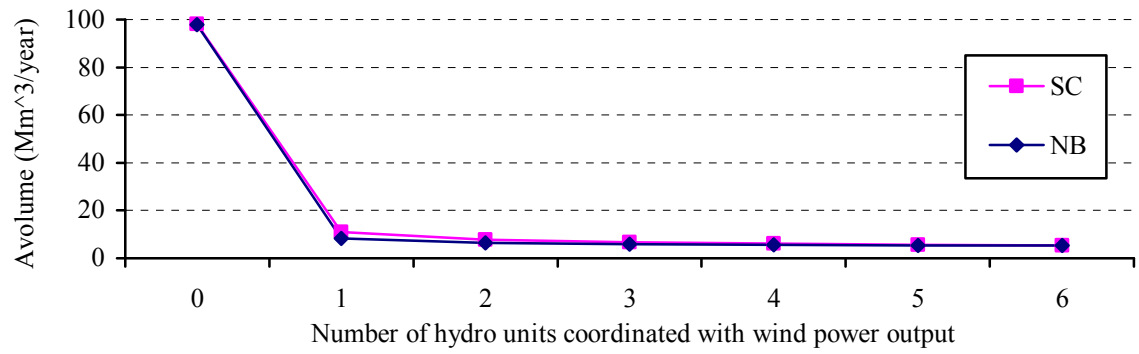


Figure 5.28: Effect of wind farm location on the AVolume with Reservoir A.

In order to further investigate the effect of wind farm location, the water inflow and the reservoir volume are multiplied by a factor of 10 by using Reservoir B in the study. The results are shown in Figures 5.29 to 5.34.

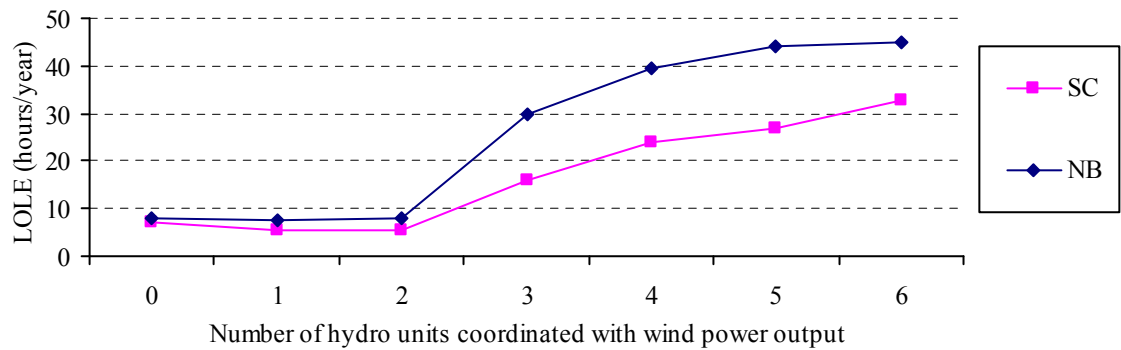


Figure 5.29: Effect of wind farm location on the system LOLE with Reservoir B.

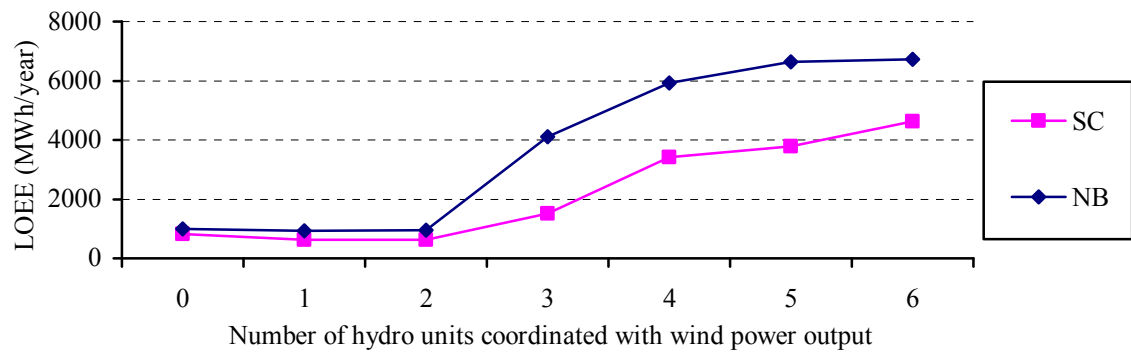


Figure 5.30: Effect of wind farm location on the system LOEE with Reservoir B.

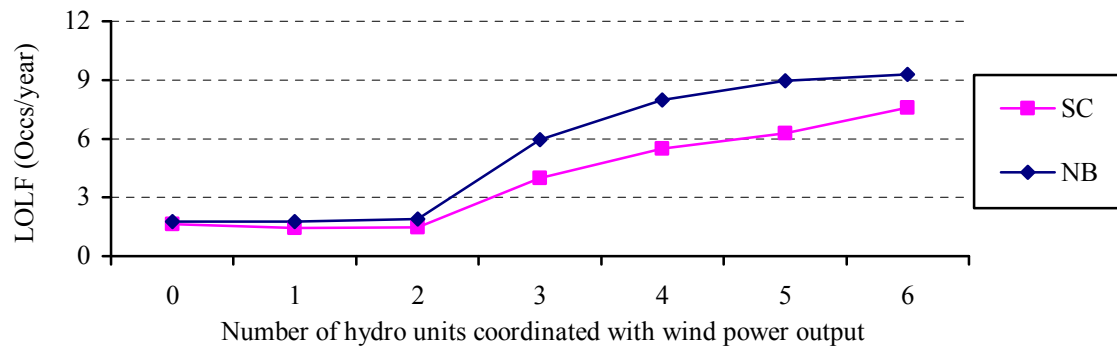


Figure 5.31: Effect of wind farm location on the system LOLF with Reservoir B.

Figures 5.29 to 5.31 show the effect of wind farm location on the system reliability indices for Reservoir B. There is an improvement in the system adequacy when wind power is coordinated with 1 or 2 hydro units for both wind farms. The reliability benefit from the North Battleford wind farm is less than that obtained from the Swift Current wind farm. When the number of hydro units assigned to coordinate with wind power is greater than 2, the water in the reservoir is insufficient, and the system adequacy is significantly reduced. There is a big difference between wind farms with Swift Current and North Battleford regimes in terms of system reliability when the number of hydro units assigned to coordinate with wind power is greater than 2.

The effect of wind farm location on the water related indices, such as AWE, AWS, AVolume when the water inflow and reservoir volume are increased is shown in Figure 5.32 to 5.34. The North Battleford wind farm output is less than the coordination criterion more often than the Swift Current wind farm output. The hydro units are therefore operated more frequently to coordinate the North Battleford wind farm output. As a result, more water is utilized, less water is spilled, and the reservoir volume is maintained at a relatively low level when the coordinated wind farm has the North Battleford wind regime.

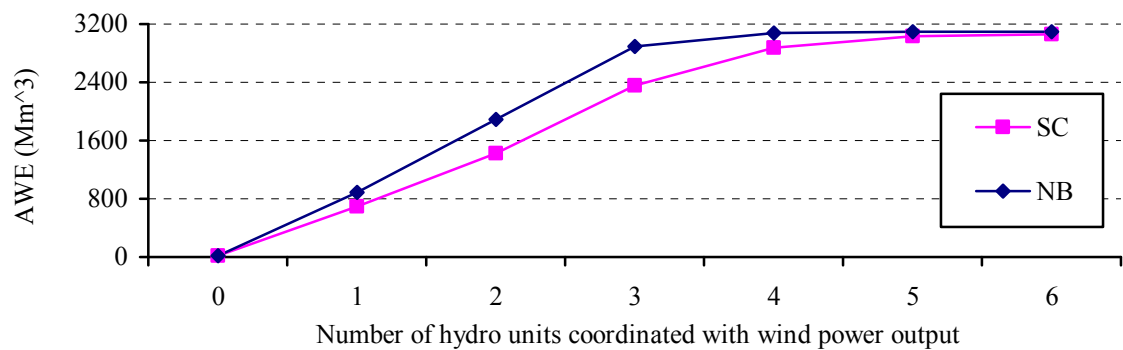


Figure 5.32: Effect of wind farm location on the AWE with Reservoir B.

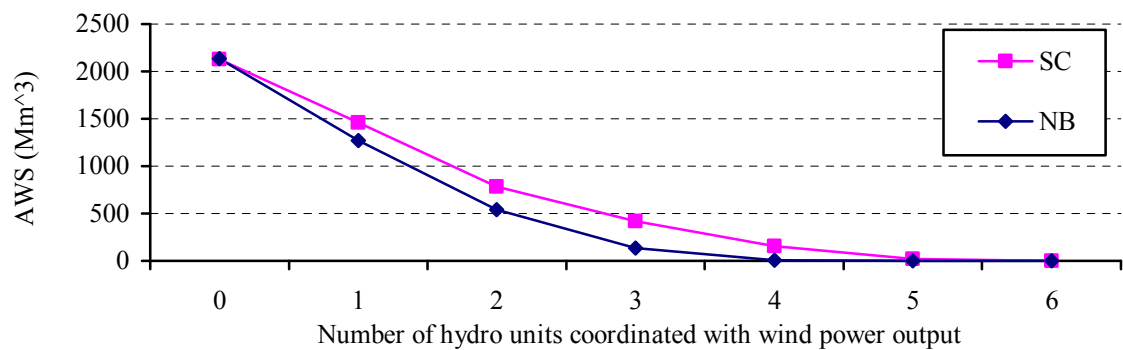


Figure 5.33: Effect of wind farm location on the AWS with Reservoir B.

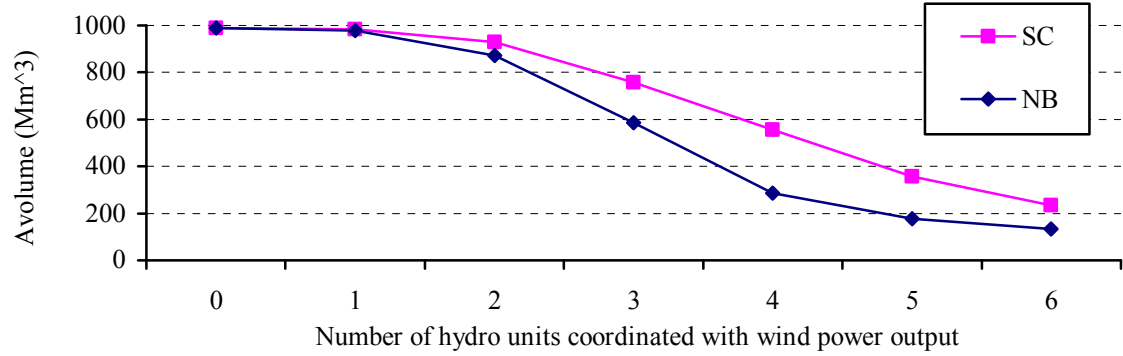


Figure 5.34: Effect of wind farm location on the AVolume with Reservoir B.

### 5.6 Effect of Wind Power Penetration Level

The effect of wind power penetration on the system adequacy is investigated in this section considering wind and hydro power coordination. The base case considered has a wind capacity equal to 300 MW, which is about 8% penetration in the IEEE-RTS. Different cases with varying wind capacities of 600, 900, and 1200 MW, i.e. wind penetration levels of 15%, 21%, and 26% respectively, are compared with the base case. The simulation results using Reservoir A are shown in Figures 5.35 to 5.40.

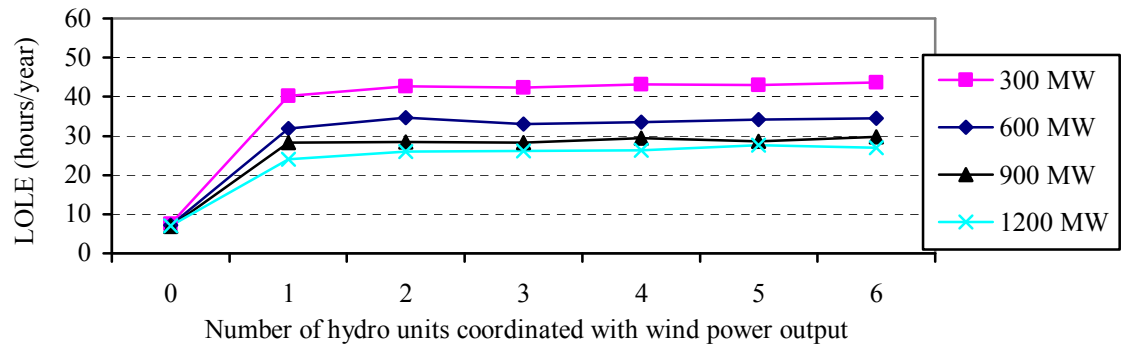


Figure 5.35: Effect of wind power penetration level on the system LOLE with Reservoir A.

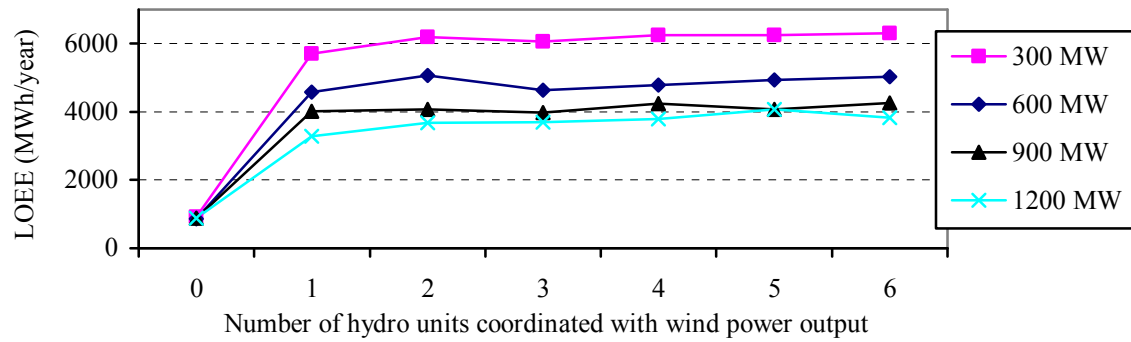


Figure 5.36: Effect of wind power penetration level on the system LOEE with Reservoir A.

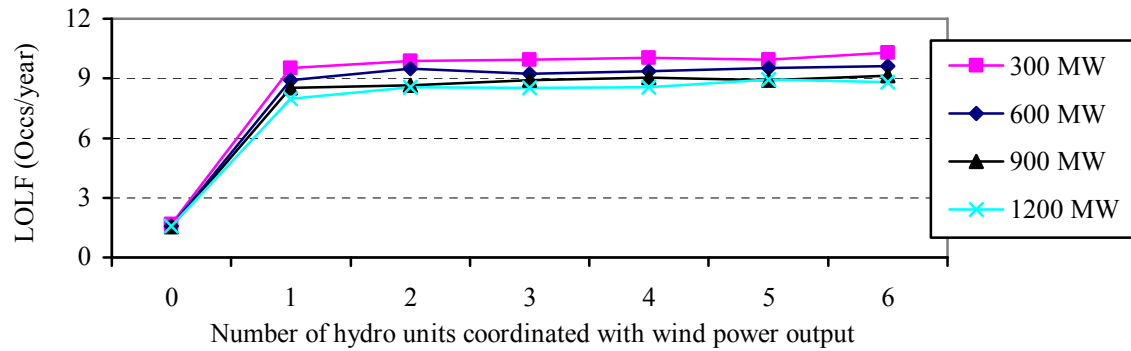


Figure 5.37: Effect of wind power penetration level on the system LOLF with Reservoir A.

Figures 5.35 to 5.37 show the effect of wind power penetration on the system adequacy indices considering the coordination between wind power and the hydro units. It can be seen that the difference in system reliability between the cases with different wind power penetration levels is small when there is no coordination between the hydro units and the wind power fluctuations. The wind power absorbed by the system is restricted to 3% of the system load in each case. The system reliability level is mainly determined by the amount of water in the reservoir. An increase in wind penetration improves the system adequacy when there is coordination between the wind power and

the hydro units. Since the water is greatly limited for Reservoir A, the system adequacy is greatly reduced due to the coordination between wind power and hydro units. There is little difference between the cases with the same wind penetration level and different numbers of hydro units assigned to coordinate with wind power.

Figures 5.38 to 5.40 show the effect of wind power penetration level on the indices such as AWE, AWS, and AVolume which relate to the water utilization. These figures show that the wind power penetration has little impact on the water utilized, spilled or the water level in the reservoir when the coordination between wind power and hydro units is considered since the water inflow is greatly limited and the reservoir is relatively small in the Reservoir A cases.

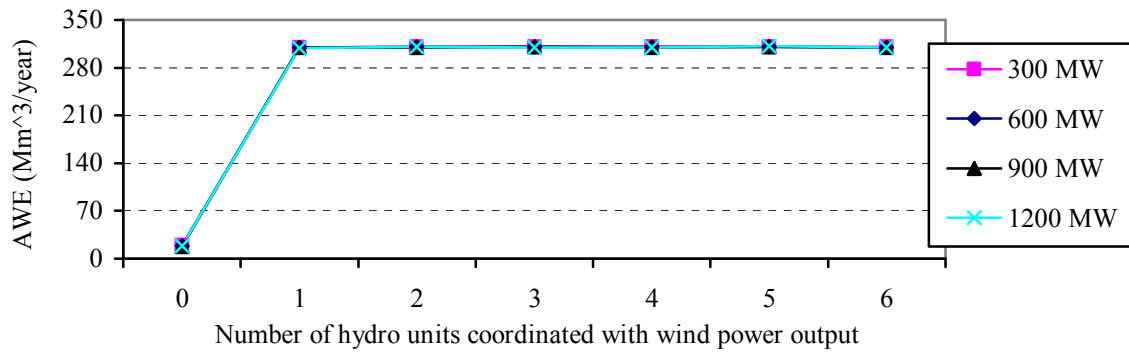


Figure 5.38: Effect of wind power penetration level on the AWE with Reservoir A.

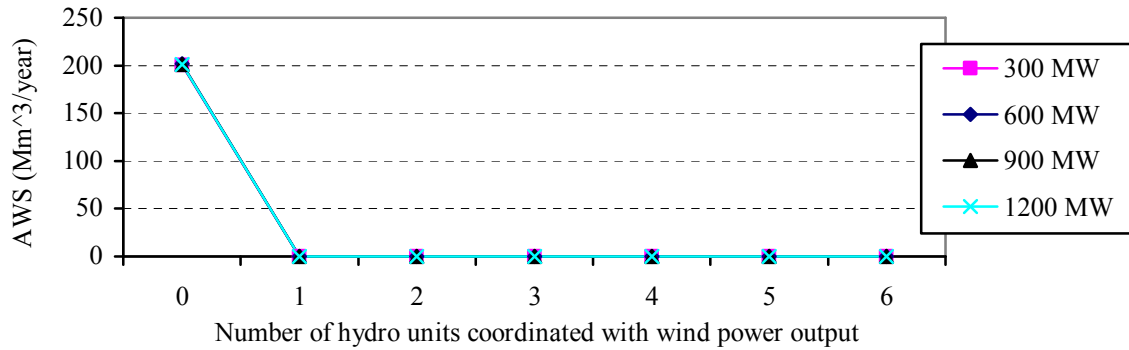


Figure 5.39: Effect of wind power penetration level on AWS with Reservoir A.

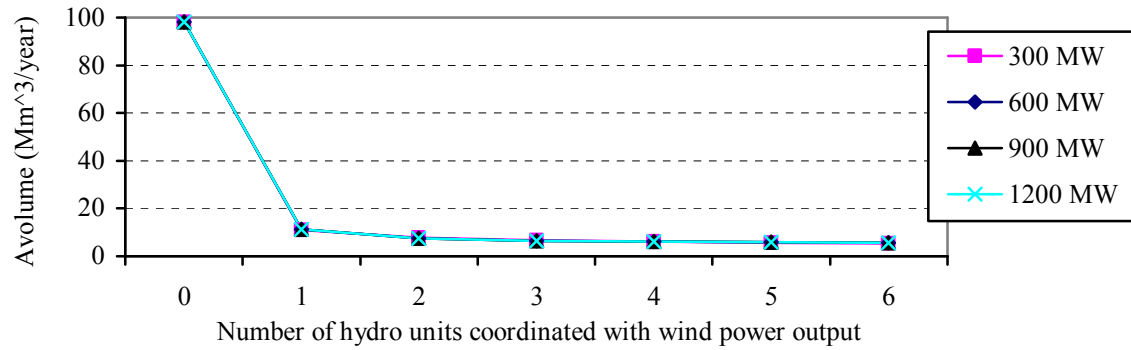


Figure 5.40: Effect of wind power penetration level on the AVolume with Reservoir A.

The effect of wind power penetration is further investigated using Reservoir B in which the water inflow and the reservoir volume are multiplied by a factor of 10. The results are shown in Figures 5.41 to 5.46.

Figures 5.41 to 5.43 show that reliability levels for systems with different wind penetration are very similar when there is no coordination of wind power and hydro units. If the number of hydro units assigned to coordinate with wind power is equal to 1 or 2, the system adequacy increases with wind power penetration. If the number of hydro units assigned to coordinate with wind power is increased further from 2, the system adequacy decreases. The system with higher wind penetration always provides higher reliability.



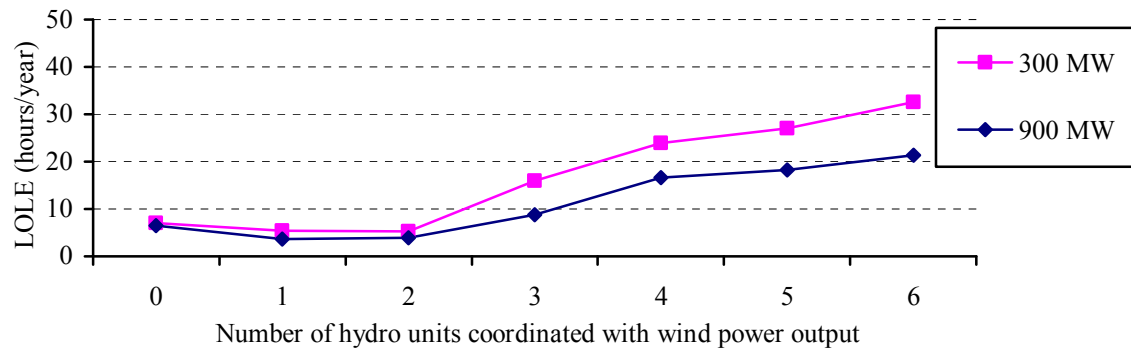


Figure 5.41: Effect of wind power penetration level on the system LOLE with Reservoir B.

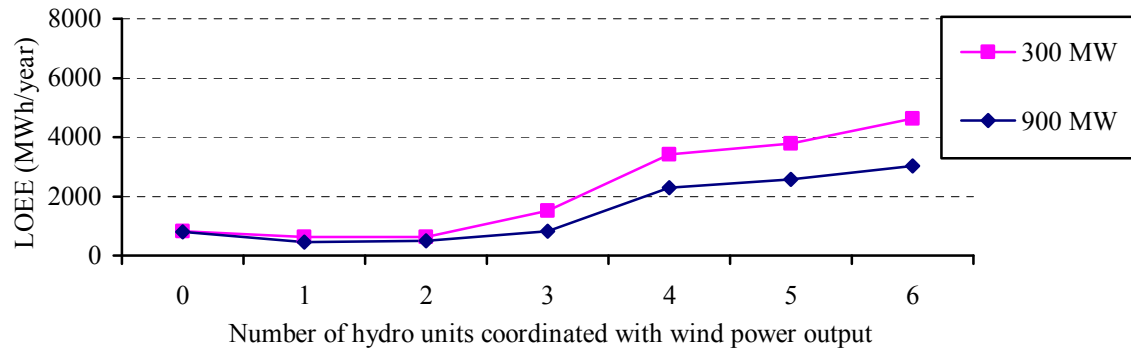


Figure 5.42: Effect of wind power penetration level on the system LOEE with Reservoir B.

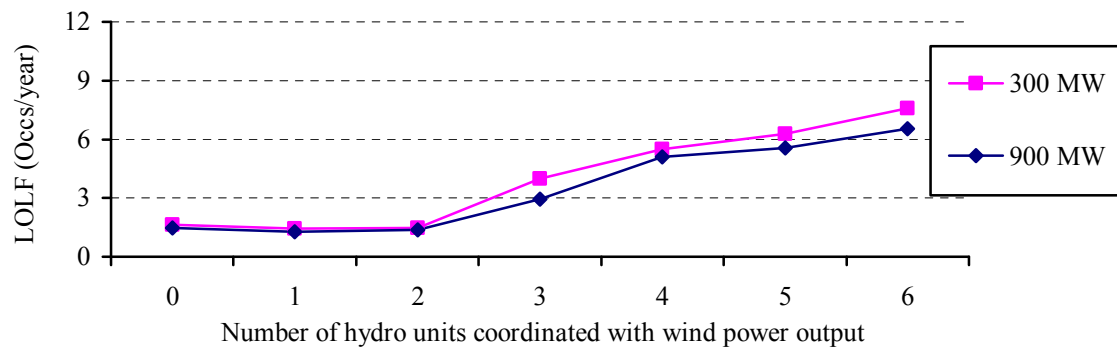


Figure 5.43: Effect of wind power penetration level on the system LOLF with Reservoir B.

Figures 5.44 to 5.46 show the effect of wind power penetration on the AWE, AWS, and AVolume when the hydro plant has a large reservoir. These figures show that the two curves for the two different wind penetration levels are close together. The wind penetration has little effect on the water utilized by the hydro generator, spilled, or the water level in the reservoir. The reason is that the water utilization is mainly determined by the number of hydro units assigned to coordinate with wind power. The coordination criterion is in terms of the percentage of rated wind capacity, and the wind penetration level does not affect the number of hydro units that should be started when the actual wind power output is less than the coordination criterion.

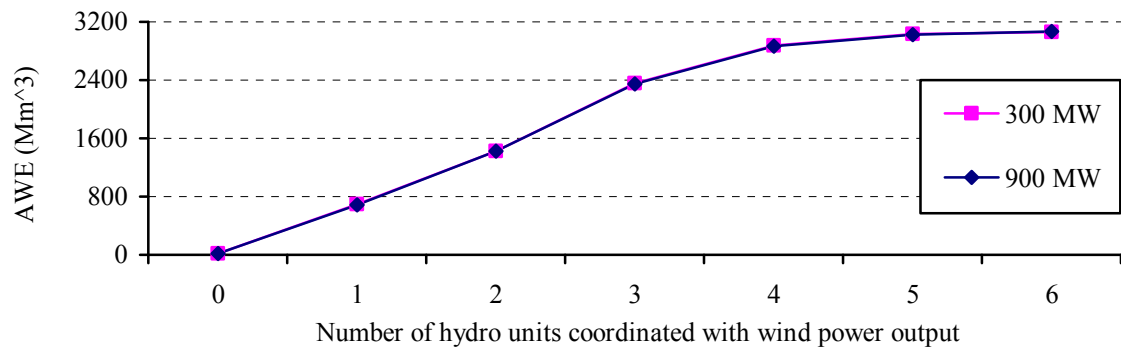


Figure 5.44: Effect of wind power penetration level on the AWE with Reservoir B.

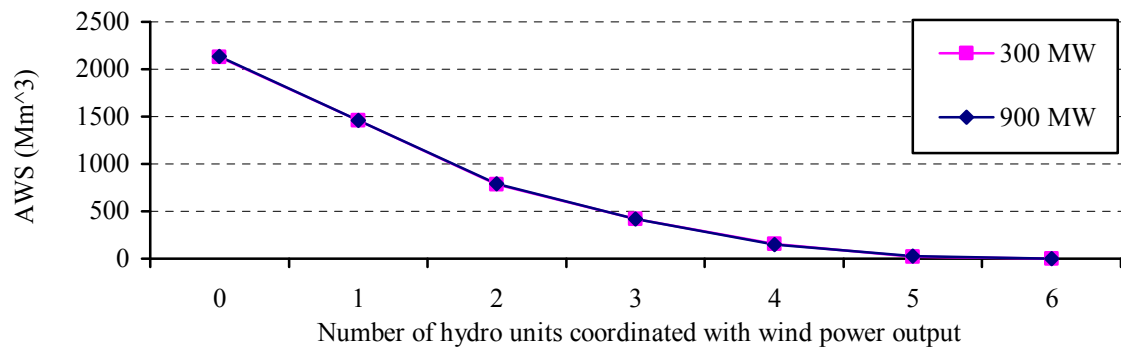


Figure 5.45: Effect of wind power penetration level on the AWS with Reservoir B.

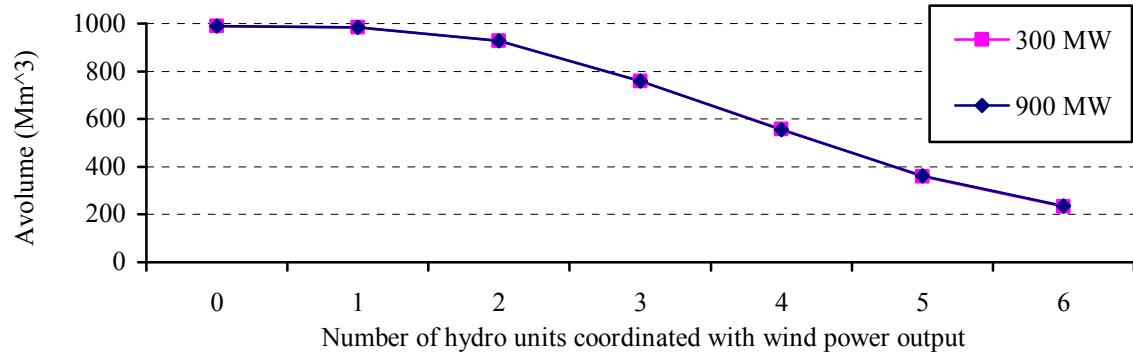


Figure 5.46: Effect of wind power penetration level on the AVolume with Reservoir B.

### 5.7 Effect of System Load Level

The effect of the system load on the system adequacy is investigated in this section considering wind and hydro power coordination. The base case considered has a peak load of 2850 MW. Different cases with peak load levels of 2800 MW, 2900 MW, and 2950 MW are compared with the base case. The simulation results are shown in Figures 5.47 to 5.52.

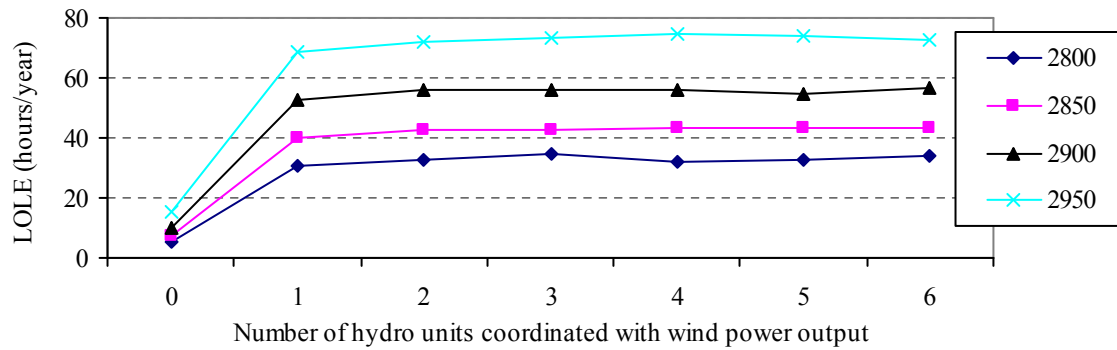


Figure 5.47: Effect of system load on the system LOLE with Reservoir A.

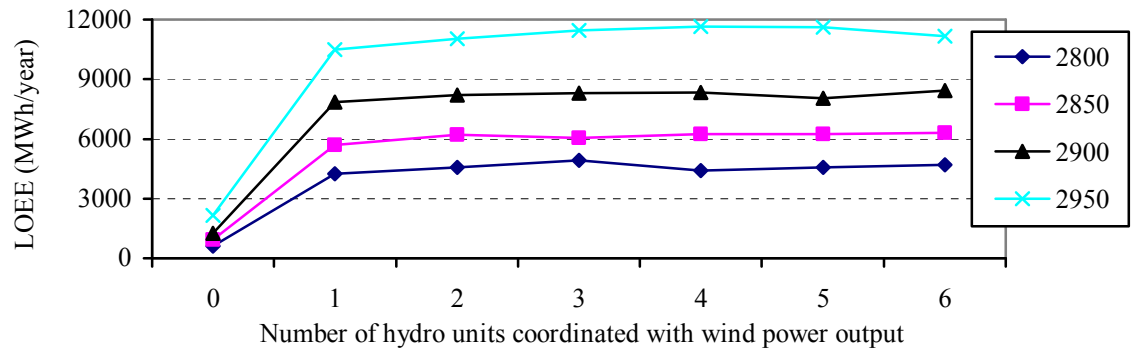


Figure 5.48: Effect of system load on the system LOEE with Reservoir A.

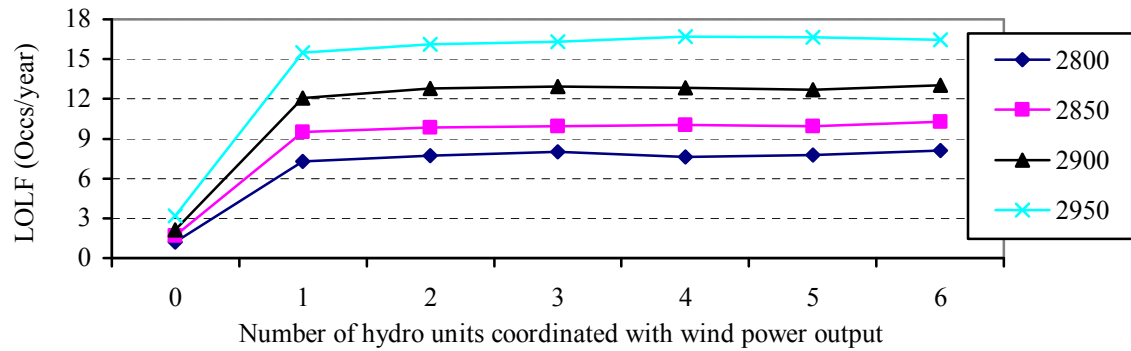


Figure 5.49: Effect of system load on the system LOLF with Reservoir A.

Figures 5.47 to 5.49 show the effect of the system load on the reliability indices. The system reliability decreases with increasing system load. For a given system load, the system reliability doesn't change significantly when the number of hydro units assigned to coordinate with wind power increases from 1 to 6.

The effect of the system load on the water utilization related indices, such as AWE, AWS, and AVolume is shown in Figures 5.50 to 5.52. When there is no coordination between wind power and the hydro units, an increased system load slightly increases the amount of water utilized by the hydro generators, and therefore, reduces the amount of water spilled. The four curves in these figures are close together when a

number of hydro units are assigned to coordinate with wind power. All the available water in the reservoir is used up, and the effect of system load level on the water utilization is very small if the reservoir volume and water inflow are relatively small.

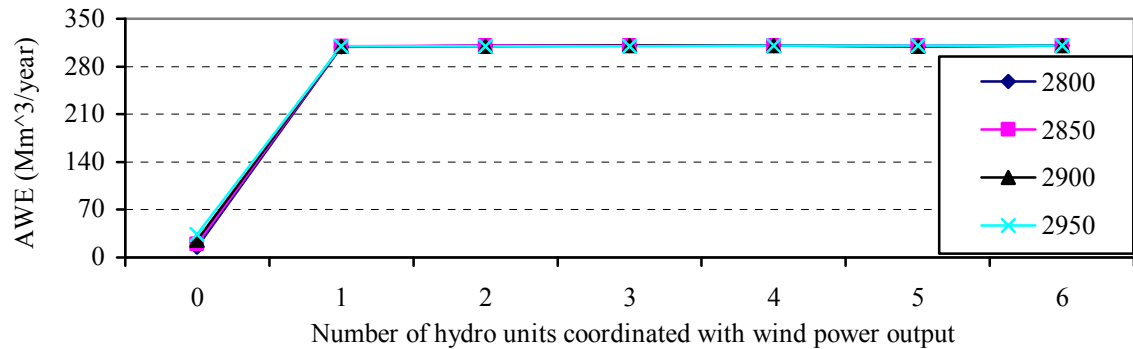


Figure 5.50: Effect of system load level on the AWE with Reservoir A.

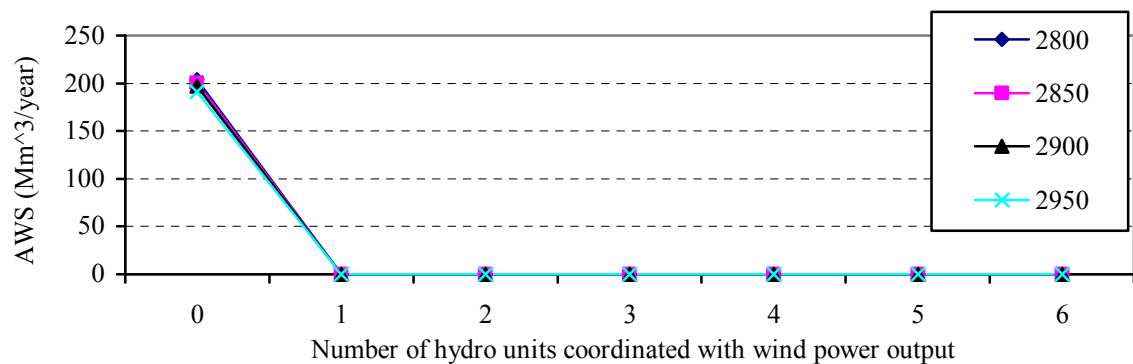


Figure 5.51: Effect of system load level on the AWS with Reservoir A.

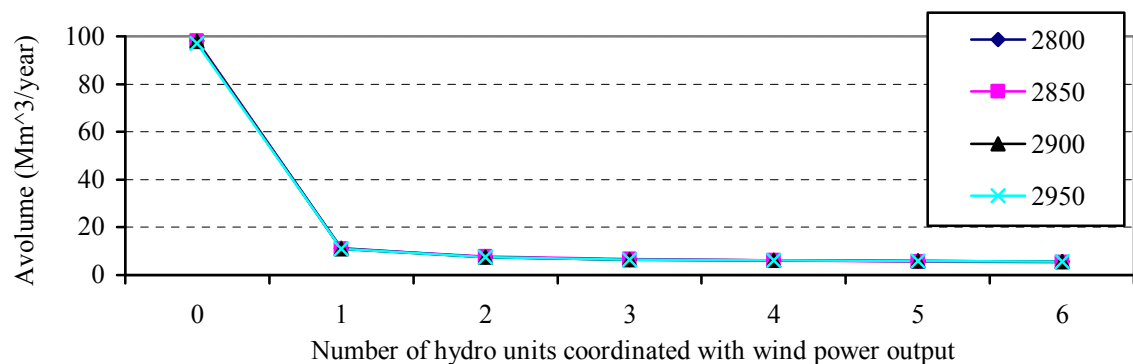


Figure 5.52: Effect of system load level on the AVolume with Reservoir A.

## 5.8 Effect of Wind-hydro Coordination Criterion

A coordination criterion is introduced to determine the amount of support required from the regulating hydro units to balance the variation in wind power. This criterion is a specific percentage of the rated wind farm capacity, and is varied to investigate the reliability benefit of the coordination between the wind farm and the hydro power station. A coordination criterion of 0.2 is applied in previous studies in the chapter. This means that hydro units assigned to respond to fluctuations of wind power will be started if the power output of the wind farm falls below 20% of its rated capacity.

In this section, two cases with coordination criteria of 0.1 and 0.5 are compared with the base case that has a coordination criterion of 0.2. Figures 5.53 to 5.55 show the effect of the coordination criteria on the system adequacy. The figures show the results as the number of hydro units assigned to coordinate with wind power is increased from 1 to 6 considering Reservoir A. It is seen that the difference between cases with different coordination criteria is very small. The effect of the coordination criteria on system adequacy is small when the hydro reservoir is relatively small.

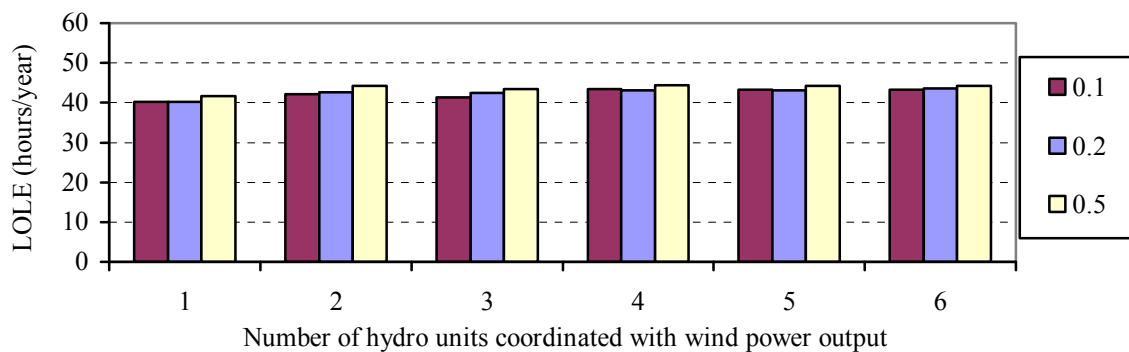


Figure 5.53: Effect of coordination criterion on the system LOLE with Reservoir A.

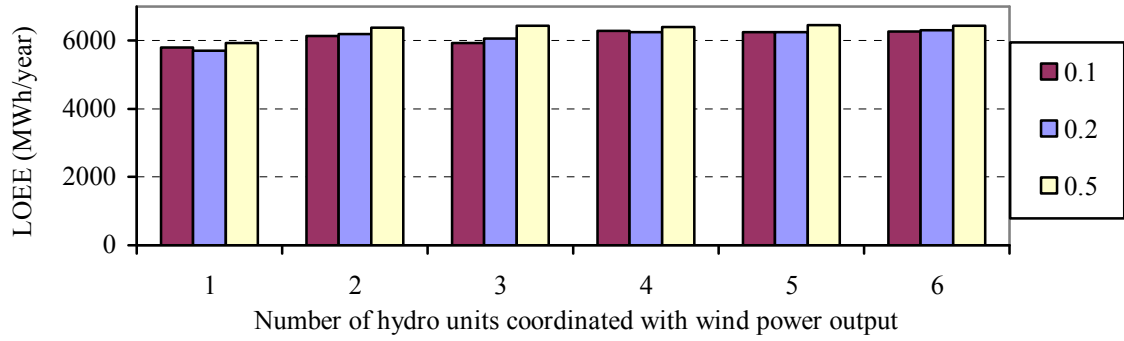


Figure 5.54: Effect of coordination criterion on the system LOEE with Reservoir A.

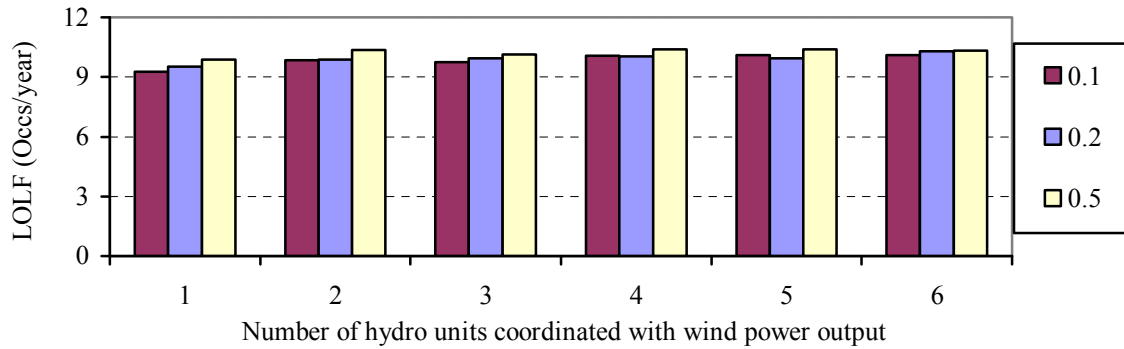


Figure 5.55: Effect of coordination criterion on the system LOLF with Reservoir A.

Figure 5.56 shows the effect of coordination criterion on the AWE. It is shown in the figure that all the available water in the reservoir is utilized for cases with different coordination criterion and different number of hydro units coordinated with wind power. Since no water is spilled for the cases with different coordination criteria as shown in the simulation results, the effect of coordination criterion on the AWS is not shown here.

Figure 5.57 shows the effect of the coordination criterion on the AVolume. It is shown in the figure that the effect of the coordination criterion on the AVolume is significant. If the coordination criterion decreases from 0.2 to 0.1, the average water volume in the reservoir is increased. If the coordination criterion increases from 0.2 to

0.5, the average water volume is decreased. The reason that this phenomenon is not significant with an increased number of coordinated units as shown in Figure 5.56 is that the water in-flow is greatly limited for Reservoir A, and the available water is used up for cases with different coordination criteria.

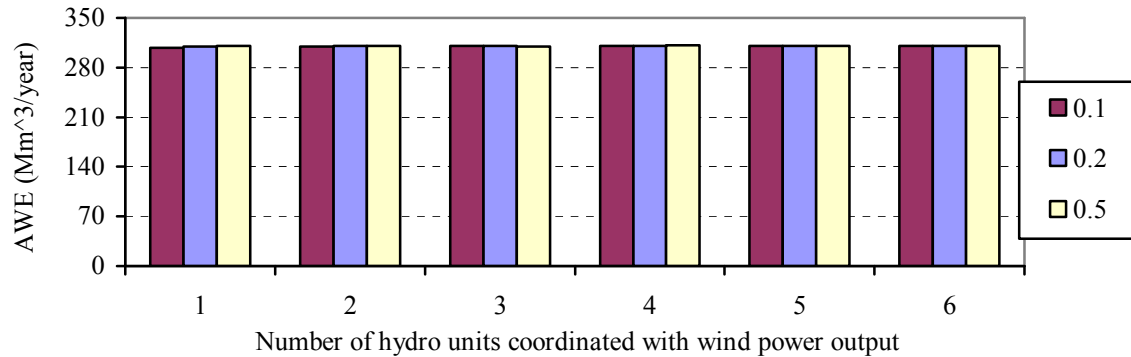


Figure 5.56: Effect of coordination criterion on the AWE with Reservoir A.

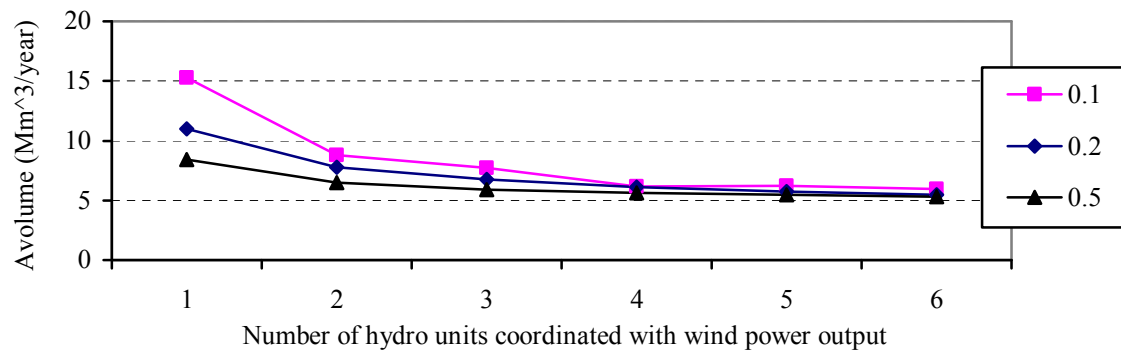


Figure 5.57: Effect of coordination criterion on the AVolume with Reservoir A.

Reservoir B with increased water inflow and the reservoir volume is used in the following studies in order to further investigate the effect of the coordination criterion on system adequacy. The results are shown in Figures 5.58 to 5.63.



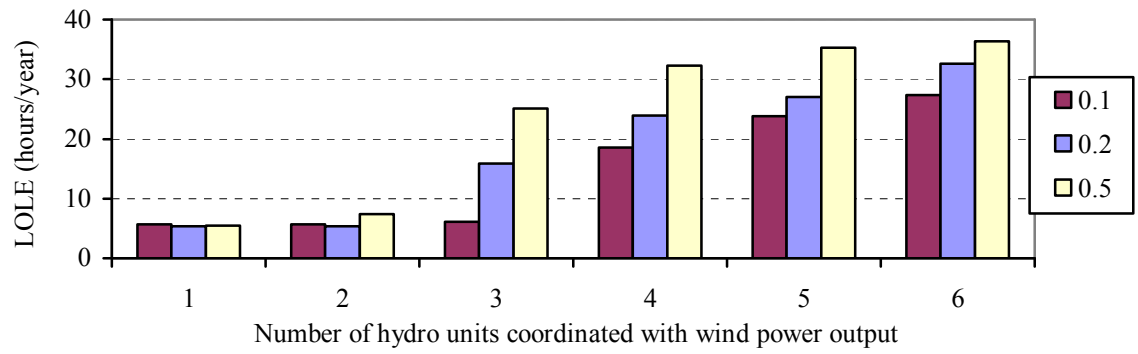


Figure 5.58: Effect of coordination criterion on the system LOLE with Reservoir B.

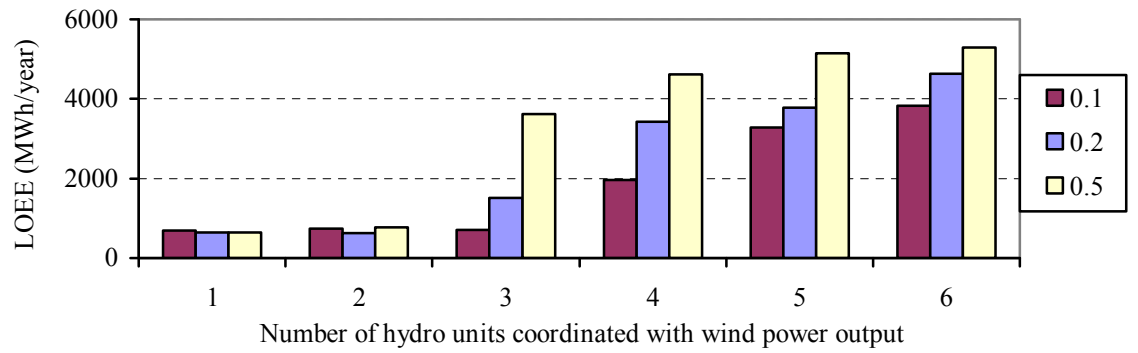


Figure 5.59: Effect of coordination criterion on the system LOEE with Reservoir B.

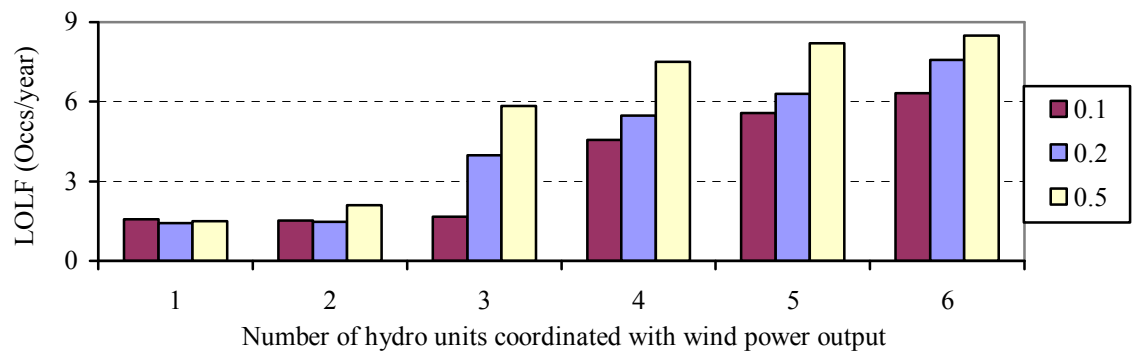


Figure 5.60: Effect of coordination criterion on the system LOLF with Reservoir B.

Figures 5.58 to 5.60 show the effect of the coordination criterion on the system adequacy indices with the increased water inflow and reservoir volume. If the

coordination criterion is decreased from 0.2 to 0.1, the system reliability level does not change when the number of hydro units assigned to coordinate with wind power is equal to 1 or 2. The system adequacy with the 0.1 criterion is higher than the 0.2 criterion when the number of coordinated hydro units is greater than 2. The reason is that less water has to be used to respond to the fluctuation of wind power, and more water is available when hydro units are required to reduce the loss of load during peak hours. If the coordination criterion is increased from 0.2 to 0.5, the system adequacy is reduced when the number of hydro units that coordinate with wind power is greater than 1. The reason is that more water has to be used to respond to the fluctuations of wind power, and less water is available when hydro units are required during the peak hours.

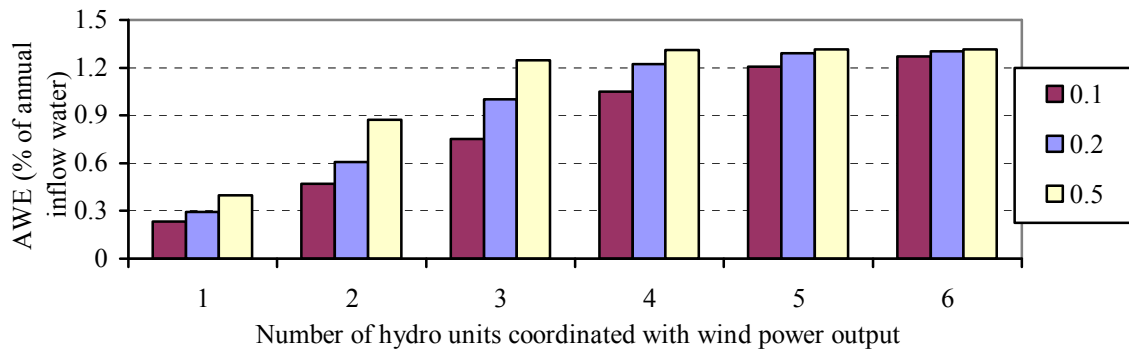


Figure 5.61: Effect of coordination criterion on the AWE with Reservoir B.

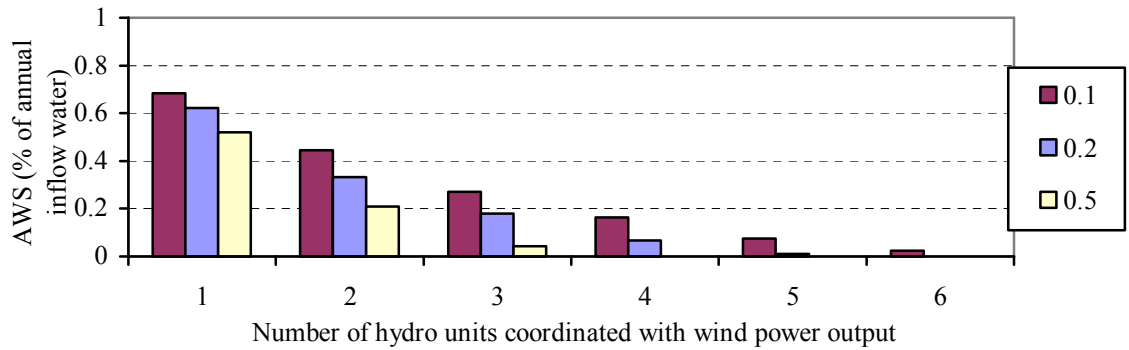


Figure 5.62: Effect of coordination criterion on the AWS with Reservoir B.

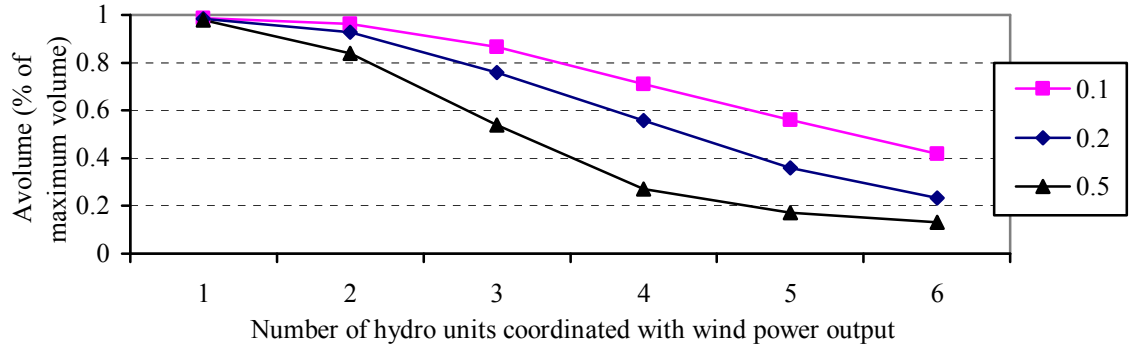


Figure 5.63: Effect of coordination criterion on the AVolume with Reservoir B.

Figures 5.61 to 5.63 respectively show the effect of the coordination criterion on the AWE, AWS, and AVolume with the increased water inflow and reservoir volume. If the coordination criterion is decreased from 0.2 to 0.1, less water is utilized by the hydro units, and more water has to be spilled. If the coordination criterion is increased from 0.2 to 0.5, more water is utilized by the hydro units, and less water has to be spilled. In Figure 5.63, the AVolume values are similar for the three coordination criteria when one hydro unit is coordinated with wind power. The AVolume decreases as the number of hydro units assigned to coordinate with wind power increases. If the number of hydro units assigned to coordinate with wind power is greater than 1, the higher coordination criterion value results in a lower water volume in the reservoir.

### 5.9 Effect of Hydro Unit Starting Failures

The effects of hydro unit starting failures on the system adequacy and water utilization in the reservoir are investigated considering wind and hydro power coordination. The starting failure probability of hydro units is considered to be 0 in the previous studies presented in this chapter. The hydro units can either start successfully or fail to start. The hydro units that fail to start will be under repair and not available for a

period of time. In this section, cases considering hydro unit starting failure probabilities of 0.1 and 0.2 are compared with the case with a hydro unit starting failure probability of 0.

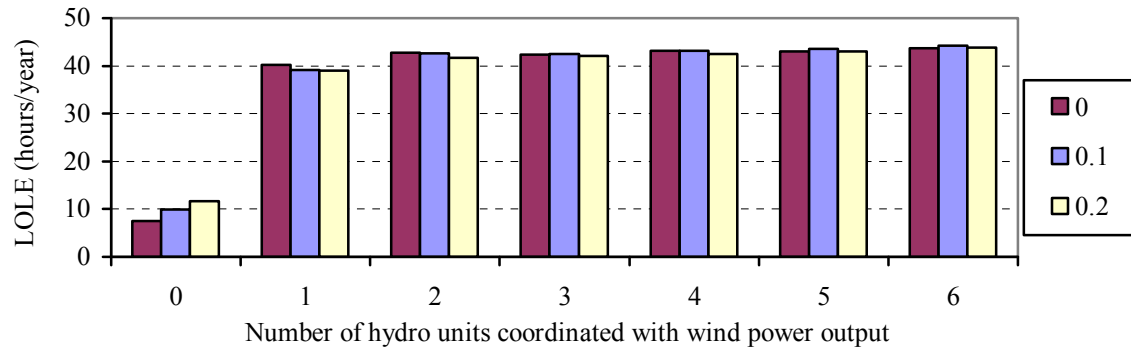


Figure 5.64: Effect of hydro unit starting failure probability on the system LOLE with Reservoir A.

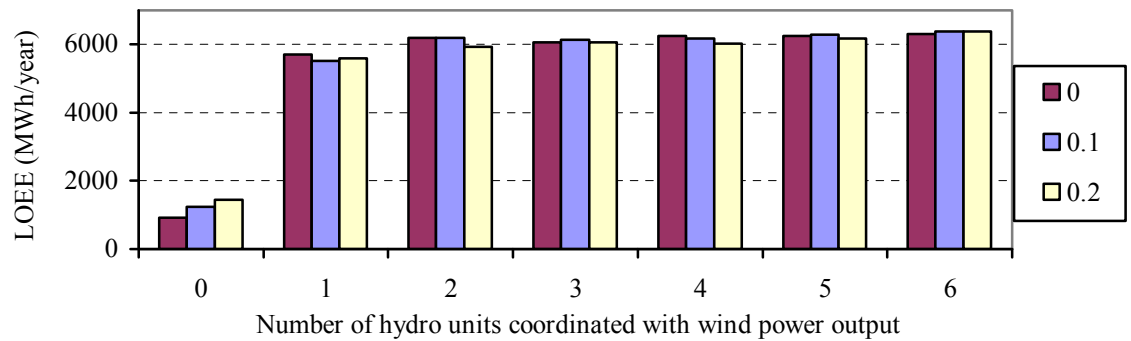


Figure 5.65: Effect of hydro unit starting failure probability on the system LOEE with Reservoir A.

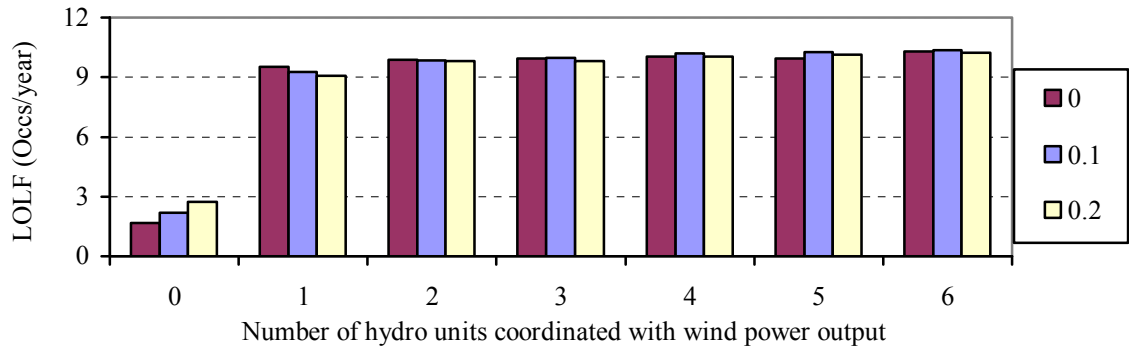


Figure 5.66: Effect of hydro unit starting failure probability on the system LOLF with Reservoir A.

Figures 5.64 to 5.66 show the effect of hydro unit starting failure probability on the system adequacy indices using Reservoir A data. It is shown in these figures that the starting failure probability of hydro units affect the system reliability level when there is no coordination between the hydro units and wind power, and the higher starting failure of hydro units result in lower system reliability. When a part of or all of the hydro units are assigned to coordinate with wind power, the effect of their starting failure probability on the system reliability is relatively small.

Figures 5.67 to 5.69 respectively show the effect of starting failure probability of the hydro units on the AWE, AWS, and AVolume. Figures 5.67 and 5.68 respectively show that the effect of the hydro unit starting failure probability on the amount of water utilized and spilled is small. Figure 5.69 shows that the consideration of starting failure of hydro units will slightly increase the water volume in the reservoir.

When no hydro units are assigned to coordinate with wind power, the water volume in the reservoir is close to its maximum limit, and starting failures of hydro units can have a significant impact on the system adequacy. When there is coordination between hydro units and wind power, the system adequacy is greatly reduced due to the

water shortage, but the impact on the system adequacy of the starting failures of hydro units is comparatively small. In the next study, the water inflow and reservoir volume are increased by using Reservoir B data, and the effect of starting failure of hydro units on the system adequacy and water utilization is further investigated.

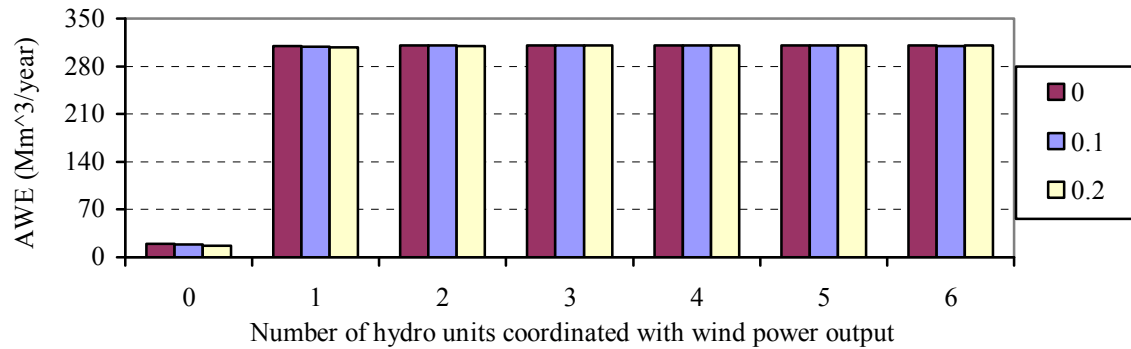


Figure 5.67: Effect of hydro unit starting failure probability on the AWE with Reservoir A.

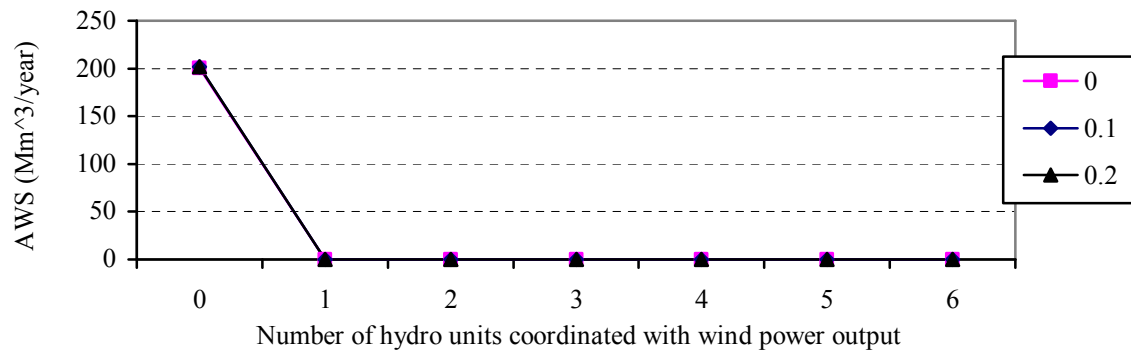


Figure 5.68: Effect of hydro unit starting failure probability on the AWS with Reservoir A.

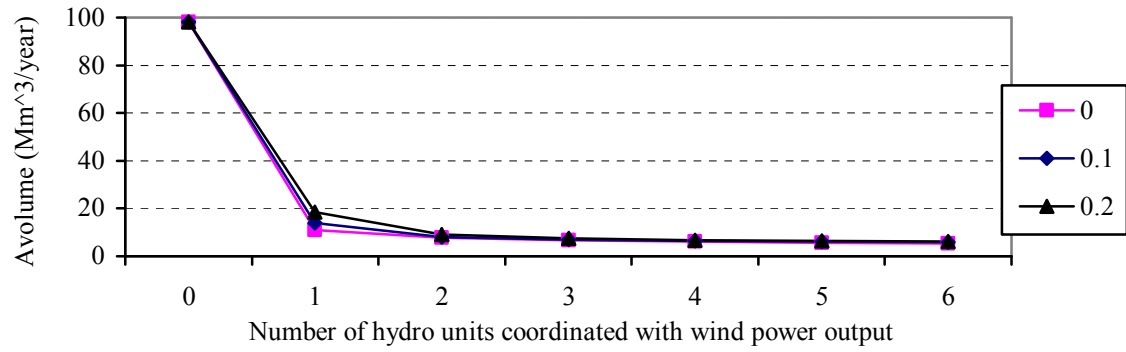


Figure 5.69: Effect of hydro unit starting failure probability on the AVolume with Reservoir A.

Figures 5.70 to 5.72 show the effect of starting failure of hydro units on the system adequacy indices when the water inflow and the hydro reservoir are increased. When the number of hydro units coordinated with wind power is less than 3, the adequacy indices are increased as the starting failure probability of hydro unit increases from 0 to 0.2. When 3 hydro units are coordinated with wind power, the adequacy indices decrease when the hydro unit starting failure probability increases from 0 to 0.1. The adequacy indices, however, increase when the hydro unit starting failure probability further increases from 0.1 to 0.2. When the number of hydro units coordinated with wind power is greater than 3, the adequacy indices decrease as the hydro unit starting failure probability increases from 0 to 0.2.

Figures 5.73 to 5.75 show the effect of hydro unit starting failure on the AWE, AWS, and AVolume. These figures show that the amount of water utilized is reduced, the amount of water spilled is increased, and the water level in the reservoir is increased if the starting failure probability of hydro units increases. The starting failure of hydro units has a significant impact on the water utilization when the water inflow and reservoir volume are increased.

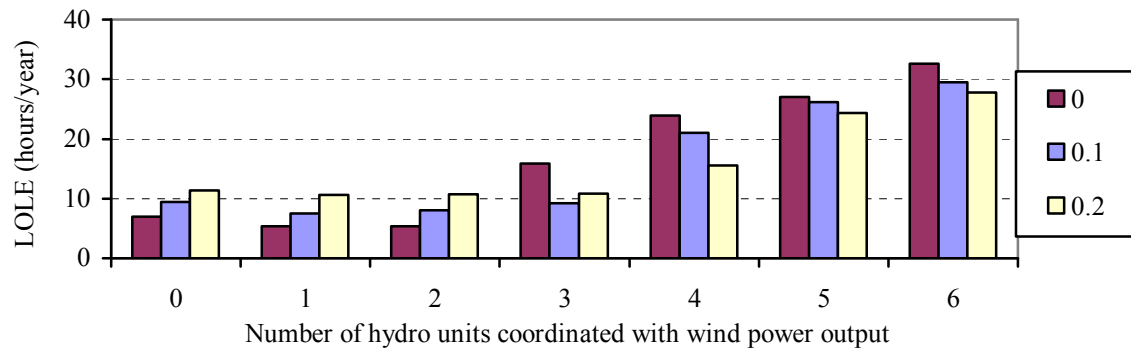


Figure 5.70: Effect of hydro unit starting failure probability on the system LOLE with Reservoir B.

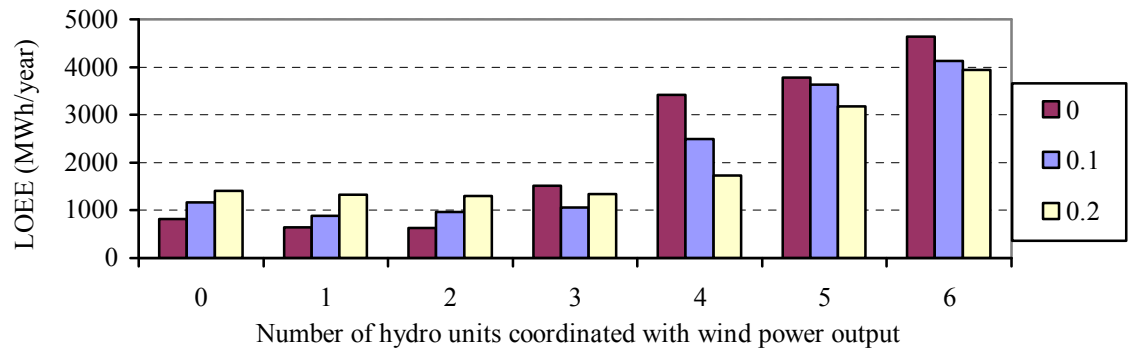


Figure 5.71: Effect of hydro unit starting failure probability on the system LOEE with Reservoir B.

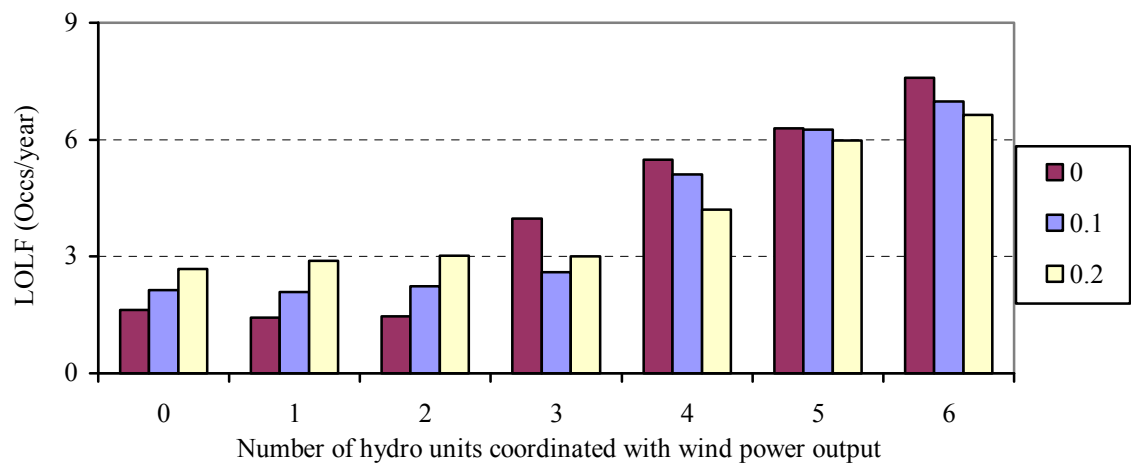


Figure 5.72: Effect of hydro unit starting failure probability on the system LOLF with Reservoir B.



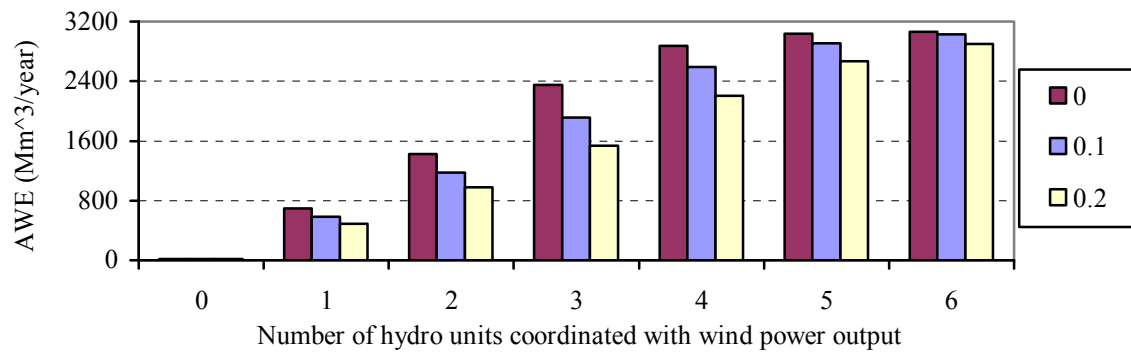


Figure 5.73: Effect of hydro unit starting failure probability on the AWE with Reservoir B.

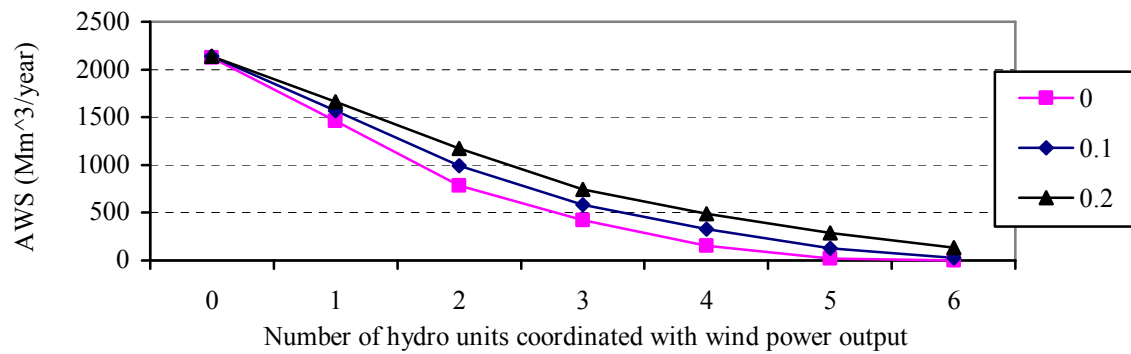


Figure 5.74: Effect of hydro unit starting failure probability on the AWS with Reservoir B.

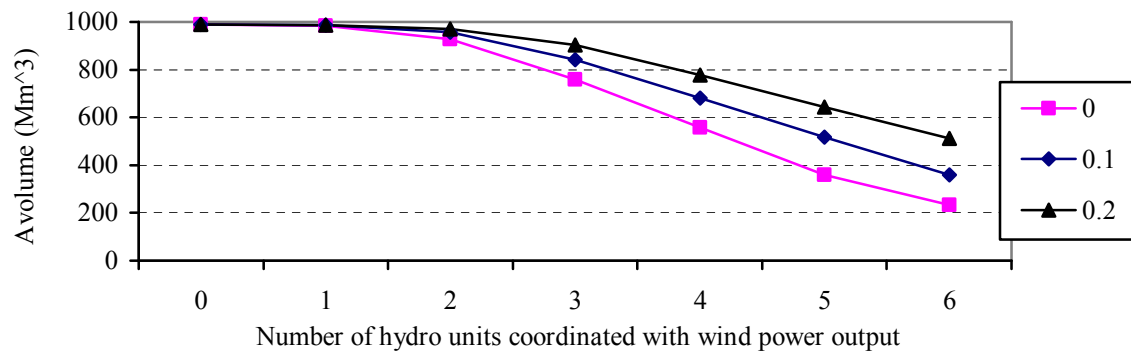


Figure 5.75: Effect of hydro unit starting failure probability on the AVolume with Reservoir B.

The consideration of hydro unit starting failure can reduce the system reliability level if sufficient water is available in the reservoir for the hydro units. When 3 or more hydro units are assigned to coordinate with wind power, the water in the reservoir is not always enough for the hydro units. The water can be saved for the peaking hydro units during the peak hours if the hydro unit starting failure is considered. This is the reason that the consideration of hydro unit starting failure can improve the system adequacy when 3 or more hydro units are assigned to coordinate with wind power.

#### **5.10 Effect of Initial Water Volume in the Reservoir**

In the previous studies in this chapter, the initial water volume in the reservoir is set at 80% of its maximum volume at the beginning of each simulated year. Two additional cases with initial reservoir water volume of 50% and 20% of the maximum volume are compared with the 80% case in this section. The effect of the initial water volume in the reservoir on the system adequacy and water utilization are investigated considering wind and hydro power coordination.

Figures 5.76 to 5.78 show the effect on the system adequacy indices of the initial water volume in the reservoir using Reservoir A data. The system reliability decreases as the initial water volume in the reservoir decreases. The impact of initial water volume on system adequacy is significant as shown in these figures when there is no coordination between hydro units and wind power. The reason is that a decrease in the initial water volume means a decrease of the available water to meet the load during the peak hours. When there is coordination between hydro units and wind power, the water in the reservoir is used up for the three cases with different initial water volumes in the reservoir and the differences in the reliability indices between the three cases are small. The effect of the initial water volume in the reservoir on the system adequacy is small

when there is coordination between hydro units and wind power.

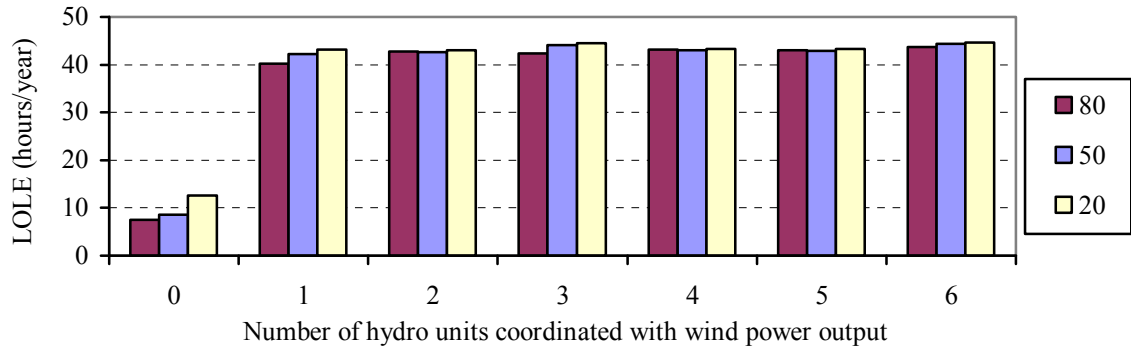


Figure 5.76: Effect of the initial water volume in the reservoir on the system LOLE with Reservoir A.

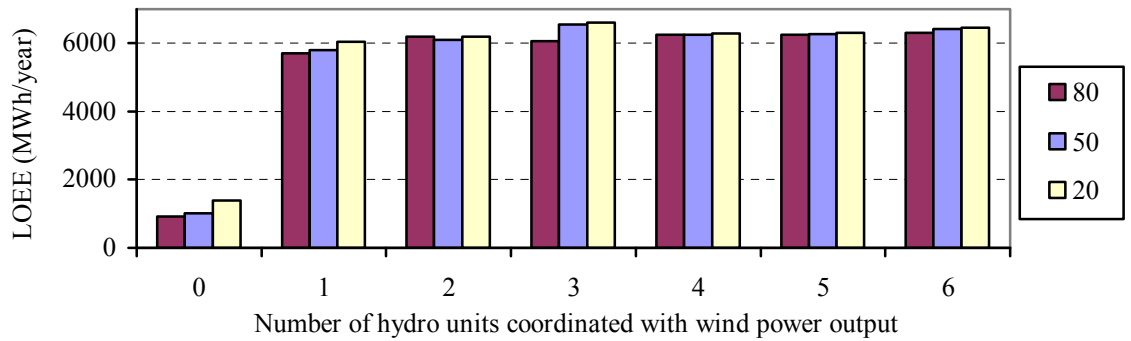


Figure 5.77: Effect of the initial water volume in the reservoir on the system LOEE with Reservoir A.

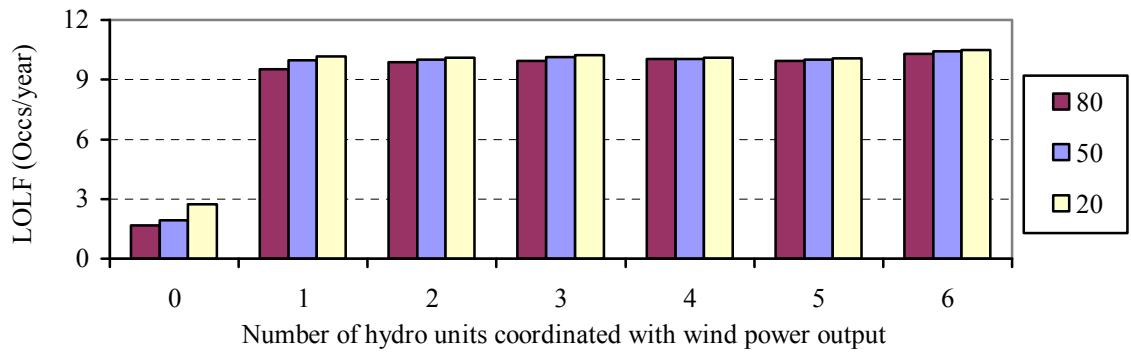


Figure 5.78: Effect of the initial water volume in the reservoir on the system LOLF with Reservoir A.

Figures 5.79 to 5.81 show the effect of the initial water volume on the water utilization indices, the AWE, AWS, and AVolume when Reservoir A data is used. When there is no coordination between the wind power and hydro units, the initial water volume has a small impact on the amount of water utilized. The amount of water spilled, and the average water volume are however reduced. When a number of hydro units are assigned to coordinate with wind power, the decrease in the initial water volume reduces the amount of water utilized and slightly reduces the average water volume in the reservoir.

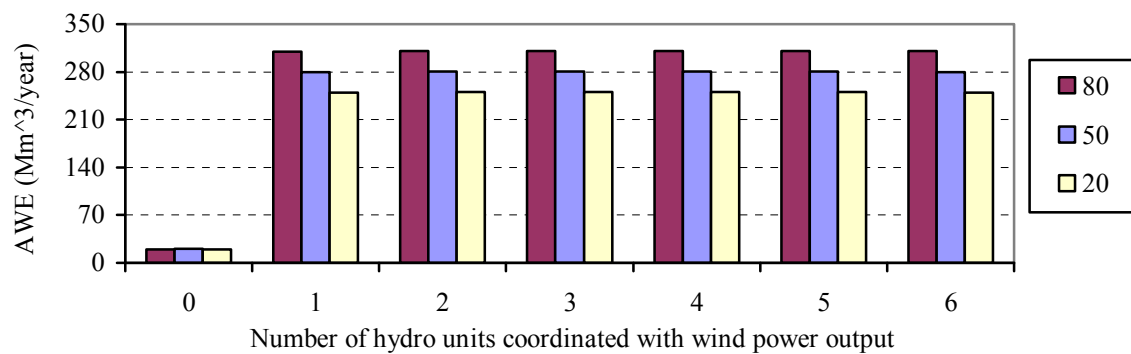


Figure 5.79: Effect of the initial water volume in the reservoir on the AWE with Reservoir A.

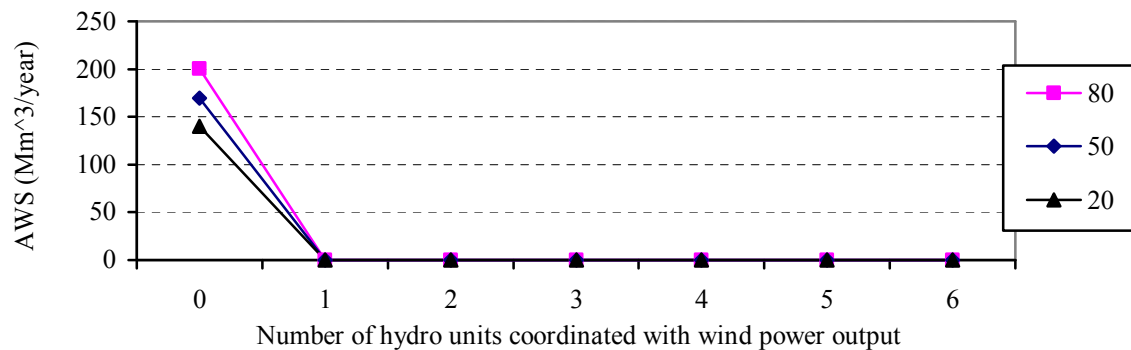


Figure 5.80: Effect of the initial water volume in the reservoir on the AWS with Reservoir A.

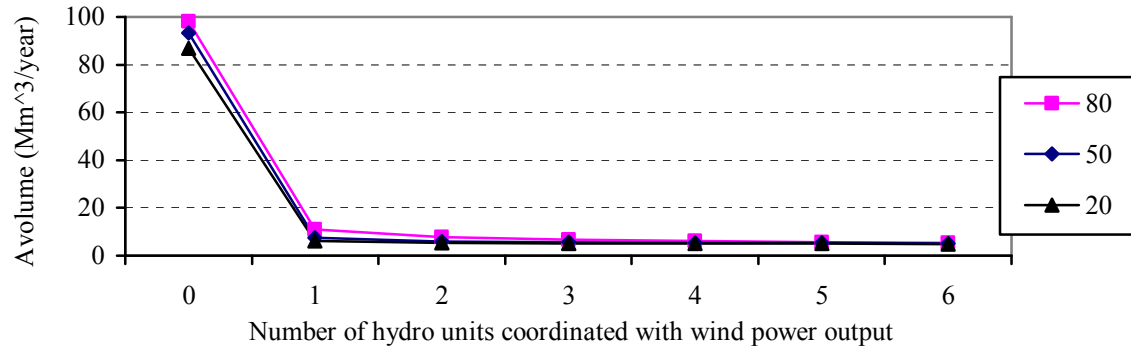


Figure 5.81: Effect of the initial water volume in the reservoir on the AVolume with Reservoir A.

In order to further investigate the effect of initial water volume in the reservoir, the water inflow and the reservoir volume are multiplied by a factor of 10 using Reservoir B, and the results are shown in Figures 5.82 to 5.87.

Figures 5.82 to 5.84 show the effect of the initial water volume on the system adequacy indices when Reservoir B is used in the study. When the initial water volume decreases from 800 Mm<sup>3</sup> to 500 Mm<sup>3</sup>, the system reliability changes slightly if there is no coordination between wind power and hydro units, or the number of hydro units assigned to coordinate with wind power equal to 1 and 2. If the number of hydro units assigned to coordinate with wind power is greater than 2, the decreased initial water volume significantly reduces the system reliability. When the initial water volume is decreased from 500 Mm<sup>3</sup> to 200 Mm<sup>3</sup>, the system reliability level is reduced for all the cases as shown in the figures.

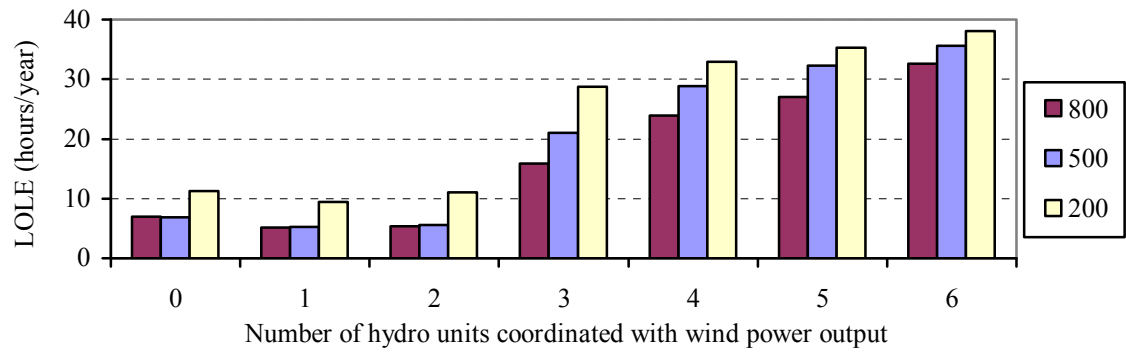


Figure 5.82: Effect of the initial water volume in the reservoir on the system LOLE with Reservoir B.

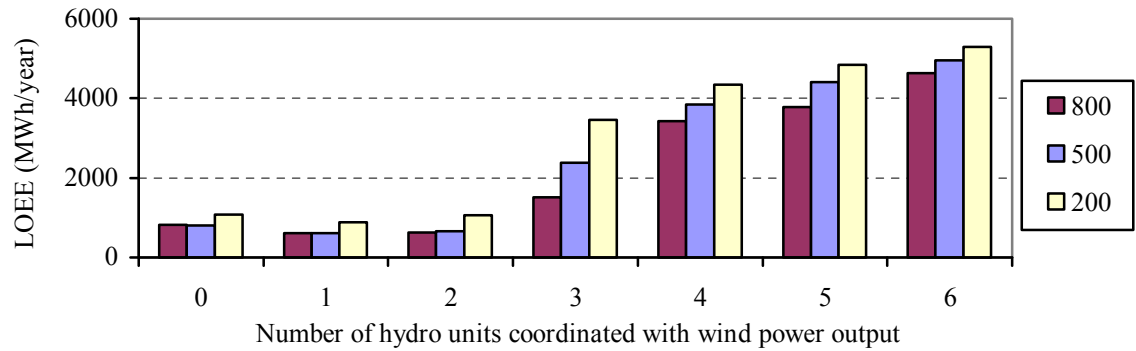


Figure 5.83: Effect of the initial water volume in the reservoir on the system LOEE with Reservoir B.

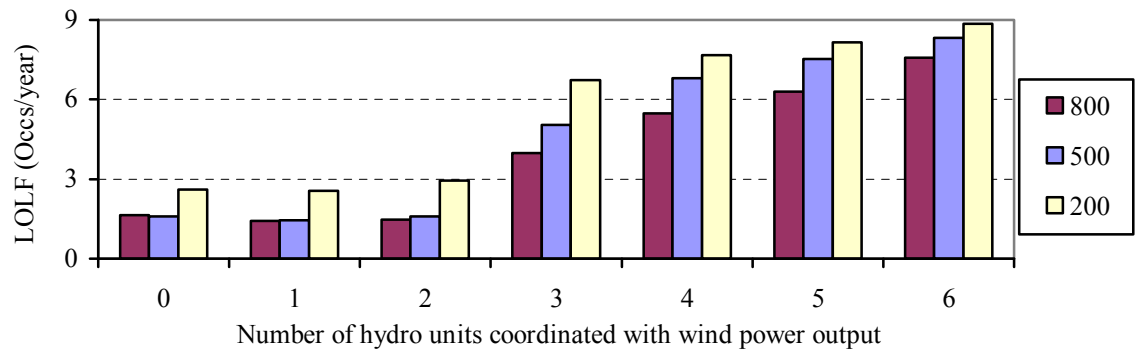


Figure 5.84: Effect of the initial water volume in the reservoir on the system LOLF with Reservoir B.

Figures 5.85 to 5.87 show the effect of the initial water volume on the AWE, AWS, and AVolume when considering the large reservoir and increased water inflow. It is interesting to see in Figure 5.85 that the AWE initially increases and then decreases with a decrease in the initial water volume as the number of coordinated hydro units is increased from 1 to 6. The AWE for cases with different initial water volumes continues to increase as the number of hydro units assigned to coordinate with wind power increases, and the AWE reach their maximum values at different levels for the different cases. Obviously, the decrease in the initial water volume in the reservoir reduces the total amount of available water. If the initial water volume is equal to 800 Mm<sup>3</sup>, the AWE reaches its maximum value when 5 hydro units are assigned to coordinate with wind power. For initial water volumes of 500 and 200 Mm<sup>3</sup>, the AWE is a maximum when the number of hydro units assigned to coordinate with the wind power is equal to 4 and 3 respectively.

Figure 5.86 shows that less water is spilled if the initial water volume in the reservoir is decreased. Figure 5.87 shows that a reduced initial water volume decreases the average water volume in the reservoir.

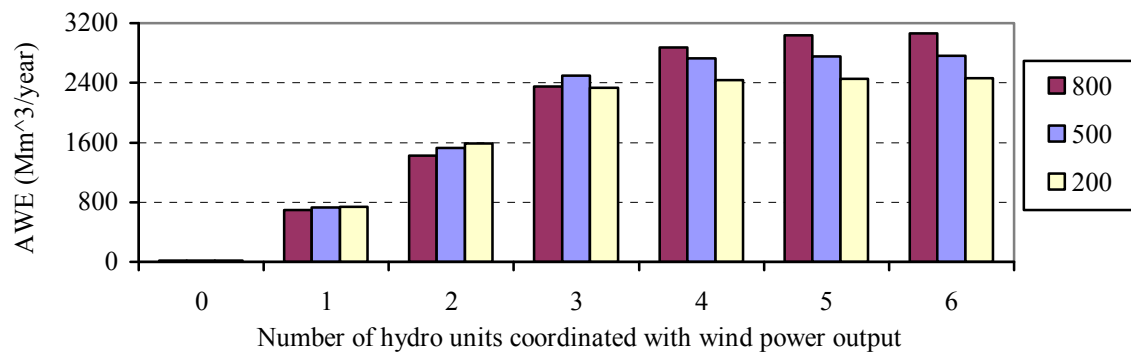


Figure 5.85: Effect of the initial water volume in the reservoir on the AWE with Reservoir B.

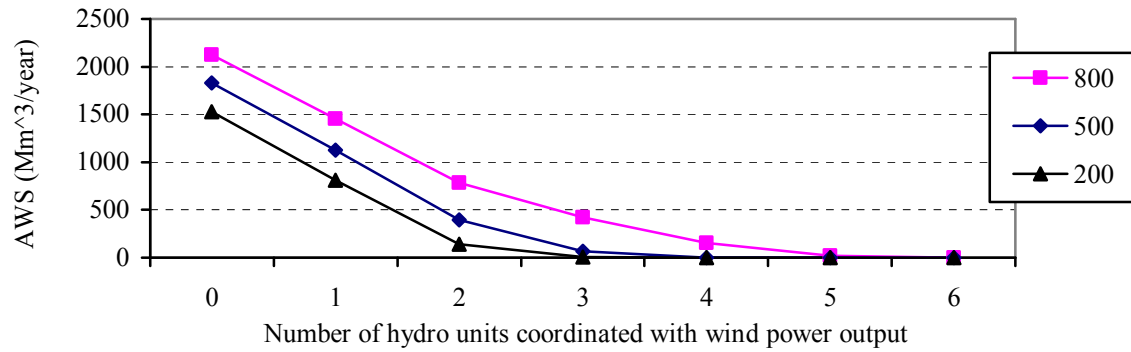


Figure 5.86: Effect of the initial water volume in the reservoir on the AWS with Reservoir B.

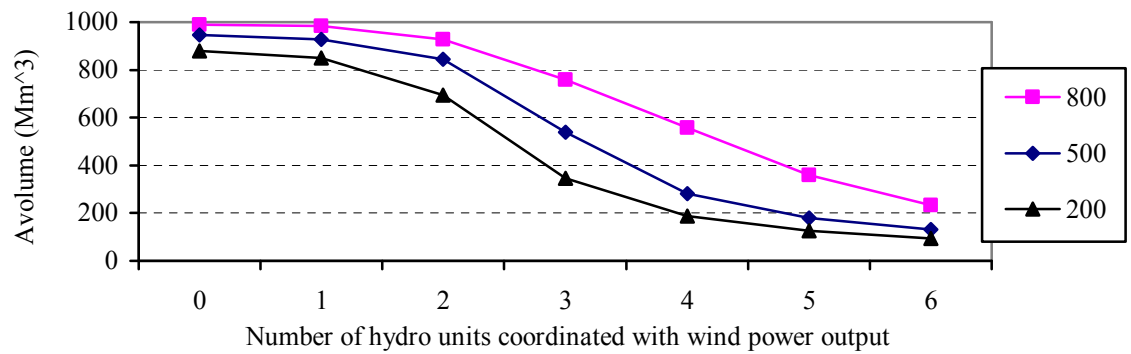


Figure 5.87: Effect of the initial water volume in the reservoir on the AVolume with Reservoir B.

## 5.11 Summary

A series of sensitivity studies are described in this chapter to illustrate the effect of important system parameters on the reliability benefits from the coordination between wind power and hydro units. An interactive simulation technique is applied for the adequacy evaluation of the generating system considering the coordination between



wind power and the hydro units. Base case studies were conducted to explore the impact of energy limited hydro units and the wind power dispatch restriction on the system adequacy using different hydro unit models. It is necessary to use the model that incorporates energy limitations and the different hydro unit resident states if the operating strategy of hydro units is to be considered in the system adequacy evaluation.

The coordination between wind power and hydro units can reduce the system adequacy due to inadequate water in the reservoir if the hydro reservoir is relatively small and the hydro unit energy limitations are considered. If there is no coordination between the wind power and the hydro units, very little water is utilized by the hydro units. All the available water in the reservoir is used by the hydro units and no water is spilled if there is coordination between the wind power and the hydro units.

The water inflow and reservoir volume are increased in the study to investigate the impacts of wind and hydro coordination as the water inflow and reservoir size in the initial studies are relatively small and inadequate to operate hydro units in coordination with wind power. The system reliability level can be maintained when the number of hydro units assigned to coordinate with wind power is 1 or 2 if the water inflow and reservoir volume are increased by a factor of 10. If the number of hydro units assigned to coordinate with wind power is greater than 2, the system adequacy decreases due to inadequate water in the reservoir. As the number of hydro units assigned to coordinate with wind power increases, more water in the reservoir is utilized by the hydro units, less water is spilled, and the average water volume continues to decrease in the reservoir. There are reliability benefits from the coordination between wind power and hydro units, and the number of hydro units assigned to coordinate with wind power has little effect on the system adequacy if the units are not energy constrained by the reservoir.

The system reliability is improved by coordination between hydro units and wind

farms located in good wind regimes as long as there is adequate water in the reservoir. The wind regime can affect the amount of water utilized, and spilled since it can affect the frequency of hydro units starts in coordination with wind power.

The system reliability is improved as the wind penetration increases, given that there is adequate water in the reservoir for the coordination between wind power and hydro units. The wind power penetration has little effect on the water in the reservoir since the coordination criterion is a fixed percentage of the rated wind capacity, which does not change with wind penetration.

An increase in the system load decreases the system adequacy. The effect of the system load on the water in the reservoir is however small.

The coordination criterion can significantly affect the reliability benefit of coordination between the wind power and the hydro units when the reservoir volume and the water inflow are increased from Reservoir A to Reservoir B data. The hydro units assigned to coordinate with wind power have to be started more often when the coordination criterion is relatively high, and therefore, more water is utilized by these hydro generators.

An increase in the hydro unit starting failure probability can reduce the system adequacy when the water in the reservoir is adequate. When the water in the reservoir is inadequate, the increase in starting failure probability can reduce the amount water utilized by the hydro units assigned to coordinate with wind power and save the water for peaking purposes during peak hours and this has the effect of reducing the system adequacy indices.

The initial water volume in the reservoir affects the amount of water available for

use in a given year. The decreased initial water volume in the reservoir therefore increases the annual system adequacy indices when there is coordination between wind power and hydro units.

## **6. SUMMARY AND CONCLUSIONS**

Global environmental concerns associated with conventional energy generation, limited reserves of fossil fuels, and increasing electricity demand have led to the rapid growth of wind energy applications in power systems. Different types of renewable energy policies, such as RPS and Fixed Feed-in-Tariffs have been implemented in various jurisdictions around the world. These policies have set high wind penetration targets in power grids within the jurisdictions. Wind is going to be an important source of electrical power generation in the near future. Large wind penetration in power systems will have serious impacts on the overall system reliability.

Due to the variable nature of wind speed, large scale integration of wind power in a power system can produce large power fluctuations, and the continuity of electric power supply to customers can be affected. Energy storage can be utilized to reduce the risk in continuously meeting the varying system load. The actual benefits associated with wind power and energy storage in relatively large power systems need to be technically investigated using quantitative evaluation methods.

There are two major techniques used by power utilities in the reliability evaluation of power systems. They can be categorized as being either deterministic or probabilistic methods. Deterministic methods cannot recognize the random system behavior and completely reflect the risk associated with a given system. Many power utilities have changed from deterministic to probabilistic criteria [43]. Probabilistic methods are suitable for adequacy evaluation of systems that include numerous random variables associated with wind power and energy storage.

The fundamental techniques utilized in the probabilistic assessment of generating capacity adequacy include direct analytical and simulation methods. Analytical techniques for adequacy evaluation use mathematical and statistical models to represent the system elements. In an analytical approach, the generation model is in the form of a capacity outage probability table that includes the capacity and the corresponding probability of each outage state of the generating system. The load model is a daily peak load duration curve or an hourly load duration curve. The main disadvantage of the analytical method is that it can not recognize the chronological variations in the generation and load elements and the correlation between subsequent events, which are very important in the assessment of power systems with wind energy and energy storage. The sequential MCS method is therefore used in the adequacy evaluation of generating systems containing wind power and energy storage. In this method, the generation model is constructed by creating an artificial operating history of each generating unit in time chronology. The load model is represented by a sequential hourly load variation profile. The system risk indices in both approaches are obtained by combining the generation model and the load model to obtain the system risk model.

The generating model for power systems including wind power is developed using the following steps. Time series auto regressive and moving average models for wind regimes with different geographical characteristics are utilized to simulate the high-order auto-correlation, the seasonal and diurnal distribution of the actual wind speed. The power curve technique is employed to obtain the available wind farm power output from the simulated wind speed. A time sequential MCS method is applied to generate a synthetic operating history of a generating system.

An energy storage facility can be used to smooth the fluctuating nature of wind power, and improve the continuity of power supply from a wind energy conversion

system. A time series model for energy storage considering its charging/discharging characteristics is developed based on the generation time series and the load time series models. A wind energy dispatch restriction is incorporated in the model, in which the wind energy utilization is restricted to a specified percentage of the system load in order to consider the power system stability concerns. The amount of wind energy that can not be directly absorbed by the system is surplus wind energy and is available to be stored in an energy storage facility. All of the surplus wind energy can not be stored since there are charging/discharging constraints and capacity limits of energy storage facilities.

A hydro plant with a reservoir acts as an indirect energy storage facility. It has the ability to quickly adjust its power output and alleviate the impact of wind power fluctuations. Hydro units are modeled by incorporating energy limitations in the IEEE four-state model in order to recognize the intermittent operation of hydro units in response to the system need. If a hydro unit is successfully started, its power output depends on the water condition in the reservoir during that time interval. A coordination strategy between wind power and energy limited hydro units are considered, and an interactive simulation model is developed for adequacy evaluations.

The overall system adequacy increases with an increase in the wind power penetration level. The incremental reliability benefits from wind power, however, decrease. The simulation results show that the expected surplus wind energy (ESWE) increases as the installed wind capacity is increased above the minimum system load level when all wind energy can be utilized by the system load. At relatively high wind penetration, the wind power must be restricted to avoid system stability problems in practical system operation. In this case, the ESWE can be relatively high, and a significant amount of ESWE that cannot be absorbed by the system is available for storage. A relatively high ESWE means more benefits can be obtained from using energy storage in wind integrated power systems.

Energy storage can improve the system adequacy of a generating system containing wind power. The charging/discharging restrictions of the storage facility greatly limit the benefits from energy storage. Different storage technologies have different charging/discharging characteristics, and therefore, provide different reliability benefits to the system.

Three different operating strategies for wind farm and energy storage are proposed and compared in terms of their contribution to the overall system reliability and the utilization of a storage facility to capture surplus wind energy. In Scenario 1, the energy stored is only used to avoid or minimize load loss situations. A fixed power dispatch commitment is made in Scenario 2 from the combined use of wind power output and energy storage. Scenario 3 is similar to Scenario 2 with additional usage for the stored energy to avoid or minimize load loss situations. There is a wind energy dispatch restriction for all three operating strategies, and the surplus wind energy above the wind energy dispatch restriction is available for storage. Energy storage in Scenario 1 is controlled by the Independent System Operator, and the stored energy is used to supply the system load when the sum of the wind power and the conventional power is inadequate to supply the system load. Energy storage in Scenario 2 and 3 are operated by wind farm owners, and a commitment is made to supply power equal to the wind energy dispatch restriction.

The wind farm and energy storage operating strategy described in Scenario 1 provides higher system reliability than Scenarios 2 and 3. Compared with Scenario 2, energy storage in Scenario 3 has more ability to improve the system reliability for a wide range of wind energy dispatch restrictions. The charging and discharging characteristics of energy storage can greatly affect the reliability benefits from energy storage in Scenario 1, but have negligible effects on the reliability benefits in Scenarios 2 and 3.

There is better utilization of the stored energy in Scenarios 2 and 3 than in Scenario 1. In other words, significantly more wind energy can be stored in Scenario 2 and 3 compared with Scenario 1. There is very little difference between Scenarios 2 and 3 on the wind energy that can be placed in the energy storage facility. The charging and discharging restrictions on energy storage have great influence on the amount of wind energy that can be stored in Scenarios 2 and 3. The reliability benefits from energy storage in all three scenarios are highly dependent on the wind energy dispatch restrictions. Energy storage in Scenario 3 has the ability to improve the system reliability, and capture relatively large amounts of surplus wind energy. Energy storage in Scenario 3 is a potentially useful option for both power system operators and wind farm owners.

An interactive simulation technique considering the coordination between wind and hydro power generation is applied in the adequacy evaluation of generating systems. Base case studies were conducted to investigate the impact of energy limited hydro units on the system adequacy using different hydro unit models, and the effect of wind power dispatch restriction on the reliability benefits of wind power. It is necessary to use a model that incorporates energy limitations and the different hydro unit resident states if the operating strategy of hydro units and WTG units are to be considered in the system adequacy evaluation. Wind power dispatch restrictions have considerable great influence on the system adequacy indices especially when the wind penetration level is relatively high.

A series of sensitivity studies have been conducted to investigate the effect on the reliability benefit from the coordination between wind power and hydro units of important factors, such as the number of hydro units assigned to coordinate with the wind power, the water in-flow and reservoir volumes, the wind farm locations, the wind power penetration levels, the system load level, the coordination criterion between the



wind power and the hydro units, the hydro unit starting failure probability, and the initial water volume of the reservoir.

The reliability benefits from the coordination between wind power and hydro units largely depends on the reservoir size, water in-flow to the reservoir, and the number of hydro units assigned to coordinate with wind power. There are significant reliability benefits from wind and hydro coordination if infinite water is available in the reservoir. In this case, the number of hydro units assigned for coordination has little effect on the system adequacy. If there is inadequate water in the reservoir due to relatively small water in-flow and reservoir volume, the coordination between wind power and hydro units can reduce the system adequacy. All the available water in the reservoir is used up by the hydro units that operate in response to wind power fluctuations, and no water is available to supply the load during peak hours. If there is no coordination between wind power and hydro units, very little water is utilized by the hydro units.

Reservoir A used in the initial studies is relatively small with a small water in-flow, and is inadequate to provide storage benefits for wind integrated power systems. Reservoir B is larger than Reservoir A by a factor of 10, and therefore, can provide relatively more benefits to the system from wind and hydro coordination. The system adequacy is improved by wind and hydro coordination if the number of assigned hydro units is less than 3. If the number of hydro units assigned to coordinate with wind power is greater than 2, the system adequacy continues to decrease due to inadequate water in the reservoir. As the number of hydro units assigned to coordinate with wind power increases, more water in the reservoir is utilized by the hydro units, less water is spilled, and the average water volume continues to decrease in the reservoir.

Better wind regimes normally mean higher average wind speed and greater

expected power output from the WTG units. If wind farms are located in better wind regimes, more reliability benefits can be obtained from the coordination between hydro units and wind farms as long as there is adequate water in the reservoir. The amount of water utilized by hydro units can be reduced if the wind farm is located at a site with good wind regime since it can decrease the frequency of hydro units started to coordinate with wind power.

The system reliability is improved as the wind penetration increases if there is adequate water in the reservoir for the coordination between the wind power and the hydro units. The wind power penetration has little impact on the water in the reservoir since the coordination criterion does not change with wind penetration as it is a fixed percentage of the rated wind capacity.

The reliability benefit from the coordination between wind power and hydro units is significantly affected by the coordination criterion when the hydro reservoir is relatively large. The hydro units assigned to coordinate with wind power have to be started more often when the coordination criterion is relatively high, and therefore, more water is utilized by these hydro generators and less water is available for peaking purposes during high load hours.

The system adequacy is reduced by an increase in the starting failure probability of hydro units when there is adequate water in the reservoir. When the water in the reservoir is inadequate, increases in the starting failure probability of hydro units reduces the amount of water utilized by the hydro units assigned to coordinate with wind power. As a result, the system adequacy is improved since more water is available for the peaking units to serve the load during the peak hours.

The amount of water available for utilization in a given year is affected by the

initial water volume in the reservoir. A decrease in the initial water volume in the reservoir increases the annual system adequacy indices with or without the coordination between wind power and hydro units. The system adequacy is decreased by an increase in the system load. The effect of the system load on the reservoir water is small if the coordination between wind power and hydro units is considered.

In conclusion, the models and methodologies developed, concepts and examples illustrated, results and discussion presented in the thesis provide valuable information to electric power utilities for planning and operating power systems containing wind power and energy storage.

## 7. REFERENCES

- [1] R. Billinton and R.N. Allan, *Reliability Evaluation of Power Systems*, 2<sup>nd</sup> Edition, Plenum Press, New York, 1996.
- [2] Global Wind Energy Council, [http:// www.gwec.net/](http://www.gwec.net/), “Wind is a Global Power Source”.
- [3] Canadian Wind Energy Association Website, <http://www.canwea.ca/>, “Wind Version for Canada”.
- [4] Windustry Website, <http://www.windustry.com/>, “Introduction to Wind Energy”.
- [5] American Wind Energy Association Website, <http://www.awea.org/>, “Renewable Portfolio Standard”.
- [6] T. Ackermann, *Historical Development and Current Status of Wind Power*, Chapter 2 of book: *Wind Power in Power Systems*, Edited by Ackermann T., John Wiley & Sons Ltd, 2005.
- [7] M. P. Connor, *The UK Renewable Obligation*, Chapter 7 of book: *Switching of Renewable Power*, Edited by V. Lauber, Earthscan, 2005.
- [8] I. Abouzahr and R. Ramakumar, “An approach to assess the performance of utility-interactive wind electric conversion systems”, *IEEE Transactions on Energy Conversion*, Vol. 6, no. 4, December, 1991, pp. 627-638.

- [9] R. Billinton, H. Chen and R. Ghajar, "Time-series models for reliability evaluation of power systems including wind energy", *Microelectronics Reliability*, Vol. 36, no. 9, September, 1996, pp. 1253-1261.
- [10] P. Giorsetto and K. F. Utsurogi, "Development of a new procedure for reliability modeling of wind turbine generators", *IEEE Transactions on Power Apparatus and Systems*, Vol. 102, no. 1, January, 1983, pp. 134-143.
- [11] X. Wang, H. Dai, and R. J. Thomas, "Reliability modeling of large wind farms and electric utility interface systems", *IEEE Transactions on Power Apparatus and Systems*, Vol. 103, no. 3, March, 1984, pp. 569-575.
- [12] R. Karki, P. Hu, "Wind power simulation model for reliability evaluation", *Proceedings of the IEEE Canadian Conference on Electrical and Computer Engineering*, Saskatoon, May 1-4, 2005, pp. 541-544.
- [13] R. Karki, P. Hu, R. Billinton, "A simplified wind power generation model for reliability evaluation", *IEEE Transactions on Energy Conversion*, Vol. 21, no. 2, June, 2006, pp.533 – 540.
- [14] R. Karki, P. Hu, R. Billinton, "Reliability evaluation of a wind power delivery system using an approximate wind model", *41st International Universities Power Engineering Conference*, Newcastle, UK, September 6<sup>th</sup>-8<sup>th</sup>, 2006.
- [15] R. Billinton and A. A. Chowdhury, "Incorporation of wind energy conversion systems in conventional generation capacity adequacy assessment", *IEE Proceedings—C*, Vol. 139, no. 1, January, 1992, pp. 47-56.

- [16] A. J. M. van Wijk, N. Halberg, and W. C. Turkenburg, "Capacity credit of wind power in the Netherlands", *Electric Power Systems Research*, vol. 23, 1992, pp. 189-200.
- [17] Rui M. G. Castro and Luís A. F. M. Ferreira, "A Comparison between chronological and probabilistic methods to estimate wind power capacity credit", *IEEE Transactions on Power Systems*, Vol. 16, no. 4, November, 2001, pp. 904-909.
- [18] R. Billinton and W. Li, *Reliability Assessment of Electrical Power Systems Using Monte Carlo Methods*, Plenum Publishing, New York, 1994.
- [19] Wijarn Wangdee, "Bulk electric system reliability simulation and application", Ph. D. thesis, University of Saskatchewan, 2005.
- [20] R. Karki, R. Billinton, "Maintaining supply reliability of small isolated power systems using renewable energy", *IEE Proceedings Generation, Transmission and Distribution*, Vol. 148, no. 6, November, 2001 pp.530 - 534.
- [21] R. Karki and R. Billinton, "Cost-effective wind energy utilization for reliable power supply", *IEEE Transactions on Energy Conversion*, Vol. 19, no. 2, June, 2004, pp. 435-440.
- [22] R. Billinton, G. Bai, "Generating capacity adequacy associated with wind energy", *IEEE Transactions on Energy Conversion*, Vol.19, no. 3, September, 2004, pp. 641-646.
- [23] R. Billinton, H. Chen, and R. Ghajar, "A sequential simulation technique for adequacy evaluation of generating systems including wind energy", *IEEE Transactions on Energy Conversion*, Vol. 11, no. 4, December, 1996, pp. 728-734.

- [24] R. Karki and R. Billinton, "Reliability/cost implications of PV and wind energy utilization in small isolated power systems", *IEEE Transactions on Energy Conversion*, Vol. 16, no. 4, December, 2001, pp. 368-373.
- [25] C. Singh, and A. Lago-Gonzalez, "Reliability modeling of generation systems including unconventional energy sources", *IEEE Transactions on Power Apparatus and Systems*, Vol. 104, no. 5, May, 1985, pp.1049-1056.
- [26] G. Desrochers, M. Blanchard, and S. Sud, "A Monte Carlo simulation method for the economic assessment of the contribution of wind energy to power systems", *IEEE Transactions on Energy Conversion*, Vol. 1, no. 4, December, 1986, pp. 50-56.
- [27] P. B. Eriksen, T. Ackermann, et al., "System operation with high wind penetration", *IEEE Power and Energy Magazine*, Vol. 3, no. 6, November/December, 2005, pp. 65-74.
- [28] M. Black, G. Strbac, "Value of bulk energy storage for managing wind power fluctuations", *IEEE Transactions on Energy Conversion*, Vol. 22, no. 1, March, 2007, pp. 197-205.
- [29] I. Abouzahr, R. Ramakumar, "Loss of power supply probability of stand-alone wind electric conversion systems: A closed form solution approach", *IEEE Transactions on Energy Conversion*, Vol. 5, no. 3, September, 1990, pp. 445-451.
- [30] A. G. Bakirtzis, "A probabilistic method for the evaluation of the reliability of stand-alone wind energy systems", *IEEE Transactions on Energy Conversion*, Vol. 7, no. 1, March, 1992, pp. 99-107.

- [31] S. H. Karaki, R. B. Chedid and R. Ramadan, "Probabilistic performance assessment of wind energy conversion systems", *IEEE Transactions on Energy Conversion*, Vol. 14, no. 2, September, 1999, pp. 217-224.
- [32] Bagen, R. Billinton, "Incorporating well-being considerations in generating systems using energy storage", *IEEE Transactions on Energy Conversion*, Vol. 20, no. 1, March, 2005, pp. 225-230.
- [33] U.S. Department of Energy, Wind and Hydropower Technologies Program, <http://www.nrel.gov/docs/fy04osti/34915.pdf>, "Wind Power: Today and Tomorrow".
- [34] J. Matevosyan, M. Olsson, and L. Soder, "Hydropower planning coordinated with wind power in areas with congestion problems for trading on the spot and the regulating market", *Electric Power Systems Research*, Vol. 79, no. 1, January, 2009, pp. 39-48.
- [35] J.K. Kaldellis, K.A. Kavadias, "Optimal wind-hydro solution for Aegean sea islands' electricity-demand fulfillment", *Applied Energy*, Vol. 70, no. 4, December, 2001, pp. 333-354.
- [36] E. D. Castronuovo, and J. A. Pecas Lopes, "On the optimization of the daily operation of a wind-hydro power plant", *IEEE Transactions on power systems*, Vol. 19, no. 3, August, 2004, pp. 1599-1606.
- [37] C. Belanger, L. Gagnon, "Adding wind energy to hydropower", *Energy Policy*, Vol. 30, no. 14, November, 2002, pp.1279-1284.



- [38] D. F. Ancona, S. Krau, G. Lafrance, P. Bezrukikh, "Operational constraints and economic benefits of wind-hydro hybrid systems analysis of systems in the U.S. / Canada and Russia", *European Wind Energy Conference*, Madrid, Spain, June 16-19, 2003.
- [39] Tapbury Management Limited, Sustainable Energy Ireland (<http://www.sei.ie>): "VRB ESS energy storage and the development of dispatchable wind turbine output".
- [40] R. N. Allan, J. Roman, "Reliability assessment of generation systems containing multiple hydro plant using simulation techniques", *IEEE Transactions on Power Systems*, Vol. 4, no. 3, August, 1989, pp. 1074-1080.
- [41] IEEE Committee Report, "A reliability test system", *IEEE Transactions on Power Apparatus and Systems*, Vol. PAS-98, no. 6, November/December, 1979, pp. 2047-2054.
- [42] Report of the IEEE Task Group on Models for Peaking Services Unit, "A four state model for estimation of outage risk for units in peaking service", *IEEE Transactions on Power Apparatus and Systems*, Vol. PAS-91, no. 2, March, 1972, pp. 618-627.
- [43] R. Billinton, "Criteria used by Canadian utilities in the planning and operation of generation capacity", *IEEE Transactions on Power Systems*, Vol. 3, no. 4, November, 1988, pp. 1488-1493.
- [44] R. Billinton and P. G. Harrington, "Reliability evaluation in energy limited generating capacity studies", *IEEE Transactions on Power Apparatus and Systems*, Vol. PAS-97, no. 6, November, 1978, pp. 2076-2086.

- [45] R. Billinton and R.N. Allan, *Reliability Evaluation of Engineering Systems: Concepts and Techniques*, Plenum Press, New York, 1992.
- [46] R. Billinton, S. Kumar, et al., "A reliability test system for educational purposes-basic data", *IEEE Transactions on Power Systems*, Vol. 4, no.3, August, 1989, pp. 1238-1244.
- [47] K. C. Chou and R. B. Corotis, "Simulation of hourly wind speed and array wind power", *Solar Energy*, Vol. 26, no. 3, 1981, pp.199-212.
- [48] M. Blanchard and G. Desrochers, "Generation of auto-correlated wind speeds for wind energy conversion system studies", *Solar Energy*, Vol. 33, no. 6, 1984, pp.571-579.
- [49] G. E. P. Box, G. M. Jenkins, *Time Series Analysis Forecasting and Control*, Holden Day Inc., 1970.
- [50] S. M. Pandit, SM. Wu, *Time Series and System Analysis with Application*, John Wiley & Sons, Inc, 1983.
- [51] Y. Gao, "Adequacy assessment of electric power systems incorporating wind and solar energy", M. Sc. Thesis, University of Saskatchewan, 2006.
- [52] R. Y. Rubinstein, *Simulation and the Monte Carlo Method*, Wiley, New York, 1981.
- [53] S. A. Papathanassiou, N. G. Boulaxis, "Power limitations and energy yield evaluation for wind farms operating in island systems", *Renewable Energy*, Vol. 31, no. 4, June, 2006, pp. 457-479.

- [54] H. Holttinen, J. Pedersen, “The effect of large-scale wind power on a thermal system operation”, *Proceedings of the 4<sup>th</sup> International Workshop on Large-Scale Integration of Wind Power and Transmission Networks for Offshore Wind Farms*, October 20-22, 2003, Billund, Denmark.

# APPENDIX A

## LOAD DATA AND GENERATING SYSTEM DATA FOR THE IEEE-RTS

Table A.1: Weekly peak load as a percentage of annual peak

Week	Peak load (%)	Week	Peak load (%)
1	86.2	27	75.5
2	90.0	28	81.6
3	87.8	29	80.1
4	83.4	30	88.0
5	88.0	31	72.2
6	84.1	32	77.6
7	83.2	33	80.0
8	80.6	34	72.9
9	74.0	35	72.6
10	73.7	36	70.5
11	71.5	37	78.0
12	72.7	38	69.5
13	70.4	39	72.4
14	75.0	40	72.4
15	72.1	41	74.3
16	80.0	42	74.4
17	75.4	43	80.0
18	83.7	44	88.1
19	87.0	45	88.5
20	88.0	46	90.9
21	85.6	47	94.0
22	81.1	48	89.0
23	90.0	49	94.2
24	88.7	50	97.0
25	89.6	51	100.0
26	86.1	52	95.2

Table A.2: Daily peak load as a percentage of weekly peak

Day	Peak load (%)
Monday	93
Tuesday	100
Wednesday	98
Thursday	96
Friday	94
Saturday	77
Sunday	75

Table A.3: Hourly peak load as a percentage of daily peak

	Winter weeks 1-8 & 44-52		Summer weeks 18-30		Spring/Fall weeks 9-17 & 31-43	
Hour	Weekday	Weekend	Weekday	Weekend	Weekday	Weekend
12-1 am	67	78	64	74	63	75
1-2	63	72	60	70	62	73
2-3	60	68	58	66	60	69
3-4	59	66	56	65	58	66
4-5	59	64	56	64	59	65
5-6	60	65	58	62	65	65
6-7	74	66	64	62	72	68
7-8	86	70	76	66	85	74
8-9	95	80	87	81	95	83
9-10	96	88	95	86	99	89
10-11	96	90	99	91	100	92
11-12 pm	95	91	100	93	99	94
12-1	95	90	99	93	93	91
1-2	95	88	100	92	92	90
2-3	93	87	100	91	90	90
3-4	94	87	97	91	88	86
4-5	99	91	96	92	90	85
5-6	100	100	96	94	92	88
6-7	100	99	93	95	96	92
7-8	96	97	92	95	98	100
8-9	91	94	92	100	96	97
9-10	83	92	93	93	90	95
10-11	73	87	87	88	80	90
11-12	63	81	72	80	70	85

Table A.4: IEEE-RTS generating unit ratings and reliability data

Unit No.	Rated Power (MW)	MTTF (Hours)	MTTR (Hours)	FOR
1	12	2940	60	0.02
2	12	2940	60	0.02
3	12	2940	60	0.02
4	12	2940	60	0.02
5	12	2940	60	0.02
6	20	450	50	0.1
7	20	450	50	0.1
8	20	450	50	0.1
9	20	450	50	0.1
10	76	1960	40	0.02
11	76	1960	40	0.02
12	76	1960	40	0.02
13	76	1960	40	0.02
14	100	1200	50	0.04
15	100	1200	50	0.04
16	100	1200	50	0.04
17	155	960	40	0.04
18	155	960	40	0.04
19	155	960	40	0.04
20	155	960	40	0.04
21	197	950	50	0.05
22	197	950	50	0.05
23	197	950	50	0.05
24	350	1150	100	0.08
25	400	1100	150	0.12
26	400	1100	150	0.12
27	50	1980	20	0.01
28	50	1980	20	0.01
29	50	1980	20	0.01
30	50	1980	20	0.01
31	50	1980	20	0.01
32	50	1980	20	0.01

**APPENDIX B**

**GENERATING UNIT RATINGS AND RELIABILITY DATA FOR**

**THE RBTS**

Table B.1: RBTS generating unit ratings and reliability data

Unit No.	Rated Power (MW)	MTTF (Hours)	MTTR (Hours)	FOR
1	40	1460	45	0.03
2	40	1460	45	0.03
3	10	2190	45	0.02
4	20	1752	45	0.025
5	5	4380	45	0.01
6	5	4380	45	0.01
7	40	2920	60	0.02
8	20	3650	55	0.015
9	20	3650	55	0.015
10	20	3650	55	0.015
11	20	3650	55	0.015